

MAGNETIC ANNIHILATION AND RECONNECTION

Craig Anderson

A Thesis Submitted for the Degree of PhD
at the
University of St Andrews



1994

Full metadata for this item is available in
St Andrews Research Repository
at:
<http://research-repository.st-andrews.ac.uk/>

Please use this identifier to cite or link to this item:
<http://hdl.handle.net/10023/14014>

This item is protected by original copyright

Magnetic Annihilation and Reconnection.

Craig Anderson,
Solar Theory Group,
St Andrews University.
April 1994.

ProQuest Number: 10167056

All rights reserved

INFORMATION TO ALL USERS

The quality of this reproduction is dependent upon the quality of the copy submitted.

In the unlikely event that the author did not send a complete manuscript and there are missing pages, these will be noted. Also, if material had to be removed, a note will indicate the deletion.



ProQuest 10167056

Published by ProQuest LLC (2017). Copyright of the Dissertation is held by the Author.

All rights reserved.

This work is protected against unauthorized copying under Title 17, United States Code
Microform Edition © ProQuest LLC.

ProQuest LLC.
789 East Eisenhower Parkway
P.O. Box 1346
Ann Arbor, MI 48106 – 1346

TL B500

Abstract

This thesis presents several analytical models of magnetic annihilation and reconnection and studies their properties. The models investigated are

1. **Steady-state magnetic annihilation.** The assumption of straight field lines reduces the resistive, viscous MHD equations to two ordinary differential equations, one for the flow and one for the magnetic field. These equations can be solved exactly (for the case of a simple stagnation-point flow) and asymptotically (for a more general stagnation-point flow). In both cases the reconnection rates can be fast due to advection effects which create large magnetic gradients.
2. **Time-dependent magnetic annihilation.** The assumption of straight field lines whose strength can vary with time reduces the MHD equations to two partial differential equations, one for the flow and one for the magnetic field. The time-modulated simple stagnation-point flow is shown to be an exact solution and the equation for the magnetic field is then solved on infinite and finite intervals. For the infinite interval the reconnection rates are shown to be dependent on the nature of the advected initial field. Also examined are self-similar solutions and the effect of variation of diffusivity with time.
3. **Annihilation in a compressible, inviscid plasma.** Here, the assumption of straight field lines and an inviscid, compressible flow reduce the MHD equations to a pair of non-linear coupled partial differential equations. Further assuming that the density only varies in one direction and the flow is of a stagnation-point type allow these equations to be solved approximately analytically and exactly numerically. It is shown that the magnetic field and reconnection rates are the same in both the compressible and incompressible cases and that the density of the plasma is greatest within the current sheet.
4. **Steady-state magnetic reconnection.** For an incompressible flow the MHD equations can be reduced to two coupled non-linear partial differential equations. These two equations are studied by seeking asymptotic solutions around the annihilation solution and then looking for series solutions to the first-order equations. It is found that the magnetic field always has a magnetic cusp and never possesses an x-type neutral point.
5. **Reconnection in a viscous plasma.** Assuming that the viscous forces dominate, the induction equation and equation of motion decouple and become linear. The magnetic field is obtained for the case of a simple stagnation-point flow. It is shown that if the inflow magnetic field is taken to be straight then the magnetic field within the region tends towards the annihilation solution as the magnetic Reynolds number increases.
6. **Magnetic flipping.** A previous ideal model of magnetic flipping is refined so that it becomes an exact solution of the MHD equations. In the refined model the streamlines are straight rather than curved. Assuming straight streamlines, the MHD equations reduce to two linear ordinary differential equations, one for the flow and one for the magnetic field. These are then solved

exactly analytically to find a flow containing a viscous boundary layer and a magnetic field that contains an x-type neutral point. The angle between the separatrices of the field is determined by the Reynolds and magnetic Reynolds numbers. It is shown that most of the ohmic heating occurs within the viscous boundary layer.

Contents

Abstract	ii
Declaration	vi
Acknowledgements	vii
1 Introduction	8
1.1 The Sun	8
1.2 Solar Flares	8
1.3 The Magnetohydrodynamic Equations	9
1.4 Magnetic Connection and Reconnection	10
1.5 Reconnection Models	11
2 Steady-State Magnetic Annihilation	16
2.1 Introduction	16
2.2 Sonnerup and Priest Case	18
2.3 Jardine Case	23
3 Time-Dependent Magnetic Annihilation	28
3.1 Introduction	28
3.2 Solution on an Infinite Interval	30
3.3 Finite Interval with a Steady Plasma Flow	36
3.4 Finite Interval with a Time-Modulated Flow	40
3.5 Self-Similar Solutions	41
3.6 Time-Dependent Diffusivity	42
4 Magnetic Annihilation in a Compressible, Inviscid Plasma	44
4.1 Introduction	44
4.2 Assumptions	46
4.3 Analytical Solution	47
4.4 Numerical Solution	50
4.5 Magnetic Field	51
4.6 Additional Thoughts	52
5 A Series Approach to Steady-State Magnetic Reconnection	55
5.1 Introduction	55
5.2 Asymptotic Solution	57
5.3 Zero-Order Equation	58
5.4 First-Order Equations	58
5.5 Series Solutions for f and g	60
5.6 Boundary Conditions	62
5.7 Solutions for the Flux and Stream Functions	62
5.8 Magnetic Field Lines	62
5.9 Necessary Conditions	63
5.10 Examples	63

6	Magnetic Reconnection in a Viscous Plasma	65
6.1	Introduction	65
6.2	Plasma Flow	65
6.3	Magnetic Field	66
6.4	Large R_m	69
6.5	Numerical Investigation of the Analytical Solution	71
7	Magnetic Flipping	73
7.1	Introduction	73
7.2	Refining the Priest and Forbes Solution	73
7.3	Straight Stream Lines	77
7.4	Plasma Flow	79
7.5	Magnetic Field	82
7.6	Reconnection Rates	85
	Conclusions	87
	Appendix A	89
	Appendix B	90
	Appendix C	91
	Appendix D	92
	Appendix E	93
	Appendix F	94
	Appendix G	95
	Appendix H	101
	Appendix I	103
	Appendix J	104
	References	105

Declaration

In accordance with the regulations of St Andrews University as of December 1993,

1. I, Craig Anderson, hereby certify that this thesis has been composed by myself, that it is a record of my own work, and that it has not been accepted in partial or complete fulfillment of any other degree of professional qualification.

Signed:

Date: 5/4/94

2. I was admitted to the Faculty of Science of the University of St Andrews under Ordinance General No 12 in October 1990 and as a candidate for the degree of PhD on the same date.

Signed:

Date: 5/4/94

3. I hereby certify that the candidate has fulfilled the conditions of the Resolution and Regulations appropriate to the Degree of PhD.

Signed:

Date: 5-4-94

4. In submitting this thesis to the University of St Andrews I understand that I am giving permission for it to be made available for use in accordance with the regulations of the University Library for the time being in force, subject to any copyright vested in the work not being affected thereby. I also understand that the title and abstract will be published, and that a copy of the work may be made and supplied to any bona fide library or research worker.

Acknowledgements

Many thanks to

Eric Priest, my supervisor, whose endless enthusiasm kept me going,

My parents, for their encouragement and support, and

Alan Hood, for putting up with lots of questions about magnetic flipping.

Thanks also to SERC for all the money, Richard Ireland for all the tea and all the members of the Solar Theory group, past and present, for making it such an interesting place to work.

The thesis was examined by David Hughes (Newcastle University) and Alan Hood (St Andrews University) and I am grateful to them for their time and effort and also for their many helpful criticisms and suggestions.

Chapter 1

Introduction

1.1 The Sun

The Sun is an object of great interest that has been studied for many thousands of years. However, only in this century has it been realised that the Sun is an intensely magnetic environment and that the magnetic field is responsible for most, if not all, of the structures and phenomena that are observed.

Some of these solar phenomena, such as flares and x-ray bright points, involve the release of vast amounts of heat and light energy in a short interval of time. It is generally believed that the source of this energy is the solar magnetic field and it has been supposed that a process known as magnetic reconnection converts magnetic energy to heat energy.

This thesis is concerned with mathematically modelling the magnetic reconnection process with the aim of showing whether or not it is capable of converting large amounts of energy within a short space of time.

1.2 Solar Flares

A solar flare can be loosely described as a localised rapid brightening of H_α emission in the low chromosphere. Usually there is a flash phase, typically lasting 5 minutes, in which the intensity and area of emission increase rapidly and a main phase, lasting about an hour, in which the intensity declines slowly.

A typical solar flare has a length scale of $\ell_0 = 2 \times 10^7$ metres and a typical time scale $t_0 = 10^2 \sim 10^3$ seconds. Parker (1957) and (1963) estimates the typical energy release in a solar flare to be around 10^{25} joules and analysis of emission lines (eg Jeffries & Smith (1959) and Jeffries & Orrall (1961)) gives a mean density in the flare of around $2 \times 10^{-10} \text{ kg m}^{-3}$. The typical velocity scale is $v_0 = \ell_0/t_0 = 2 \times 10^5 \text{ ms}^{-1}$.

Since solar flares invariably occur in regions of strong magnetic field and other sources of energy seem inadequate it is usually assumed that the magnetic field supplies the energy for a flare. For example the magnetic energy available from a cube of side $\ell_0 = 2 \times 10^7$ metres containing a magnetic field of strength $B_0 = 0.05$ tesla (500 gauss) is

$$E_m = \int_V \frac{B^2}{2\mu} dV \approx \ell_0^3 \frac{B_0^2}{2\mu_0} \approx 10^{25} \text{ joules,}$$

which is roughly the same as the energy released in a flare.

1.3 The Magnetohydrodynamic Equations

Solar flares, and many other solar phenomena, have length scales larger than the mean free paths of the particles in the plasma that comprises the solar atmosphere. This implies that the plasma can be regarded as a continuous fluid and can be modelled by the set of magnetohydrodynamic (MHD) equations. These equations consist of Maxwell's equations of electromagnetism along with Ohm's law and the hydrodynamic equations which describe the behaviour of a fluid.

Maxwell's Equations

Assuming plasma neutrality and that the typical velocities are much less than the speed of light, Maxwell's equations reduce to

$$\bar{\nabla} \times \bar{\mathbf{B}} = \mu \bar{\mathbf{j}} \quad \text{Ampere's law,} \quad (1.1)$$

$$\bar{\nabla} \times \bar{\mathbf{E}} = -\frac{\partial \bar{\mathbf{B}}}{\partial t} \quad \text{Faraday's law,} \quad (1.2)$$

$$\bar{\nabla} \cdot \bar{\mathbf{B}} = 0, \quad (1.3)$$

where $\bar{\mathbf{B}}$ is the magnetic induction (usually called the magnetic field), $\bar{\mathbf{E}}$ is the electric field and $\bar{\mathbf{j}}$ is the current density. The quantity μ , the magnetic permeability, is usually approximated to its value in a vacuum, $\mu_0 = 1.26 \times 10^{-6} \text{ Hm}^{-1}$.

Ohm's Law

The simplest (resistive) form of Ohm's law is

$$\bar{\mathbf{E}} + \bar{\mathbf{v}} \times \bar{\mathbf{B}} = \frac{1}{\sigma} \bar{\mathbf{j}}. \quad (1.4)$$

Hydrodynamic Equations

The equations describing the behaviour of a fluid are the equation of motion,

$$\bar{\rho} \left[\frac{\partial \bar{\mathbf{v}}}{\partial t} + (\bar{\mathbf{v}} \cdot \bar{\nabla}) \bar{\mathbf{v}} \right] = -\bar{\nabla} \bar{p} + \bar{\mathbf{j}} \times \bar{\mathbf{B}} + \nu \bar{\rho} \bar{\nabla}^2 \bar{\mathbf{v}} + \frac{1}{3} \nu \bar{\rho} \bar{\nabla} (\bar{\nabla} \cdot \bar{\mathbf{v}}), \quad (1.5)$$

the equation of mass continuity,

$$\frac{\partial \bar{\rho}}{\partial t} + \bar{\nabla} \cdot (\bar{\rho} \bar{\mathbf{v}}) = 0, \quad (1.6)$$

the ideal gas law,

$$\bar{p} = \frac{R}{\mu_a} \bar{\rho} T, \quad (1.7)$$

and an energy equation,

$$\frac{\bar{\rho}^\gamma}{\gamma - 1} \frac{D}{Dt} \left(\frac{\bar{p}}{\bar{\rho}^\gamma} \right) = -\bar{\nabla} \cdot \mathbf{q} - L + \frac{1}{\sigma} \bar{j}^2. \quad (1.8)$$

In these equations, $\bar{\rho}$ is the fluid density, R is the gas constant, T is the absolute temperature and μ_a is the mean atomic weight. In the energy equation, γ is the ratio of the specific heat at constant pressure to the specific heat at constant volume, \mathbf{q} is the heat flux due to particle conduction, L is the radiative loss and \bar{j}^2/σ is the ohmic heating rate. Note that the effects of gravity are neglected in the equation of motion as they are considered to be negligible in comparison to the other terms.

Non-Dimensionalisation

Equations (1.1) to (1.6) are usually non-dimensionalised according to

$$\bar{\mathbf{B}} = B_0 \mathbf{B}, \quad \bar{\mathbf{v}} = v_0 \mathbf{v}, \quad \bar{\mathbf{r}} = \ell_0 \mathbf{r}, \quad \bar{\rho} = \rho_0 \rho, \quad \bar{p} = p_0 p$$

and

$$\bar{\mathbf{j}} = \frac{B_0}{\mu \ell_0} \mathbf{j}, \quad \bar{\mathbf{E}} = v_0 B_0 \mathbf{E}, \quad \bar{t} = \frac{\ell_0}{v_0} t,$$

to obtain

$$\begin{aligned} M_A^2 \rho \left[\frac{\partial \mathbf{v}}{\partial t} + (\mathbf{v} \cdot \nabla) \mathbf{v} \right] &= -\beta \nabla p + \mathbf{j} \times \mathbf{B} + \frac{M_A^2}{R} \rho \nabla^2 \mathbf{v}, \\ \mathbf{E} + \mathbf{v} \times \mathbf{B} &= \frac{1}{R_m} \mathbf{j}, \\ \nabla \times \mathbf{E} &= -\frac{\partial \mathbf{B}}{\partial t}, \\ \nabla \cdot \mathbf{B} &= 0, \\ \frac{\partial \rho}{\partial t} + \nabla \cdot (\rho \mathbf{v}) &= 0, \\ \mathbf{j} &= \nabla \times \mathbf{B}, \end{aligned}$$

where $M_A = \sqrt{\rho_0 \mu} v_0 / B_0$ is the Alfvén mach number, $\beta = p_0 \mu / B_0^2$ is the plasma beta, $R_m = v_0 \ell_0 / \eta$ is the magnetic Reynolds number and $R = v_0 \ell_0 / \nu$ is the Reynolds number. The magnetic energy and ohmic heating rate,

$$E_m = \frac{1}{2\mu_0} \int_V \bar{B}^2 d\bar{V} \quad \text{and} \quad R_\Omega = \frac{1}{\sigma} \int_V \bar{j}^2 d\bar{V},$$

become

$$E_m = \frac{B_0^2 \ell_0^3}{\mu_0} E_m \quad \text{and} \quad R_\Omega = \frac{B_0^2 \ell_0^2}{\mu_0} R_\Omega,$$

where

$$E_m = \frac{1}{2} \int_V B^2 dV \quad \text{and} \quad R_\Omega = \frac{1}{R_m} \int_V j^2 dV$$

are the dimensionless magnetic energy and ohmic heating rate.

1.4 Magnetic Connection and Reconnection

Taking the curl of Ohm's law and using Faraday's and Ampere's laws gives the induction equation,

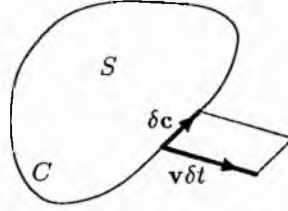
$$\frac{\partial \mathbf{B}}{\partial t} = \nabla \times (\mathbf{v} \times \mathbf{B}) + \frac{1}{R_m} \nabla^2 \mathbf{B},$$

where $R_m = v_0 \ell_0 \mu_0 \sigma$. The conductivity, σ , of the solar atmosphere is not well known and consequently R_m is not known exactly but is believed to lie in the range $10^6 \sim 10^{12}$. Since R_m is large the $\nabla^2 \mathbf{B} / R_m$ term can usually be assumed to be negligible so that the induction equation reduces to

$$\frac{\partial \mathbf{B}}{\partial t} = \nabla \times (\mathbf{v} \times \mathbf{B}). \quad (1.9)$$

Consider the flux F through a closed curve C bounding a simple surface S which is moving with the plasma, as shown in figure 1.1. In time δt the line element $\delta \mathbf{c}$ sweeps out an area of $\mathbf{v} \delta t \times \delta \mathbf{c}$ and intuitively we have

$$\frac{DF}{Dt} = \int_S \frac{\partial \mathbf{B}}{\partial t} \cdot d\mathbf{S} + \int_C \mathbf{B} \cdot \mathbf{v} \times d\mathbf{c}, \quad (1.10)$$

Figure 1.1: A surface S moving with the plasma.

where the first term on the right-hand side is due to field changes in time and the second term on the right-hand side is due to the motion of the boundary. The second term can be rewritten as

$$-\int_C \mathbf{v} \times \mathbf{B} \cdot d\mathbf{c}$$

and Stokes' theorem can be applied so that this becomes

$$-\int_S \nabla \times (\mathbf{v} \times \mathbf{B}) \cdot d\mathbf{S}.$$

Equation (1.10) thus becomes

$$\frac{DF}{Dt} = \int_S \left[\frac{\partial \mathbf{B}}{\partial t} - \nabla \times (\mathbf{v} \times \mathbf{B}) \right] \cdot d\mathbf{S}$$

which, if (1.9) holds, reduces to

$$\frac{DF}{Dt} = 0.$$

Physically, this result says that the magnetic flux through a closed loop moving with the fluid is conserved, the implication being that flux tubes move with the fluid, their strength remaining constant. In the limit of zero cross section a magnetic flux tube becomes a magnetic field line and so we can say that magnetic field lines move with the fluid, behaving as if they were "frozen" into it. (The transport of magnetic field lines by fluid motion is known as magnetic advection.) Elements of the fluid which are initially connected by a common field line thus continue to be connected.

This result only holds true if the $\nabla^2 \mathbf{B}/R_m$ term remains negligible. It is possible for fluid motions to carry part of the field line through some region where this term is locally large and the frozen flux theorem becomes locally invalid. Within this region the magnetic field may diffuse slightly and fluid elements that were connected by a field line before it passed through the region become disconnected and connected afterwards to different fluid elements. Within the small region where the term $\nabla^2 \mathbf{B}/R_m$ is non-negligible magnetic reconnection is said to have taken place.

1.5 Reconnection Models

Diffusion Model

The simplest reconnection or annihilation process is the diffusion of magnetic field through a static plasma. Taking $\mathbf{v} = 0$ and $\mathbf{B} = (B(y, t), 0, 0)$ the induction equation reduces to

$$\frac{\partial B}{\partial t} = \frac{1}{R_m} \frac{\partial^2 B}{\partial y^2} \quad (1.11)$$

which can be solved (see chapter 3 for details) to obtain

$$B(y, t) = \frac{1}{\sqrt{\pi}} \int_{-\infty}^{+\infty} B_0 \left(y + 2\epsilon t^{\frac{1}{2}} R_m^{-\frac{1}{2}} \right) e^{-\epsilon^2} d\epsilon,$$

where $B_0(y)$ is the initial magnetic field. Taking $B_0(y) = \text{erf } y$, which consists of two regions of oppositely directed field lines with a narrow region of large magnetic gradient between them, gives the results shown in figure 1.2.

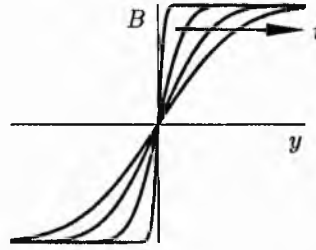


Figure 1.2: Diffusion of a magnetic field.

The oppositely directed field lines diffuse through the plasma and cancel (or annihilate) each other. The region of magnetic gradient (known as a current sheet) widens with a velocity $1/(\ell R_m)$, where ℓ is the scale width of the current sheet. This velocity, known as the diffusion velocity, is obtained by an order of magnitude analysis of the diffusion equation, (1.11). The rate of change of magnetic energy is

$$\frac{\partial}{\partial t} E_m = \frac{1}{2} \frac{\partial}{\partial t} \int_V B^2 dV = \int_{-\infty}^{\infty} B \frac{\partial B}{\partial t} dy$$

and substituting from (1.11) gives

$$\frac{\partial}{\partial t} E_m = \frac{1}{R_m} \int_{-\infty}^{\infty} B \frac{\partial^2 B}{\partial y^2} dy.$$

Integrating this by parts and assuming that $\partial B / \partial y \rightarrow 0$ as $y \rightarrow \pm\infty$ yields

$$\frac{\partial}{\partial t} E_m = -\frac{1}{R_m} \int_{-\infty}^{\infty} \left(\frac{\partial B}{\partial y} \right)^2 dy = -\frac{1}{R_m} \int_{-\infty}^{\infty} j^2 dy = -R_\Omega,$$

from which we see that magnetic energy is dissipating through ohmic heating and that the magnetic energy in the system is converted to heat energy.

Note that the current sheet widens and the magnetic gradient (and hence the current) decreases with time. Since the ohmic heating decreases with time, this simple mechanism cannot explain the rapid heating observed in solar flares for long times.

Sweet-Parker Reconnection Model

Parker (1957) and Sweet (1958) noted that the currents could be kept constant if the outward diffusion of the current sheet is counterbalanced by an inward flow of fluid. They proposed the idealised situation shown in figure 1.3a. As the field lines move towards each other the x -components of the magnetic field diffuse and annihilate. At the ends of the current sheet only the y -component of the field remains and reconnection has taken place.

The current sheet length, L , is fixed by the geometry of the field lines and energy and momentum considerations give $v_o = B_i / \sqrt{\mu_0 \rho}$. Non-dimensionalising against B_i , v_o and L gives the situation of figure 1.3b in which the plasma outflow velocity, current sheet length and the field outside the sheet are unity. Note that the region outside the current sheet is current-free and the dimensionless current in the sheet is $1/\ell$.

Conservation of mass gives

$$v_i = \ell. \quad (1.12)$$

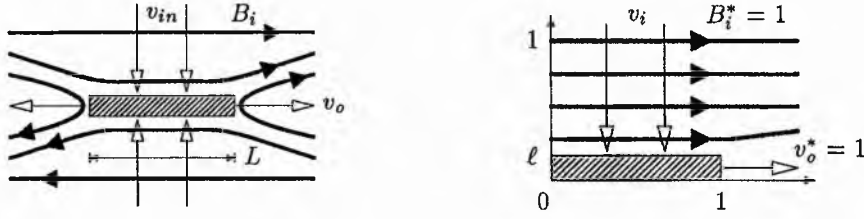


Figure 1.3: Sweet-Parker reconnection model

and the outward diffusion of the current sheet will be balanced by the plasma inflow if

$$v_i = \frac{1}{R_m \ell}. \quad (1.13)$$

Eliminating ℓ between (1.12) and (1.13) gives

$$v_i = R_m^{-\frac{1}{2}}.$$

The magnitude of v_i gives a measure of how much flux is being transported into the the current sheet and is thus a measure of the reconnection rate. In dimensional units this result becomes

$$v_{in} = v_o v_i = \frac{B_i}{\sqrt{\mu_0 \rho_0}} R_m^{-\frac{1}{2}} \quad (1.14)$$

and, in applying this result to solar flares, Parker (1963) found that v_{in} was too slow compared to the typical velocity scale of a solar flare. Taking, for example,

$$B_i = 0.05 \text{ T (500 G)}, \quad \rho_0 = 2 \times 10^{-7} \text{ kg m}^{-3} \quad \text{and} \quad R_m = 10^6 \sim 10^{12},$$

then (1.14) gives $v_{in} = 5 \times 10^3 \text{ ms}^{-1} \sim 5 \text{ ms}^{-1}$ which is several orders of magnitude short of the typical flare velocity scale of 10^5 ms^{-1} . The Sweet-Parker model is thus said to be a *slow* reconnection process.

Classes of Magnetic Reconnection

Magnetic reconnection models can be classified in several different ways. One of the classifications is based on the behaviour of the reconnection rate. If the reconnection rate is less than, equal to or greater than $R_m^{-\frac{1}{2}}$, as R_m tends to infinity, the reconnection is said to be very slow, slow or fast, respectively.

Reconnection models can also be classified on whether they are steady-state or time-dependent and according to the global state of the magnetic field (ie current sheet or x-point).

Reconnection Rates

In the Sweet-Parker model the dimensionless inflow velocity, v_i , is used as a measure of the reconnection rate. Since the inflow region is assumed to be current-free and the inflow field is unity then Ohm's law gives $E + v_i = 0$ and hence the v_i and E can be used interchangeably as a measure of reconnection. Since, in a two-dimensional model, the electric field is uniform throughout space then at a neutral point Ohm's law becomes $E = j/R_m$ and hence it is quite common to take j_{np}/R_m , where j_{np} is the magnitude of the current at a neutral point, as the reconnection rate.

Also of interest is the ohmic heating rate and throughout this thesis we will consider the reconnection and ohmic heating rates R_E and R_Ω , where

$$R_E = E = \frac{1}{R_m} j_{np} \quad \text{and} \quad R_\Omega = \frac{1}{R_m} \int_V j^2 dV.$$

Petschek Reconnection

The first fast reconnection model was that of Petschek (1964). The main features of this model, sketched in figure 1.4a, are the slow-mode shocks propagating from the corners of the current sheet which accelerate the inflowing plasma up to the outflow velocity. These shocks are treated as discontinuities within the field and flow. The most important assumptions in the Petschek model are that the inflow magnetic field is current free (and hence potential) and that the inflow magnetic field lines are almost straight. Petschek considered a linear potential perturbation to a uniform magnetic field in the inflow region which is matched to an approximate resistive solution for the current sheet in which the current sheet length and width are allowed to vary. The reconnection rate for this model was estimated by Petschek to be

$$R_E \leq \frac{\pi}{8 \log(2R_E^2 R_m)},$$

which is only weakly dependent on the magnetic Reynolds number. Axford (1984) argues that it is the changing current sheet length that leads to a fast reconnection process; provided that the diffusion region is small compared with the dimensions of the flow then changes in the the conductivity produce compensating changes in the size of the diffusion region and the reconnection rate is then ultimately determined by boundary conditions and not by the conductivity.

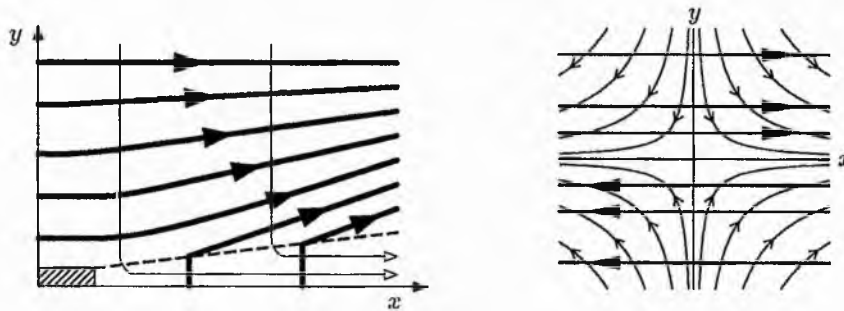


Figure 1.4: Petschek reconnection model and Sonnerup and Priest annihilation model.

Sonnerup (1970) proposed a similar model with an extra set of shocks and obtained a reconnection rate of order unity. Many details of these models were clarified by Vasyliunas (1975) who points out that Petschek's inflow region has the character of a weak fast-mode expansion and that Sonnerup's extra discontinuity is a slow-mode expansion generated at some external point. Sonnerup and Wang (1987) studied the structure of the downstream region in detail by treating it as a narrow boundary layer.

Magnetic Annihilation

The first reconnection model which is an exact solution of the resistive and viscous MHD equations was investigated by Parker (1973) and Sonnerup & Priest (1975). As shown in figure 1.4b, they supposed the field lines to be straight, ie $\mathbf{B} = (B(y), 0, 0)$, and carried together by the stagnation-point flow $\mathbf{v} = (x, -y, 0)$. The induction equation can then be solved for the magnetic field and the equation of motion for the plasma pressure. This model is similar to the Sweet-Parker model in that the incoming flow of plasma prevents the outward diffusion of the current sheet and maintains a constant magnetic gradient. Since field lines cancel exactly within the diffusion region and no magnetic flux is expelled outwards, then this is termed magnetic annihilation.

Models of this sort can be adapted to study a wide range of phenomena. For example Gratton *et al* (1988), Phan and Sonnerup (1990) and Jardine *et al* (1992) (1993) consider more general types of stagnation point flows. Kirkland and Sonnerup (1979) find self-similar solutions for the induction, mass continuity, energy and pressure balance equations.

Numerical Reconnection Experiments

The magnetic reconnection process is not straightforward to model numerically as the mixture of length-scales (large length scale of the inflow/outflow regions and small length scale of current sheets and slow-mode shocks) requires a lot of effort to resolve the finer details. Numerical models can only examine part of a parameter regime and can only apply certain types of boundary conditions so any scaling laws deduced may not be applicable to different parameter regimes or different boundary conditions.

Scholer (1989) has shown (in contrast to Biskamp (1986)) that at high magnetic Reynolds numbers fast Petschek reconnection can occur when the appropriate boundary conditions are imposed and the central current sheet possesses an anomalous resistivity. Forbes & Priest (1986), Biskamp (1986) and Fu & Lee (1986) have found clear evidence of the slow-mode shock waves.

However, numerical experiments on steady magnetic reconnection (Biskamp (1984) (1986), Forbes & Priest (1982) (1983) (1984), Lee (1986), Lee & Fu (1986), Fu & Lee (1986), Scholer (1989)) have revealed many new features, namely

1. the inflow is generally not a weak fast-mode expansion,
2. the inflow magnetic field can have strong curvature,
3. there may be jets of plasma along the separatrices,
4. there may be regions of "reversed" current near the ends of the current sheet.

Many time-dependent models of reconnection exist, eg Tsuda & Ugai (1977) and Hayashi & Sato (1978) use time-dependent codes and find that an initial configuration evolves to a quasi-steady state similar to Petschek's and Deluca & Craig (1992) and Rickard & Craig (1993) investigate time-dependent reconnection near an x-type neutral point.

Recent Reconnection Models

Priest and Forbes (1986) produced a unified theory for linear reconnection (linear in the sense that the inflow magnetic field is a linear perturbation to a uniform state) by generalising the assumption that the inflow is potential. They obtain a continuous series of reconnection regimes with the upper (inflow) boundary condition determining which regime is produced. The inflow may have the character of a slow mode compression, fast-mode expansion or slow-mode expansion, depending on whether the inflow is converging or diverging. This theory was developed by Jardine and Priest (1988a-c) who extended it to include compressibility and to allow weakly non-linear inflow by considering the second-order terms.

Separatrix jets have been studied by Habbal & Tuan (1979), Soward & Priest (1986) whilst Jardine & Priest (1988d) give physical arguments for the existence of reversed currents.

Priest & Lee (1990) present a model in which the inflow field has significant curvature and possesses plasma jets and reverse current. This model is developed by Strachan and Priest (1994).

Chapter 2

Steady-State Magnetic Annihilation

2.1 Introduction

In this section the equations describing two-dimensional, steady-state, magnetic annihilation models are derived from the steady-state MHD equations.

Equations

The dimensionless, steady-state, resistive, viscous MHD equations for an incompressible plasma are

$$\begin{aligned}M_A^2 (\mathbf{v} \cdot \nabla) \mathbf{v} &= -\beta \nabla p + \mathbf{j} \times \mathbf{B} + \frac{M_A^2}{R} \nabla^2 \mathbf{v}, \\ \mathbf{E} + \mathbf{v} \times \mathbf{B} &= \frac{1}{R_m} \mathbf{j}, \\ \nabla \times \mathbf{E} &= 0, \\ \nabla \cdot \mathbf{B} &= 0, \\ \nabla \cdot \mathbf{v} &= 0, \\ \mathbf{j} &= \nabla \times \mathbf{B}.\end{aligned}$$

Assumptions

The basis of all magnetic annihilation models is the assumption that the magnetic field lines are straight so that the non-linear magnetic tension term drops out of the equation of motion. Taking the field lines to be parallel to the x -axis then to satisfy $\nabla \cdot \mathbf{B} = 0$ they must be of the form

$$\mathbf{B} = (B(y), 0, 0). \quad (2.1)$$

The equation of mass continuity, $\nabla \cdot \mathbf{v} = 0$, will be satisfied if $\mathbf{v} = \nabla \times \psi$, where ψ is the stream function. Assuming that the flow is two-dimensional gives

$$\mathbf{v} = \nabla \times \psi(x, y) \hat{\mathbf{z}} = (\psi_y, -\psi_x, 0). \quad (2.2)$$

Faraday's Law

The components of Faraday's Law are

$$\begin{aligned}\partial_y E_z &= 0, \\ \partial_x E_z &= 0, \\ \partial_x E_y - \partial_y E_x &= 0.\end{aligned} \quad (2.3)$$

The first two of these imply that

$$E_{\hat{z}} = \text{constant} = k.$$

Ohm's Law

With \mathbf{B} and \mathbf{v} of the forms (2.1) and (2.2) the components of Ohm's law are

$$\begin{aligned} E_{\hat{x}} &= 0, \\ E_{\hat{y}} &= 0, \\ E_{\hat{z}} + \psi_x B &= -\frac{1}{R_m} B'. \end{aligned}$$

The first two of these equations determine $E_{\hat{x}}$ and $E_{\hat{y}}$, which now satisfy (2.3) identically. Noting that $E_{\hat{z}} = k$, the third component becomes

$$\frac{1}{R_m} B' + \psi_x B = -k \quad (2.4)$$

and since B is a function of y this equation can only be consistent if

$$\psi_x = f(y),$$

implying that

$$\psi = x f(y) + g(y) \quad (2.5)$$

and reducing (2.4) to

$$\frac{1}{R_m} B' + f B = -k.$$

The Equation of Motion

As the field lines are straight the equation of motion reduces to

$$M_A^2 (\mathbf{v} \cdot \nabla) \mathbf{v} = -\nabla \left(\beta \nabla p + \frac{1}{2} B^2 \right) + \frac{M_A^2}{R} \nabla^2 \mathbf{v}.$$

The pressure terms can be eliminated by taking the curl of this (see appendix A) to produce

$$(\mathbf{v} \cdot \nabla) \boldsymbol{\omega} - (\boldsymbol{\omega} \cdot \nabla) \mathbf{v} = \frac{1}{R} \nabla^2 \boldsymbol{\omega},$$

where $\boldsymbol{\omega} = \nabla \times \mathbf{v}$ is the vorticity. Since the model is two-dimensional, $\boldsymbol{\omega} = \omega \hat{z}$ and this simplifies to

$$(\mathbf{v} \cdot \nabla) \omega = \frac{1}{R} \nabla^2 \omega.$$

Substituting \mathbf{v} of the form (2.2) into this equation we find

$$(\psi_y \partial_x - \psi_x \partial_y) (\psi_{xx} + \psi_{yy}) = \frac{1}{R} (\partial_x^2 + \partial_y^2) (\psi_{xx} + \psi_{yy}),$$

and with ψ of the form (2.5) this becomes

$$((x f' + g') \partial_x - f \partial_y) (x f'' + g'') = \frac{1}{R} (\partial_x^2 + \partial_y^2) (x f'' + g'')$$

or

$$x \left(\frac{1}{R} f^{(4)} + f f''' - f' f'' \right) + \frac{1}{R} g^{(4)} + f g''' - g' f'' = 0.$$

Since f is a function of y this equation will only be consistent if

$$\frac{1}{R} f^{(4)} + f f''' - f' f'' = 0,$$

leaving

$$\frac{1}{R} g^{(4)} + f g''' - g' f'' = 0.$$

Summary

For two-dimensional steady-state magnetic annihilation models where

$$\mathbf{B} = (B(y), 0, 0) \quad \text{and} \quad \mathbf{v} = (\psi_y, -\psi_x, 0),$$

the MHD equations will be satisfied if

$$\psi = xf(y) + g(y),$$

$$\frac{1}{R_m} B' + fB = -k, \quad (2.6)$$

$$\frac{1}{R} f^{(4)} + ff''' - f'f'' = 0, \quad (2.7)$$

$$\frac{1}{R} g^{(4)} + fg''' - f''g' = 0, \quad (2.8)$$

where the arbitrary constant k is the electric field component in the \hat{z} direction.

Notes

1. The function g does not appear in the equation for B and has no influence on the magnetic field. Accordingly, only the solution $g = 0$ of equation (2.8) will be considered here.
2. With $g = 0$ the flow becomes $\mathbf{v} = (xf', -f, 0)$. Assuming that v_y is an odd function (so that only the region $0 \leq y \leq 1$ has to be considered) gives the boundary condition $f(0) = 0$. Due to the non-dimensionalisation process, f must also satisfy $f(1) = 1$.
3. Similarly, B must satisfy the boundary conditions $B(0) = 0$ and $B(1) = 1$.

2.2 Sonnerup and Priest Case

Introduction

Equation (2.7) has the simple solution $f = y$ giving $\psi = xy$ (which is the simple stagnation-point flow $\mathbf{v} = (x, -y, 0)$) and equation (2.6) becomes

$$\frac{1}{R_m} B' + yB = -k. \quad (2.9)$$

This is the equation examined by Sonnerup & Priest (1975). In this section we solve this equation to obtain B and examine the reconnection rates and the advection process in more detail.

Ideal Solution for the Magnetic Field

Equation (2.9) has two terms on the left-hand side, one resistive and the other advective. If R_m is large, the resistive term becomes negligible and the equation reduces to

$$yB = -k,$$

giving

$$B = -\frac{k}{y}. \quad (2.10)$$

This solution, in which only the process of advection acts on the magnetic field, is singular on $y = 0$, giving unphysical behaviour near this line. The unphysical behaviour can only be eliminated if some extra, non-ideal, effect becomes important near $y = 0$ creating a boundary layer.

Mathematically, we can note that the resistive term, B'/R_m , was dropped on the basis that its magnitude is small if R_m is large. With $B = -k/y$ the resistive term is

$$\frac{1}{R_m} B' = \frac{1}{R_m y^2},$$

which is negligible if y and R_m are large but, irrespective of the magnitude of R_m , becomes non-negligible close to $y = 0$.

From these arguments, it can be surmised that the ideal approximation becomes untenable near $y = 0$ and resistive effects become important to create a resistive boundary layer. The large magnetic gradients in this boundary layer will give rise to large currents and, consequently, strong ohmic heating. The ideal solution, in which advection is dominant and controls the behaviour of the magnetic field, is valid outside the boundary layer.

Since (2.10) is valid away from $y = 0$, the boundary condition $B(1) = 1$ can be applied to give $k = -1$ and so

$$B = \frac{1}{y}. \quad (2.11)$$

At $y = 0$ equation (2.9) reduces to

$$\frac{1}{R_m} B' = k.$$

Solving this equation, applying $k = -1$ and the boundary condition $B(0) = 0$ yields

$$B = R_m y, \quad (2.12)$$

which is an approximate inner solution for B . The inner solution (2.12) and the outer solution (2.11) have the same value at $y = R_m^{-\frac{1}{2}}$, giving the patched solution

$$B \approx \begin{cases} R_m y & 0 \leq y \leq R_m^{-\frac{1}{2}} \\ 1/y & R_m^{-\frac{1}{2}} < y \leq 1 \end{cases} \quad \text{as } R_m \rightarrow \infty. \quad (2.13)$$

This implies that the inner region, where resistive effects are important, is $0 \leq y \leq R_m^{-\frac{1}{2}}$ and the outer region, where the advection process dominates, is $R_m^{-\frac{1}{2}} \leq y \leq 1$.

Note that for a current sheet of width ℓ the outward diffusion velocity is $1/(R_m \ell)$. If this is balanced by the inflow $v_y = -y$ then we must have

$$\frac{1}{\ell R_m} = \ell,$$

giving $\ell = R_m^{-\frac{1}{2}}$. This result for the current sheet width agrees with the analysis above.

Resistive Solution for the Magnetic Field

As shown in appendix D, equation (2.9) has the general solution

$$B = c_0 e^{-\frac{1}{2} R_m y^2} - k R_m y e^{-\frac{1}{2} R_m y^2} M\left(\frac{1}{2}, \frac{3}{2}, \frac{1}{2} R_m y^2\right), \quad (2.14)$$

where M is the confluent hypergeometric Kummer function. Applying the boundary conditions $B(0) = 0$ and $B(1) = 1$ gives

$$c_0 = 0, \quad k = -\frac{1}{R_m e^{-\frac{1}{2} R_m} M\left(\frac{1}{2}, \frac{3}{2}, \frac{1}{2} R_m\right)}, \quad (2.15)$$

and so

$$B = \frac{y e^{-\frac{1}{2} R_m y^2} M\left(\frac{1}{2}, \frac{3}{2}, \frac{1}{2} R_m y^2\right)}{e^{-\frac{1}{2} R_m} M\left(\frac{1}{2}, \frac{3}{2}, \frac{1}{2} R_m\right)}. \quad (2.16)$$

The asymptotic approximation

$$M(a, b, z) \rightarrow \frac{\Gamma(b)}{\Gamma(a)} e^z z^{a-b} \quad \text{as} \quad z \rightarrow \infty, \quad (2.17)$$

can be used on (2.16) to give

$$B \rightarrow R_m y e^{-\frac{1}{2} R_m y^2} M\left(\frac{1}{2}, \frac{3}{2}, \frac{1}{2} R_m y^2\right) \quad \text{as} \quad R_m \rightarrow \infty.$$

If $y \rightarrow 1$ then (2.17) can be used again to give $B \rightarrow 1/y$ whereas if $y \rightarrow 0$ then $M(a, b, z) \rightarrow 1$ as $z \rightarrow 0$ can be used to give $B \rightarrow R_m y$. This agrees with the patched solution (2.13).

Solution (2.16) gives the results plotted in figure 2.1. Figure 2.1a shows the magnetic field for several values of R_m and we can note that as R_m becomes large the solution contains a boundary layer at $y = 0$, outside which the field behaves like $1/y$. Figure 2.1b shows the current sheet width (taken to be twice the distance from the origin to the point maximum B) as a function of R_m . The gradient of the line in this figure is -0.5 , indicating that ℓ varies as $R_m^{-0.5}$, in agreement with the arguments of the previous section.

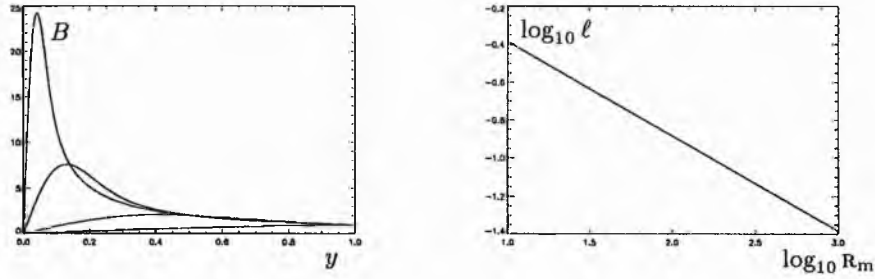


Figure 2.1: (a) Magnetic field profile for $R_m = 10^0, 10^1, 10^2, 10^3$ (b) Current sheet width as a function of R_m .

Reconnection Rates

The reconnection rate is given by $R_E = k$ and from (2.15) this becomes

$$R_E = \frac{1}{R_m e^{-\frac{1}{2} R_m} M\left(\frac{1}{2}, \frac{3}{2}, \frac{1}{2} R_m\right)}.$$

Using the asymptotic approximation (2.17) gives

$$R_E \rightarrow 1 \quad \text{as} \quad R_m \rightarrow \infty,$$

which indicates a fast reconnection process.

The ohmic heating rate is

$$R_\Omega = \frac{1}{R_m} \int_0^1 j^2 dy$$

and since $\mathbf{j} = -B' \hat{\mathbf{z}}$, this becomes

$$R_\Omega = \frac{1}{R_m} \int_0^1 (B')^2 dy.$$

Approximating B with the patched solution (2.13) this becomes

$$R_\Omega = R_\Omega^i + R_\Omega^o,$$

where

$$R_{\Omega}^i = \frac{1}{R_m} \int_0^{R_m^{-\frac{1}{2}}} R_m^2 dy = R_m^{\frac{1}{2}}$$

is the ohmic heating rate within the current sheet, and

$$R_{\Omega}^o = \frac{1}{R_m} \int_{R_m^{-\frac{1}{2}}}^1 \left(-\frac{1}{y^2} \right)^2 dy = \frac{1}{3} R_m^{\frac{1}{2}} - \frac{1}{3} R_m^{-1}$$

is the ohmic heating rate in the advection region. As R_m becomes large R_{Ω}^i and R_{Ω}^o are $R_m^{\frac{1}{2}}$ and $\frac{1}{3}R_m^{\frac{1}{2}}$ respectively, suggesting that the ohmic heating in the advection region is just as strong as in the current sheet and giving

$$R_{\Omega} \rightarrow \frac{4}{3} R_m^{\frac{1}{2}} \quad \text{as} \quad R_m \rightarrow \infty. \quad (2.18)$$

Solution (2.16) can be used to numerically calculate the reconnection and ohmic heating rates to give the results plotted in figure 2.2. Figure 2.2a shows that R_E tends to one as R_m increases. In figure 2.2b the gradient of the lines tends to 0.5, showing that R_{Ω}^i and R_{Ω}^o both vary as $R_m^{0.5}$. These results agree with the analytical results above.

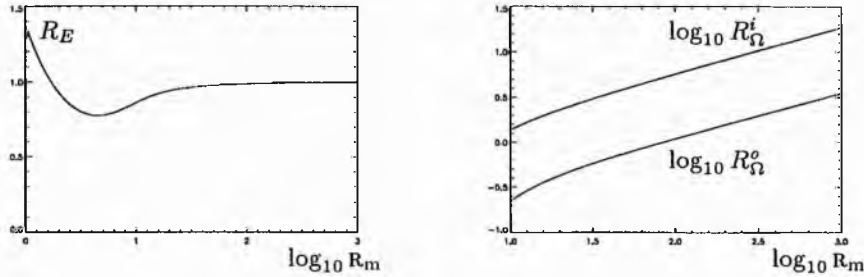


Figure 2.2: The reconnection and ohmic heating rates as a function of R_m .

From chapter 1, the reconnection rate R_{Ω} is related to the actual ohmic heating by

$$\Omega = \frac{B_0^2 v_0}{\mu_0 l_0} R_{\Omega}$$

where B_0 , v_0 and l_0 are the typical values for the field, velocity and length. Using (2.18) this becomes

$$\Omega \rightarrow \frac{4B_0^2 v_0}{3\mu_0 l_0} R_m^{\frac{1}{2}} \quad \text{as} \quad R_m \rightarrow \infty.$$

and with $B_0 = 0.05$ tesla (500 G), $l_0 = 10^7$ m, $v_0 = 10^5$ ms⁻¹ and $R_m = 10^6 \sim 10^{12}$ we find that $\Omega \approx 10^{25} \sim 10^{27}$ watts. Over 10^2 s around $10^{27} \sim 10^{29}$ joules of heat will be released. This is more than observed in a large solar flare but the model is highly idealised.

Note that the current sheet width varies as $R_m^{-\frac{1}{2}}$ and thus decreases as R_m becomes large. The MHD equations are only valid down to about 100 km (mean free path) or 10 km (ion gyroradius) and the current sheet width in this model will drop below these limits when R_m exceeds 10^4 .

The ohmic heating produced by this model increases with the magnetic Reynolds number. As the boundary conditions remain constant the question arises as to where all this energy is coming from?

The Effects of Advection

With the flow $\mathbf{v} = (x, -y, 0)$ plasma moves along the y -axis according to

$$\frac{dy}{dt} = -y,$$

and so the position of any point in the flow is given by

$$y = y_0 e^{-t}$$

where y_0 is the initial position. Thus, as shown in figure 2.3, a plasma element that initially lies between a and $a - \delta$ will, at time t , lie between ae^{-t} and $(a - \delta)e^{-t}$.

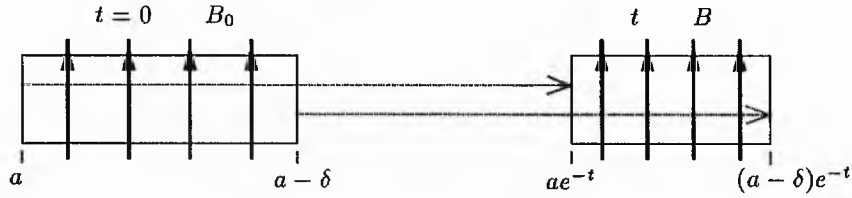


Figure 2.3: Movement of a plasma element along the y -axis.

The width of the plasma element, δe^{-t} , decreases with time and since the magnetic flux is conserved then the magnetic field within the plasma element must increase. If the field within the element at times t and $t = 0$ is B and B_0 then equating magnetic flux gives

$$B\delta e^{-t} = B_0\delta$$

and hence

$$B = B_0 e^t,$$

showing that the field increases exponentially with time. Since the field lines are being pushed together against the force of magnetic pressure, the flow has to do work on the plasma element. As the magnetic energy in the element,

$$E_M = \frac{1}{2} \int_{(a-\delta)e^{-t}}^{ae^{-t}} B^2 dy \approx \frac{1}{2} (B_0 e^t)^2 \delta e^{-t} = \frac{1}{2} B_0^2 e^t,$$

increases with time then at least some of this work is stored as magnetic energy.

Thus, in the advection region the magnetic field and magnetic energy are increasing because of the work done by the flow. Hence, in this model, the energy released through ohmic heating has its origin in whatever process is driving the flow. This process drives the flow, which builds up the magnetic field, which creates strong currents and gives strong ohmic heating. As R_m becomes larger the extent of the advection region increases allowing more work to be done, which explains the increase in ohmic heating with R_m .

The Even Solution

The even solution from (2.14) is

$$B = -kR_m e^{-\frac{1}{2}R_m y^2}$$

and applying the boundary condition $B(1) = 1$ gives

$$B = e^{\frac{1}{2}R_m} e^{-\frac{1}{2}R_m y^2}. \quad (2.19)$$

Note that

1. as R_m increases, the flux sheet width decreases and the maximum value of the magnetic field rises, and
2. although there is no reconnection occurring there are still magnetic gradients giving current and ohmic heating.

The magnetic field (2.19) does not give rise to any electric field and R_E is thus zero, reflecting the fact that no reconnection is taking place. As

$$j = B' = -R_m y e^{\frac{1}{2}R_m} e^{-\frac{1}{2}R_m y^2}$$

the ohmic heating rate is

$$R_\Omega = \frac{1}{R_m} \int_0^1 j^2 dy = R_m e^{R_m} \int_0^1 y^2 e^{-R_m y^2} dy.$$

As shown in appendix H, the integral tends to $\frac{1}{2}R_m^{-\frac{3}{2}}$ as $R_m \rightarrow \infty$ and so

$$R_\Omega \rightarrow \frac{1}{2} R_m^{-\frac{1}{2}} e^{R_m} \quad \text{as} \quad R_m \rightarrow \infty.$$

This is a very fast ohmic heating rate.

2.3 Jardine Case

The set of equations

$$\psi = x f(y),$$

$$\frac{1}{R_m} B' + f B = -k, \quad (2.20)$$

$$\frac{1}{R} f^{(4)} + f f''' - f' f'' = 0, \quad (2.21)$$

has been dealt with by several authors. In particular, Jardine *et al* (1992) solve equation (2.21) by asymptotic means and find some unusual "cellular" flows where the direction of v_y changes along the y -axis. In this section we follow the same analysis but use slightly different boundary conditions and find that cellular flows do not occur.

Equation (2.21) is fourth-order and will be solved subject to the four boundary conditions

$$f(0) = 0, \quad f''(0) = 0, \quad f(1) = 1 \quad \text{and} \quad f'(1) = u_b. \quad (2.22)$$

As $\mathbf{v} = (x f', -f, 0)$ and $\omega = -x f'' \hat{z}$, the first of these boundary conditions comes from requiring v_y to be an odd function (so that only the region $0 \leq y \leq 1$ has to be considered), the second from requiring that there is no vorticity on $y = 0$, the third comes from non-dimensionalisation and the fourth is a boundary condition for v_x on $y = 1$.

Solution

Looking for asymptotic solutions of the form

$$f = f_0 + \frac{1}{R} f_1 \dots$$

equation (2.21) leads to the zero-order equation

$$f_0 f_0''' - f_0' f_0'' = 0 \quad (2.23)$$

and first-order equation

$$f_0^{(4)} + f_0 f_1''' + f_1 f_0''' - f_0' f_1'' - f_1' f_0'' = 0. \quad (2.24)$$

Equation (2.23) can be solved to give f_0 , which then allows equation (2.24) to be solved for f_1 .

Boundary Conditions on f_0 and f_1

The boundary conditions (2.22) are applied to the zero-order solution and homogeneous boundary conditions applied to all other orders, ie

$$f_0(0) = f_0''(0) = 0, \quad f_0(1) = 1, \quad f_0'(1) = u_b \quad (2.25)$$

and

$$f_1(0) = f_1''(0) = f_1(1) = f_1'(1) = 0. \quad (2.26)$$

Note that the equation for f_0 , (2.23), is third-order and the solution will contain three arbitrary constants. Normally it would be impossible to satisfy all four boundary conditions in (2.25) but here, because of the nature of equation (2.23), satisfying $f_0(0) = 0$ automatically gives $f_0''(0) = 0$. Hence only the three boundary conditions $f_0(0) = 0$, $f_0(1) = 1$ and $f_0'(1) = u_b$ have to be considered.

Likewise, the solution for f_1 contains three arbitrary constants but, due to the nature of equation (2.24), satisfying $f_1(0) = 0$ automatically gives $f_1''(0) = 0$ and so all four boundary conditions in (2.26) can be satisfied.

This is an unusual feature of the problem but quite a useful one - normally the asymptotic solution would only be able to satisfy the outer boundary conditions, necessitating the calculation of an inner solution satisfying the inner boundary conditions and matching the two to give a composite solution. Here we are spared the extra work as the asymptotic solution satisfies both inner and outer boundary conditions.

The Zero-Order Equation

Dividing the zero-order equation, (2.23), by f_0^2 produces

$$\frac{d}{dy} \left(\frac{f_0''}{f_0} \right) = 0,$$

which can be integrated to give

$$f_0'' - m f_0 = 0, \quad (2.27)$$

where m is an arbitrary constant. This equation has three distinct cases, depending on the sign of m , and gives the solution

$$f_0 = \begin{cases} a_0 y + b_0 & m = 0 \\ a_0 \sinh \lambda y + b_0 \cosh \lambda y & m > 0, \quad m = \lambda^2 \\ a_0 \sin \mu y + b_0 \cos \mu y & m < 0, \quad m = -\mu^2. \end{cases}$$

Since both the positive and negative square roots of m are incorporated into the solution, λ and μ can be taken to be positive without any loss of generality.

Applying the boundary conditions $f_0(0) = 0$ and $f_0(1) = 1$ determines a_0 and b_0 and gives

$$f_0 = \begin{cases} y & m = 0 \\ \frac{\sinh \lambda y}{\sinh \lambda} & m > 0, \quad m = \lambda^2 \\ \frac{\sin \mu y}{\sin \mu} & m < 0, \quad m = -\mu^2. \end{cases}$$

Note that the $m = 0$ case is the Sonnerup and Priest solution. The third boundary condition, $f_0'(1) = u_b$, will now determine the last arbitrary constant, m . With the above solution for f_0 ,

$$f_0'(1) = \begin{cases} 1 & m = 0 \\ \frac{\lambda}{\tanh \lambda} & m > 0, \quad m = \lambda^2 \\ \frac{\mu}{\tan \mu} & m < 0, \quad m = -\mu^2, \end{cases}$$

which is plotted in figure 2.4a as a function of m . The graph has multiple branches and so the boundary condition $f'_0(1) = u_b$ can be satisfied by multiple values of m ; m is not determined uniquely. However, if we argue that some particular value of u_b has to give a stagnation-point flow (where $m = 0$) then this is only possible on the branch lying between $-\pi^2 < m < \infty$ and gives the unique solution

$$m = \begin{cases} \lambda^2 & u_b > 1, \quad \lambda / \tanh \lambda = u_b, \quad \lambda > 0 \\ 0 & u_b = 1 \\ \mu^2 & u_b < 1, \quad \mu / \tan \mu = u_b, \quad 0 < \mu < \pi. \end{cases}$$

The solution for f_0 is thus

$$f_0 = \begin{cases} \frac{\sinh \lambda y}{\sinh \lambda} & u_b > 1, \quad \lambda / \tanh \lambda = u_b, \quad \lambda > 0 \\ y & u_b = 1 \\ \frac{\sin \mu y}{\sin \mu} & u_b < 1, \quad \mu / \tan \mu = u_b, \quad 0 < \mu < \pi. \end{cases} \quad (2.28)$$

Note that since μ is restricted to lie between zero and π then f_0 is always positive on the range $0 \leq y \leq 1$. This implies that v_y is always negative and, as the flow is always towards the x -axis, there can be no cellular flows. Figure 2.4b shows the above solution for several values of u_b .

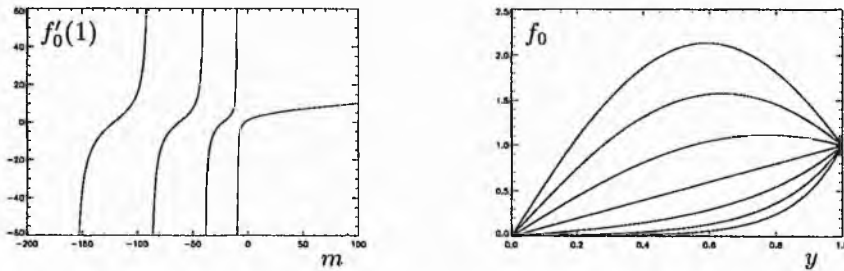


Figure 2.4: (a) $f'_0(1)$ as a function of m , (b) solutions for f_0 for various values of u_b .

Magnetic Field

For f of the form $f = f_0 + f_1/R \dots$ equation (2.20) becomes

$$\frac{1}{R_m} B' + \left(f_0 + \frac{1}{R} f_1 \dots \right) B = -k$$

and assuming that $R \gg R_m$ this reduces to

$$B' + R_m f_0 B = -R_m k.$$

The solution for f_0 in (2.28) is slightly involved so the above equation is best solved by means of an integrating factor to obtain

$$B = -k R_m e^{-R_m \int_0^y f(\xi) d\xi} \int_0^y e^{R_m \int_0^\xi f(\xi_0) d\xi_0} d\xi + c_0 e^{-R_m \int_0^y f(\xi) d\xi}.$$

Applying the boundary conditions $B(0) = 0$, $B(1) = 1$ gives

$$B = \frac{e^{-R_m \int_0^y f(\xi) d\xi} \int_0^y e^{R_m \int_0^\xi f(\xi_0) d\xi_0} d\xi}{e^{-R_m \int_0^1 f(\xi) d\xi} \int_0^1 e^{R_m \int_0^\xi f(\xi_0) d\xi_0} d\xi}. \quad (2.29)$$

This solution is straightforward to evaluate using numerical integration routines. Figure 2.5 shows the magnetic field for several values of u_b with $R_m = 10^2$. It is found that as R_m increases, the maximum

value of the magnetic field increases, irrespective of the value of u_b . The magnetic energy is thus being increased by advection in a similar manner to the Sonnerup and Priest case. The reconnection and ohmic heating rates shown in figure 2.5b and c, also behave in the same way as the Sonnerup and Priest case with R_E tending to one and R_Ω scaling as $R_m^{-\frac{1}{2}}$.

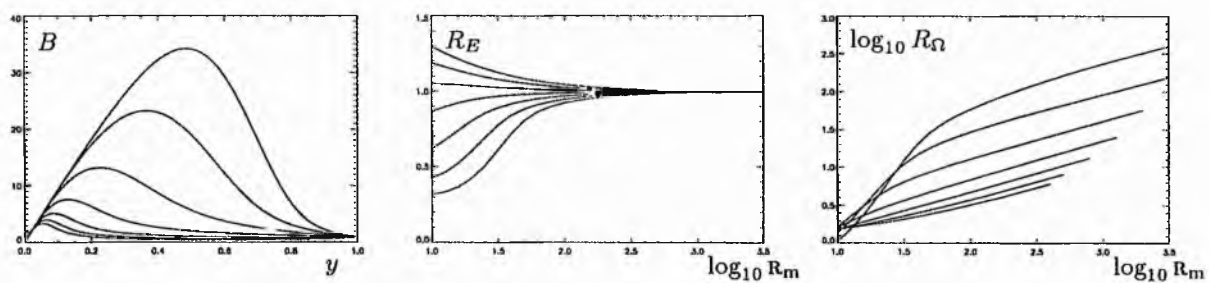


Figure 2.5: With $u_b = -5$ to 7 in steps of 2 (a) the solution for B , (b) the reconnection rate R_E and (c) ohmic heating rate R_Ω .

Chapter 3

Time-Dependent Magnetic Annihilation

3.1 Introduction

In this section the equations describing two-dimensional, time-dependent, magnetic annihilation models are derived from the time-dependent MHD equations.

Equations

The dimensionless, time-dependent, resistive, viscous MHD equations for an incompressible plasma are

$$\begin{aligned}M_A^2 \left[\frac{\partial \mathbf{v}}{\partial t} + (\mathbf{v} \cdot \nabla) \mathbf{v} \right] &= -\beta \nabla p + \mathbf{j} \times \mathbf{B} + \frac{M_A^2}{R} \nabla^2 \mathbf{v}, \\ \mathbf{E} + \mathbf{v} \times \mathbf{B} &= \frac{1}{R_m} \mathbf{j}, \\ \nabla \times \mathbf{E} &= -\frac{\partial \mathbf{B}}{\partial t}, \\ \nabla \cdot \mathbf{B} &= 0, \\ \nabla \cdot \mathbf{v} &= 0, \\ \mathbf{j} &= \nabla \times \mathbf{B}.\end{aligned}$$

Assumptions

Assuming that the field lines are straight simplifies the equation of motion as the non-linear magnetic tension term drops out. If the field lines are taken to be parallel to the x -axis then $\nabla \cdot \mathbf{B} = 0$ implies that they must be of the form

$$\mathbf{B} = (B(y, t), 0, 0). \quad (3.1)$$

Assuming that the flow is two-dimensional, then $\nabla \cdot \mathbf{v} = 0$ implies that it has the form

$$\mathbf{v} = \nabla \times \psi(x, y, t) \hat{\mathbf{z}} = (\psi_y, -\psi_x, 0). \quad (3.2)$$

Faraday's Law

The components of Faraday's Law are

$$\partial_y E_z = -\partial_t B \quad (3.3)$$

$$\begin{aligned}\partial_x E_z &= 0 \\ \partial_x E_y - \partial_y E_x &= 0\end{aligned}\quad (3.4)$$

The second of these implies that E_z is not a function of x .

Ohm's Law

With \mathbf{B} and \mathbf{v} of the forms (3.1) and (3.2) the components of Ohm's law are

$$\begin{aligned}E_x &= 0, \\ E_y &= 0, \\ E_z + \psi_x B &= -\frac{1}{R_m} B_y.\end{aligned}\quad (3.5)$$

The first two of these determine E_x and E_y , which now satisfy (3.4). Since B and E_z are not functions of x , the third equation can only be consistent if

$$\psi_x = f(y, t),$$

implying that

$$\psi = x f(y, t) + g(y, t) \quad (3.6)$$

and reducing (3.5) to

$$E_z + f B = -\frac{1}{R_m} B_y.$$

Differentiating this with respect to y and using (3.3) yields

$$\frac{1}{R_m} B_{yy} + f B_y + f_y B = B_t.$$

The Equation of Motion

As the field lines are straight the equation of motion reduces to

$$M_A^2 \left[\frac{\partial \mathbf{v}}{\partial t} + (\mathbf{v} \cdot \nabla) \mathbf{v} \right] = -\nabla \left(\beta \nabla p + \frac{1}{2} B^2 \right) + \frac{M_A^2}{R} \nabla^2 \mathbf{v}.$$

The pressure terms can be eliminated by taking the curl of this (see appendix A) to produce

$$\frac{\partial \omega}{\partial t} + (\mathbf{v} \cdot \nabla) \omega - (\omega \cdot \nabla) \mathbf{v} = \frac{1}{R} \nabla^2 \omega$$

where $\omega = \nabla \times \mathbf{v}$ is the vorticity. Since the model is two-dimensional $\omega = \omega \hat{z}$ and this simplifies to

$$\frac{\partial \omega}{\partial t} + (\mathbf{v} \cdot \nabla) \omega = \frac{1}{R} \nabla^2 \omega.$$

Substituting \mathbf{v} of the form (3.2) into this equation gives

$$\partial_t (\psi_{xx} + \psi_{yy}) + (\psi_y \partial_x - \psi_x \partial_y) (\psi_{xx} + \psi_{yy}) = \frac{1}{R} (\partial_x^2 + \partial_y^2) (\psi_{xx} + \psi_{yy})$$

and with ψ of the form (3.6) this becomes

$$\partial_t (x f_{yy} + g_{yy}) + ((x f_y + g_y) \partial_x - f \partial_y) (x f_{yy} + g_{yy}) = \frac{1}{R} (\partial_x^2 + \partial_y^2) (x f_{yy} + g_{yy})$$

or

$$x \left(\frac{1}{R} f_{yyy} + f f_{yy} - f_y f_{yy} - f_{yyt} \right) + \frac{1}{R} g_{yyy} + f g_{yy} - g_y f_{yy} - g_{yyt} = 0.$$

Since f and g are not functions of x , this will only be consistent if

$$\frac{1}{R} f_{yyy} + f f_{yy} - f_y f_{yy} - f_{yyt} = 0$$

leaving

$$\frac{1}{R} g_{yyy} + f g_{yy} - g_y f_{yy} - g_{yyt} = 0.$$

Summary

For two-dimensional time-dependent magnetic annihilation models where

$$\mathbf{B} = (B(y, t), 0, 0) \quad \text{and} \quad \mathbf{v} = \nabla \times \psi(x, y, t) \hat{\mathbf{z}} = (\psi_y, -\psi_x, 0),$$

the MHD equations are satisfied if

$$\begin{aligned} \psi &= xf(y, t) + g(y, t), \\ \frac{1}{R_m} B_{yy} + f B_y + f_y B &= B_t, \\ \frac{1}{R} f_{yyy} + f f_{yy} - f_y f_{yy} - f_{yyt} &= 0, \\ \frac{1}{R} g_{yyy} + f g_{yy} - f_{yy} g_y - g_{yyt} &= 0. \end{aligned} \tag{3.7}$$

Simple Solutions

Since g does not influence the magnetic field only the solution $g = 0$ of equation (3.8) will be considered. Equation (3.7) has the simple solution $f_{yy} = 0$, implying that $f = v(t)y + w(t)$, where $v(t)$ and $w(t)$ are arbitrary functions determined by the boundary conditions. Taking $w(t) = 0$, the set of equations in the summary reduce to

$$\psi = v(t)xy \quad \text{and} \quad \frac{1}{R_m} B_{yy} + v(t)y B_y + v(t)B = B_t.$$

These are the equations considered in the rest of this chapter. Note that with $\psi = v(t)xy$ the plasma flow will be $\mathbf{v} = v(t)(x, -y, 0)$, which is a time-modulated stagnation-point flow.

3.2 Solution on an Infinite Interval

Introduction

In this section magnetic annihilation on an infinite interval is examined. This is slightly simpler than a finite interval as the boundary conditions are easier. The problem may be expressed as

$$\frac{1}{R_m} B_{yy} + v(t)y B_y + v(t)B = B_t \quad -\infty < y < \infty \quad 0 \leq t < \infty \tag{3.9}$$

$$B(y, 0) = B_0(y) \quad -\infty < y < \infty, \tag{3.10}$$

where $B_0(y)$ is an initial condition and $v(t)$ is a prescribed function.

Simplifying the Equation for B

Equation (3.9) is already in canonical form but the term involving $y B_y$ can be eliminated by a change of variable. Changing from y, t to $\gamma(y, t), \tau(y, t)$ the equation becomes

$$\frac{1}{R_m} (\gamma_{yy} B_\gamma + \tau y B_\tau + \gamma_y^2 B_{\gamma\gamma} + 2\gamma_y \tau_y B_{\gamma\tau} + \tau_y^2 B_{\tau\tau}) + v y (\gamma_y B_\gamma + \tau_y B_\tau) + v B = \gamma_t B_\gamma + \tau_t B_\tau$$

or

$$\frac{1}{R_m} (\gamma_y^2 B_{\gamma\gamma} + 2\gamma_y \tau_y B_{\gamma\tau} + \tau_y^2 B_{\tau\tau}) + B_\gamma \left(\frac{\gamma_{yy}}{R_m} + v y \gamma_y - \gamma_t \right) + B_\tau \left(\frac{\tau_{yy}}{R_m} + v y \tau_y - \tau_t \right) + v B = 0.$$

If $\tau = \tau(t)$ and $\gamma(y, t) = yg(t)$ then this reduces to

$$\frac{1}{R_m} g^2 B_{\gamma\gamma} + y B_\gamma (vg - \dot{g}) - \dot{\tau} B_\tau + v B = 0.$$

Choosing g and τ to satisfy $vg - \dot{g} = 0$ and $\dot{\tau} = g^2$ reduces this even further to

$$\frac{1}{R_m} B_{\gamma\gamma} - B_\tau + \frac{v}{g^2} B = 0. \quad (3.11)$$

Since v/g^2 can be regarded as a function of τ this equation is separable and is thus easier to deal with than the original, (3.9).

Note that for a given $v(t)$, the new variables are $\gamma = yg(t)$ and $\tau(t)$ where

$$\frac{dg}{dt} = vg \quad (3.12)$$

and

$$\frac{d\tau}{dt} = g^2. \quad (3.13)$$

For convenience, suppose initial conditions of $g(0) = 1$ and $\tau(0) = 0$ so that initially $\tau = 0$, $\gamma = y$ and the initial condition (3.10) becomes

$$B(\gamma, \tau = 0) = B_0(\gamma). \quad (3.14)$$

Solving for B

Equation (3.11) and initial condition (3.14) form a problem very similar to that of solving the heat equation on an infinite interval. Many of the techniques developed to solve the heat equation can also be used here. Following Chester (1971), looking for solutions to equation (3.11) of the form $B(y, t) = Y(y)T(t)$ leads to

$$\frac{Y''}{R_m Y} - \frac{\dot{T}}{T} + \frac{v}{g^2} = 0,$$

which implies that

$$\frac{Y''}{R_m Y} = \lambda \quad \text{and} \quad \frac{\dot{T}}{T} - \frac{v}{g^2} = \lambda, \quad (3.15)$$

where λ is an arbitrary constant.

The equation for T can be integrated to give

$$\log T - \int \frac{v}{g^2} d\tau = \lambda t.$$

Using equation (3.13) this becomes

$$\log T - \int v dt = \lambda t$$

and using equation (3.12) gives

$$\log T - \int \frac{1}{g} dg = \lambda t.$$

Hence

$$T = g e^{\lambda \tau}.$$

The equation for Y in (3.15) has the solutions

$$Y = e^{\pm \sqrt{\lambda R_m} \gamma}.$$

Assuming that the initial magnetic field is not growing exponentially with γ implies that λ is not positive and so $\lambda = -\mu^2$, giving

$$Y = e^{\pm i\mu R_m^{\frac{1}{2}} \gamma}.$$

Allowing μ to take on all real values from $-\infty$ to ∞ , the solution $e^{i\mu R_m^{\frac{1}{2}} \gamma}$ is sufficient and it is not necessary to consider $e^{-i\mu R_m^{\frac{1}{2}} \gamma}$.

Putting together the solutions for Y and T , we find that a solution for B is

$$B(\gamma, \tau) = g e^{-\mu^2 \tau + i \mu R_m^{\frac{1}{2}} \gamma}.$$

Since equation (3.11) is linear, these solutions can be superimposed to give the more general solution

$$B(\gamma, \tau) = g \int_{-\infty}^{+\infty} b(\mu) e^{-\mu^2 \tau + i \mu R_m^{\frac{1}{2}} \gamma} d\mu \quad (3.16)$$

where b is an arbitrary function of μ . Satisfying the initial condition (3.14) requires that

$$\int_{-\infty}^{+\infty} b(\mu) e^{i \mu R_m^{\frac{1}{2}} \gamma} d\mu = B_0(\gamma)$$

and, after the simple transformation $\bar{\mu} = R_m^{\frac{1}{2}} \mu$ to obtain

$$\int_{-\infty}^{+\infty} b(\bar{\mu}) e^{i \bar{\mu} \gamma} d\bar{\mu} = R_m^{\frac{1}{2}} B_0(\gamma),$$

the Fourier inversion formula can be used to give

$$b(\bar{\mu}) = \frac{R_m^{\frac{1}{2}}}{2\pi} \int_{-\infty}^{+\infty} B_0(\xi) e^{-i \bar{\mu} \xi} d\xi$$

or

$$b(\mu) = \frac{R_m^{\frac{1}{2}}}{2\pi} \int_{-\infty}^{+\infty} B_0(\xi) e^{-i \mu R_m^{\frac{1}{2}} \xi} d\xi.$$

Substituting this into (3.16) gives

$$B(\gamma, \tau) = \frac{g R_m^{\frac{1}{2}}}{2\pi} \int_{-\infty}^{+\infty} \int_{-\infty}^{+\infty} B_0(\xi) e^{-\mu^2 \tau - i \mu R_m^{\frac{1}{2}} (\xi - \gamma)} d\xi d\mu.$$

Since μ occurs only in the exponential the integral over μ can be evaluated. To do this first complete the square in the exponent by writing

$$-\mu^2 \tau - i \mu R_m^{\frac{1}{2}} (\xi - \gamma) = - \left[\mu \tau^{\frac{1}{2}} + i \mu R_m^{\frac{1}{2}} \frac{\xi - \gamma}{2\tau^{\frac{1}{2}}} \right]^2 - \frac{R_m (\xi - \gamma)^2}{4\tau}$$

so that

$$B(\gamma, \tau) = \frac{g R_m^{\frac{1}{2}}}{2\pi} \int_{-\infty}^{+\infty} B_0(\xi) e^{-R_m \frac{(\xi - \gamma)^2}{4\tau}} d\xi \int_{-\infty}^{+\infty} e^{- \left[\mu \tau^{\frac{1}{2}} - R_m^{\frac{1}{2}} \frac{i(\xi - \gamma)}{2\tau^{\frac{1}{2}}} \right]^2} d\mu. \quad (3.17)$$

In the integral

$$I = \int_{-\infty}^{+\infty} e^{- \left[\mu \tau^{\frac{1}{2}} - R_m^{\frac{1}{2}} \frac{i(\xi - \gamma)}{2\tau^{\frac{1}{2}}} \right]^2} d\mu$$

let

$$z = \mu \tau^{\frac{1}{2}} - R_m^{\frac{1}{2}} \frac{i(\xi - \gamma)}{2\tau^{\frac{1}{2}}}$$

to obtain

$$I = \tau^{-\frac{1}{2}} \int_{-\infty + i\epsilon}^{\infty + i\epsilon} e^{-z^2} dz,$$

where $\epsilon = R_m^{\frac{1}{2}} (\xi - \gamma) / (2\tau^{\frac{1}{2}})$. Since the integrand is analytic and tends to zero as $|Re z| \rightarrow \infty$ the integration path can be moved back to the real axis to obtain

$$I = \tau^{-\frac{1}{2}} \int_{-\infty}^{+\infty} e^{-z^2} dz = \pi^{\frac{1}{2}} \tau^{-\frac{1}{2}}.$$

Equation (3.17) thus becomes

$$B(\gamma, \tau) = \frac{gR_m^{\frac{1}{2}}}{2\tau^{\frac{1}{2}}\pi^{\frac{1}{2}}} \int_{-\infty}^{+\infty} B_0(\xi) e^{-R_m \frac{(\xi-\gamma)^2}{4\tau}} d\xi. \quad (3.18)$$

To show more clearly that this tends to the initial state as $\tau \rightarrow 0$, a change of variables, from ξ to $\epsilon = R_m^{\frac{1}{2}}(\xi - \gamma)/(2\sqrt{\tau})$ can be made, to give

$$B(\gamma, \tau) = \frac{g}{\pi^{\frac{1}{2}}} \int_{-\infty}^{+\infty} B_0\left(\gamma + 2\epsilon\tau^{\frac{1}{2}}R_m^{-\frac{1}{2}}\right) e^{-\epsilon^2} d\epsilon,$$

which at $\tau = t = 0$ is

$$B(\gamma, 0) = \frac{g(0)}{\pi^{\frac{1}{2}}} B_0(\gamma) \int_{-\infty}^{\infty} e^{-\epsilon^2} d\epsilon.$$

Since $g(0) = 1$ and the integral evaluates to $\pi^{\frac{1}{2}}$ this reduces to $B(\gamma, 0) = B_0(\gamma)$ or $B(y, 0) = B_0(y)$, as required.

Solution (3.18) is exact, analytical, and gives the time-evolution of an initial magnetic field B_0 under any time-modulated stagnation-point flow.

Diffusion and Advection Regions

The solution (3.18) is difficult to analyse due to its integral form, but it can be approximated under some circumstances.

The major contribution to the integral in equation (3.18) comes from near the point $\xi = \gamma$ where the exponent is close to zero. Changing from ξ to $\epsilon = \xi/\gamma$ gives

$$B(\gamma, \tau) = \frac{gR_m^{\frac{1}{2}}\gamma}{2\pi^{\frac{1}{2}}\tau^{\frac{1}{2}}} \int_{-\infty}^{+\infty} B_0(\gamma\epsilon) e^{-\frac{\gamma^2}{4\tau}(\epsilon-1)^2} d\epsilon.$$

If $\gamma^2/(4\tau)$ is large, ie if $\gamma^2 > 4\tau$ or, since $\gamma = yg$, if

$$y^2 > \frac{4\tau}{g^2}, \quad (3.19)$$

then Laplace's method (which says that

$$\int_a^b g(t) e^{-xh(t)} dt \approx \left[\frac{2\pi}{h''(c)x} \right]^{\frac{1}{2}} g(c) e^{-xh(c)}$$

where x is large and $h(t)$ has a turning point at $t = c$) can be used to obtain

$$B(y, t) \approx g B_0(\gamma). \quad (3.20)$$

Note that if the diffusion term in the original equation for B , (3.9), is considered to be negligible, then solving the resulting first-order partial differential equation by the method of characteristics and applying the initial condition $B(y, 0) = B_0(y)$ gives

$$B = e^{\int v(t) dt} B_0 \left(y e^{\int v(t) dt} \right) = g B_0(\gamma).$$

This is the same as (3.20) and hence (3.19) splits the infinite interval into two regions, one in which diffusion is negligible and advection determines the magnetic field according to (3.20), and the other in which diffusion is important.

Reconnection Rate

The current is given by $j = -\partial_y B$ and differentiating (3.18) with respect to y gives

$$j = \frac{g^2 R_m^{\frac{3}{2}}}{4\pi^{\frac{1}{2}} \tau^{\frac{3}{2}}} \int_{-\infty}^{+\infty} B_0(\xi) (\xi - yg) e^{-R_m \frac{(\xi - yg)^2}{4\tau}} d\xi.$$

Since the magnetic field is zero on $y = 0$, the reconnection rate $R_E = j_{np}/R_m$ is

$$R_E = \frac{g^2 R_m^{\frac{1}{2}}}{4\pi^{\frac{1}{2}} \tau^{\frac{3}{2}}} \int_{-\infty}^{+\infty} B_0(\xi) \xi e^{-R_m \frac{\xi^2}{4\tau}} d\xi.$$

and integrating by parts gives

$$R_E = \frac{g^2}{2R_m^{\frac{1}{2}} \pi^{\frac{1}{2}} \tau^{\frac{1}{2}}} \int_{-\infty}^{+\infty} B'_0(\xi) e^{-R_m \frac{\xi^2}{4\tau}} d\xi.$$

If $R_m/(4\tau)$ is large then the integral can be approximated by Laplace's method to obtain

$$R_E = R_m^{-1} g^2 B'_0(0),$$

which is a slow reconnection rate. However, this result is not valid when τ is large.

Steady Flow

For the case of steady flow where $v(t) = \text{constant} = 1$, equations (3.12) and (3.13) with the boundary conditions $g(0) = 1$, $\tau(0) = 0$ have solutions

$$g = e^t \quad \text{and} \quad \tau = \frac{1}{2} (e^{2t} - 1).$$

Using these in (3.19) and (3.20) we find that the advection region is given by

$$y^2 > 2(1 - e^{-2t}) \quad (3.21)$$

and the magnetic field in the advection region is

$$B = e^t B_0(ye^t). \quad (3.22)$$

The first of these, (3.21), implies that in the limit of large t , the diffusion region is $y < \sqrt{2}$ and thus diffusion effects are confined to a small layer near $y = 0$. In the second, (3.22), supposing that $B_0 \sim y^{-n}$ as $y \rightarrow \infty$ gives

$$B = y^{-n} e^{(1-n)t}.$$

This is a curious result as it implies that if $n < 1$ advection causes the field to decay exponentially in time, if $n > 1$ advection causes the field to increase exponentially in time and if $n = 1$ the advected field does not change in time. In particular, the exponential increase of field will build up large magnetic gradients giving rise to large ohmic heating rates.

Investigating the General Solution

In this section the three initial conditions

$$B_0 = \frac{y}{1+y^2}, \quad B_0 = \frac{y}{1+y^{2.1}} \quad \text{and} \quad B_0 = \frac{y}{1+y^{1.9}}$$

are examined to determine their effect on the reconnection rates. Close to the origin all these initial conditions behave like y while further away from the origin they behave like y^{-1} , $y^{-1.1}$ and $y^{-0.9}$.

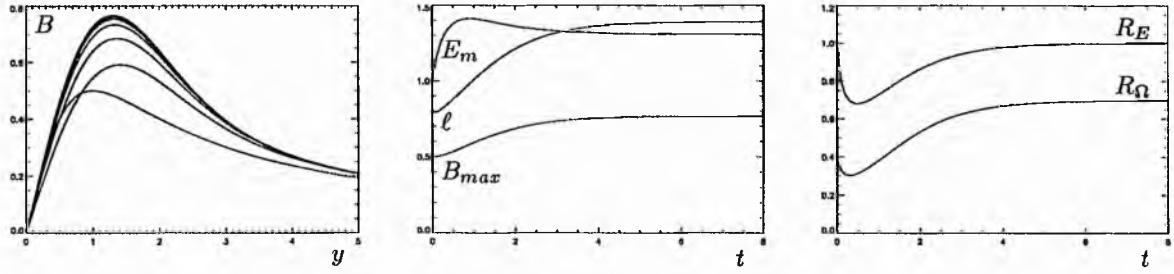


Figure 3.1: For the initial condition $B_0 = y/(1 + y^2)$ (a) The magnetic field (b) some characteristics of the magnetic field, and (c) the reconnection and ohmic heating rates.

With $B_0 = y/(1 + y^2)$ and $R_m = 1$ the solution (3.18) is evaluated numerically and gives the results plotted in figure 3.1. Figure 3.1a shows the magnetic field at several times, figure 3.1b shows the peak magnetic field, the current sheet width and the magnetic energy of the evolving magnetic field as functions of time and figure 3.1c shows the reconnection and ohmic heating rates as functions of time. From these results it is apparent that a steady state is reached.

Figure 3.2 shows results for the initial condition $B_0 = y/(1 + y^{2.1})$ with $R_m = 1$. As suggested in the previous section the magnetic field in the advection region decays away, decreasing the current within the diffusion region and the reconnection rate. Note that the current sheet width remains constant for large t , as expected.

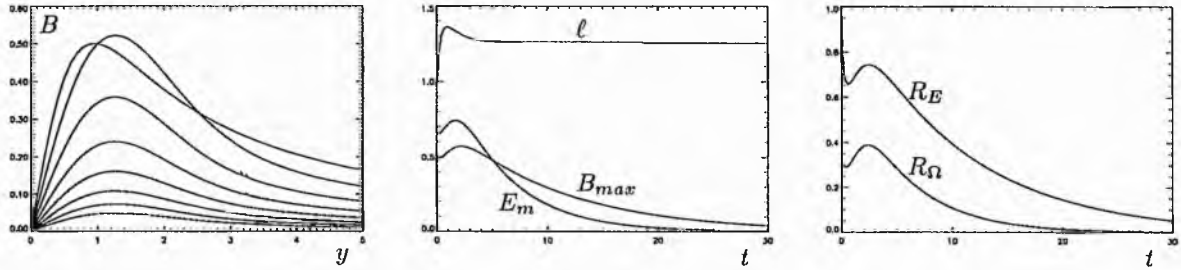


Figure 3.2: For the initial condition $B_0 = y/(1 + y^{2.1})$ (a) The magnetic field (b) some properties of the magnetic field, and (c) the reconnection and ohmic heating rate.

Figure 3.3 shows results for the initial condition $B_0 = y/(1 + y^{1.9})$ with $R_m = 1$. As expected, the magnetic field in the advection region increases rapidly, building up large gradients within the diffusion region and increasing the reconnection and ohmic heating rates. Note that the current sheet width again remains approximately constant.

Plasma Flow and Advection

As shown above, advection of the initial magnetic field leads to a variety of effects and it is necessary to determine why this is happening. During magnetic advection the frozen-in condition applies and the magnetic flux in any element of plasma is conserved. If $\mathbf{v} = (x, -y, 0)$ then plasma moves along the y -axis according to $dy/dt = -y$ and its position is thus $y = y_0 e^{-t}$ where y_0 is its initial position. Hence, as shown in figure 3.4, a plasma element which at a time t_0 lies between $y = a$ and $y = a + \delta$, will at time $t = 0$ have been lying between $y = a e^{t_0}$ and $y = (a + \delta) e^{t_0}$.

If the magnetic field in the element at $t = 0$ is $1/y^n$ and at time t is B , then conservation of flux

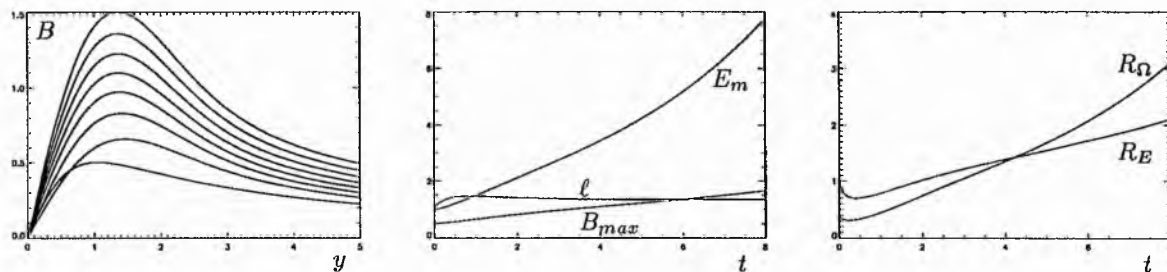


Figure 3.3: For the initial condition $B_0 = y/(1 + y^{1.9})$ (a) The magnetic field (b) some properties of the magnetic field, and (c) the reconnection and ohmic heating rates.

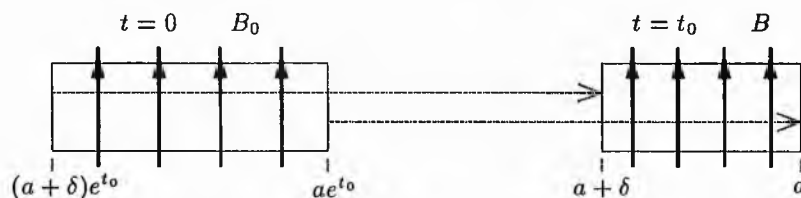


Figure 3.4: Movement of a plasma element along the y -axis.

gives

$$B\delta = \frac{1}{(ae^t)^n} \delta e^t \quad (3.23)$$

or

$$B = \frac{1}{a^n} e^{(1-n)t},$$

showing that the behaviour of the advected field depends on the value of n .

Physically, equation (3.23) is showing that

1. due to the initial condition, the magnetic field passing through $y = a$ is falling off as e^{-nt} , and
2. due to the plasma flow, the flux element in which the magnetic field lies is being "compressed" (the field lines being piled together) by a factor of e^t .

Depending on the value of n , these two effects will either balance or one will dominate the other.

If the field is increasing then the magnetic energy within the plasma element is also increasing. This energy increase comes from work done on the element by the flow. This implies that the energy released by reconnection is derived from whatever process is driving the flow as well as the initial magnetic field.

3.3 Finite Interval with a Steady Plasma Flow

Introduction

In this section it is assumed that $v(t) = 1$ and we examine magnetic annihilation in a finite interval of space, $-1 \leq y \leq 1$, with prescribed boundary and initial conditions. As the magnetic field is assumed to be an odd function, only the range $0 \leq y \leq 1$ need be considered and the lower boundary condition taken to be $B(0, t) = 0$. This problem is then

$$\frac{1}{R_m} B_{yy} + y B_y + B = B_t \quad 0 \leq y \leq 1 \quad 0 \leq t < \infty, \quad (3.24)$$

with initial condition

$$B(y, 0) = B_0(y) \quad 0 \leq y \leq 1 \quad (3.25)$$

and boundary conditions

$$B(0, t) = 0, \quad B(1, t) = B_b(t). \quad (3.26)$$

As equation (3.24) is linear, this problem can be split into two parts, namely an initial condition problem, in which equation (3.24) is solved subject to

$$B(y, 0) = B_0(y), \quad B(0, t) = 0, \quad B(1, t) = 0$$

and a boundary condition problem, in which equation (3.24) is solved subject to

$$B(y, 0) = 0, \quad B(0, t) = 0, \quad B(1, t) = B_b(t).$$

The sum of the solutions of these two problems gives a solution of (3.24) which satisfies the initial condition (3.25) and the boundary conditions (3.26).

Initial Condition Subproblem

For the first of these subproblems, looking for separable solutions of the form $B(y, t) = Y(y)T(t)$ leads to

$$\frac{1}{R_m} \frac{Y''}{Y} + y \frac{Y'}{Y} + 1 = \frac{\dot{T}}{T} = \lambda,$$

where λ is an arbitrary constant.

The spatial dependence is given by

$$\frac{1}{R_m} Y'' + yY' + (1 - \lambda)Y = 0,$$

which, as shown in appendix C, has general solution

$$Y = ae^{-\frac{1}{2}R_my^2} M\left(\frac{1}{2}\lambda, \frac{1}{2}, \frac{1}{2}R_my^2\right) + bye^{-\frac{1}{2}R_my^2} M\left(\frac{1}{2} + \frac{1}{2}\lambda, \frac{3}{2}, \frac{1}{2}R_my^2\right).$$

The time dependence is given by

$$\frac{\dot{T}}{T} = \lambda,$$

which has solution

$$T = ce^{\lambda t}.$$

The general solution to equation (3.24) is thus

$$B(y, t) = \sum_{\text{all } \lambda} e^{\lambda t - \frac{1}{2}R_my^2} \left[a_\lambda M\left(\frac{1}{2}\lambda, \frac{1}{2}, \frac{1}{2}R_my^2\right) + b_\lambda y M\left(\frac{1}{2} + \frac{1}{2}\lambda, \frac{3}{2}, \frac{1}{2}R_my^2\right) \right].$$

Satisfying the lower boundary condition, $B(0, t) = 0$, is only possible if $a_\lambda = 0$ and so the solution becomes

$$B(y, t) = \sum_{\text{all } \lambda} e^{\lambda t - \frac{1}{2}R_my^2} b_\lambda y M\left(\frac{1}{2} + \frac{1}{2}\lambda, \frac{3}{2}, \frac{1}{2}R_my^2\right).$$

Applying the upper boundary condition, $B(1, t) = 0$, leads to

$$\sum_{\text{all } \lambda} e^{\lambda t - \frac{1}{2}R_m} b_\lambda M\left(\frac{1}{2} + \frac{1}{2}\lambda, \frac{3}{2}, \frac{1}{2}R_m\right) = 0,$$

which is only possible if

$$M\left(\frac{1}{2} + \frac{1}{2}\lambda, \frac{3}{2}, \frac{1}{2}R_m\right) = 0. \quad (3.27)$$

This equation will be satisfied by certain values of λ , denoted by λ_n . The solution then becomes

$$B(y, t) = \sum_{n=0}^{\infty} b_n e^{\lambda_n t - \frac{1}{2} R_m y^2} y M\left(\frac{1}{2} + \frac{1}{2} \lambda_n, \frac{3}{2}, \frac{1}{2} R_m y^2\right). \quad (3.28)$$

To satisfy the initial condition, we must have

$$B_0(y) = \sum_{n=0}^{\infty} b_n e^{-\frac{1}{2} R_m y^2} y M\left(\frac{1}{2} + \frac{1}{2} \lambda_n, \frac{3}{2}, \frac{1}{2} R_m y^2\right).$$

As shown in appendix E, this equation can be multiplied by $y M\left(\frac{1}{2} + \frac{1}{2} \lambda_n, \frac{3}{2}, \frac{1}{2} R_m y^2\right)$ and integrated from 0 to 1 to give

$$b_n = \frac{\int_0^1 B_0(y) y M\left(\frac{1}{2} + \frac{1}{2} \lambda_n, \frac{3}{2}, \frac{1}{2} R_m y^2\right) dy}{\int_0^1 e^{-\frac{1}{2} R_m y^2} y^2 M^2\left(\frac{1}{2} + \frac{1}{2} \lambda_n, \frac{3}{2}, \frac{1}{2} R_m y^2\right) dy},$$

which completes the solution of the initial condition problem.

Large R_m

The asymptotic approximation $M(a, b, z) \rightarrow \Gamma(b) e^z z^{a-b} / \Gamma(a)$ as $z \rightarrow \infty$ suggests that as R_m becomes large equation (3.27) becomes

$$\frac{\Gamma\left(\frac{3}{2}\right)}{\Gamma\left(\frac{1}{2} + \frac{1}{2} \lambda\right)} e^{\frac{1}{2} R_m} \left(\frac{1}{2} R_m\right)^{\frac{1}{2} \lambda - 1} = 0$$

which can only be satisfied if

$$\frac{1}{2} + \frac{1}{2} \lambda = -n \quad n = 0, 1, 2, 3 \dots$$

implying that

$$\lambda_n \rightarrow -2n - 1 \quad n = 0, 1, 2, 3 \dots \quad \text{as } R_m \rightarrow \infty. \quad (3.29)$$

The numerical results plotted in figure 3.5a, in which λ_0 , λ_1 and λ_3 tend to -1, -3 and -5 as R_m increases, confirm this behaviour.

This result implies that the functions $M\left(\frac{1}{2} + \frac{1}{2} \lambda, \frac{3}{2}, \frac{1}{2} R_m y^2\right)$ tend to $M(-n, \frac{3}{2}, \frac{1}{2} R_m y^2)$ as R_m becomes large. Since, when n is a positive integer and b is non-integer,

$$M(-n, b, z) = \sum_{i=0}^n \frac{(-n)_i}{(b)_i} \frac{z^i}{i!}$$

we thus obtain

$$M\left(\frac{1}{2} + \frac{1}{2} \lambda_n, \frac{3}{2}, \frac{1}{2} R_m y^2\right) \rightarrow \frac{(-n)_n}{\left(\frac{3}{2}\right)_n} \frac{1}{n!} \left(\frac{1}{2} R_m y^2\right)^n \quad \text{as } R_m \rightarrow \infty. \quad (3.30)$$

This result appears to contradict the boundary condition $M\left(\frac{1}{2} + \frac{1}{2} \lambda, \frac{3}{2}, \frac{1}{2} R_m\right) = 0$. However numerical solutions (an example of which is plotted in figure 3.5b for λ_0) show that the result is correct and that a boundary layer forms at $y = 1$ ensuring that the boundary condition is satisfied. The thickness of this boundary layer decreases as R_m increases.

Making use of (3.29) and (3.30) the solution (3.28) becomes

$$B(y, t) \rightarrow \sum_{n=0}^{\infty} b_n \frac{(-n)_n}{\left(\frac{3}{2}\right)_n} \frac{1}{n!} e^{-(2n+1)t - \frac{1}{2} R_m y^2} y \left(\frac{1}{2} R_m y^2\right)^n \quad \text{as } R_m \rightarrow \infty,$$

where the b_n are determined by the initial condition. After a few time intervals the higher-order components die away to leave

$$B(y, t) \approx b_0 e^{-t - \frac{1}{2} R_m y^2} y. \quad (3.31)$$

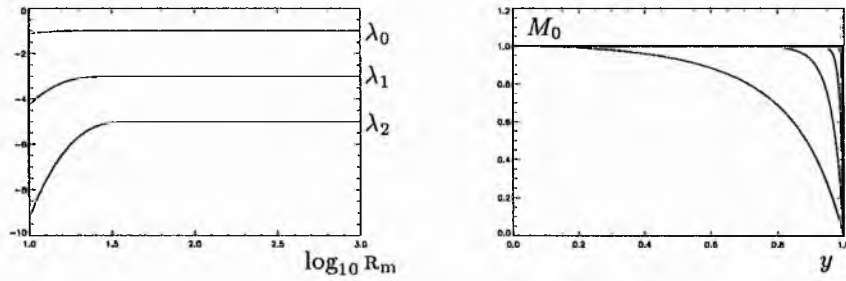


Figure 3.5: (a) $\lambda_1, \lambda_2, \lambda_3$ as functions of R_m (b) $M(\frac{1}{2} + \frac{1}{2}\lambda_0, \frac{3}{2}, \frac{1}{2}R_m y)$ for several values of R_m .

Now

$$b_0 = \frac{\int_0^1 B_0(y) y M(\frac{1}{2} + \frac{1}{2}\lambda_0, \frac{3}{2}, \frac{1}{2}R_m y^2) dy}{\int_0^1 e^{-\frac{1}{2}R_m y^2} y^2 M^2(\frac{1}{2} + \frac{1}{2}\lambda_0, \frac{3}{2}, \frac{1}{2}R_m y^2) dy}$$

and using (3.30) this becomes

$$b_0 \rightarrow \frac{\int_0^1 B_0(y) y dy}{\int_0^1 e^{-\frac{1}{2}R_m y^2} y^2 dy} \quad \text{as } R_m \rightarrow \infty.$$

The top line evaluates to some constant and, as shown in appendix H, the bottom line tends to $R_m^{-\frac{3}{2}}$ and so

$$b_0 \rightarrow c_0 R_m^{\frac{3}{2}} \quad \text{as } R_m \rightarrow \infty.$$

Equation (3.31) thus becomes

$$B(y, t) = c_0 R_m^{\frac{3}{2}} y e^{-t - \frac{1}{2}R_m y^2}. \quad (3.32)$$

This is an interesting result as it implies that every initial condition eventually ends up behaving in the same manner. The only influence the initial condition has is to change the value of c_0 .

Reconnection and Ohmic Heating Rates

From (3.32) the current $j = -\partial_y B$ is

$$j = c_0 R_m^{\frac{3}{2}} e^{-t - \frac{1}{2}R_m y^2} (R_m y^2 - 1),$$

which implies that ℓ (the current sheet width, taken to be the distance between $y = 0$ and the point where $j = 0$) is

$$\ell = R_m^{-\frac{1}{2}}.$$

The maximum value of B occurs at $y = \ell$ and, from (3.32), is

$$B_{max} = B(y, t) = c_0 R_m e^{-t - \frac{1}{2}}.$$

The reconnection rate is

$$R_E = \frac{1}{R_m} j(0, t) = c_0 e^{-t} R_m^{\frac{1}{2}}$$

and the ohmic heating rate is

$$R_\Omega = \frac{1}{R_m} \int_0^1 j^2 dy = c_0^2 e^{-2t} R_m^2 \int_0^1 e^{-R_m y^2} (R_m^2 y^4 - 2R_m y^2 + 1) dy.$$

As shown in appendix H

$$\int_0^1 e^{-R_m y^2} dy \rightarrow R_m^{-\frac{1}{2}}, \quad \int_0^1 e^{-R_m y^2} y^2 dy \rightarrow \frac{1}{2} R_m^{-\frac{3}{2}} \quad \text{and} \quad \int_0^1 e^{-R_m y^2} y^4 dy \rightarrow \frac{1}{4} R_m^{-\frac{5}{2}}$$

as R_m tends to ∞ and hence

$$R_\Omega \rightarrow \frac{1}{4} c_0^2 e^{-2t} R_m^{\frac{3}{2}}.$$

Boundary Condition Subproblem

Taking the Laplace transform of equation (3.24) and applying the homogeneous initial condition gives

$$\frac{1}{R_m} \bar{B}_{yy} + y \bar{B}_y + (1-s) \bar{B} = 0,$$

which (see appendix C) has solution

$$\bar{B}(y, s) = a(s) e^{-\frac{1}{2} R_m y^2} M\left(\frac{1}{2}s, \frac{1}{2}, \frac{1}{2} R_m y^2\right) + b(s) e^{-\frac{1}{2} R_m y^2} y M\left(\frac{1}{2} + \frac{1}{2}s, \frac{3}{2}, \frac{1}{2} R_m y^2\right).$$

The transformed boundary conditions are

$$\bar{B}(0, s) = 0 \quad \text{and} \quad \bar{B}(1, s) = \bar{B}_b(s).$$

Applying the first of these gives $a(s) = 0$ and applying the second gives

$$b(s) = \frac{\bar{B}_b(s)}{e^{-\frac{1}{2} R_m} y M\left(\frac{1}{2} + \frac{1}{2}s, \frac{3}{2}, \frac{1}{2} R_m\right)}$$

and so

$$\bar{B}(y, s) = \frac{\bar{B}_b(s) y e^{-\frac{1}{2} R_m y^2} M\left(\frac{1}{2} + \frac{1}{2}s, \frac{3}{2}, \frac{1}{2} R_m y^2\right)}{e^{-\frac{1}{2} R_m} M\left(\frac{1}{2} + \frac{1}{2}s, \frac{3}{2}, \frac{1}{2} R_m\right)}.$$

Having found $\bar{B}(y, s)$, $B(y, t)$ can be obtained through the reverse transform, ie

$$B(y, t) = \frac{1}{2\pi i} \int_P e^{st} \bar{B}(y, s) ds,$$

where P is a path in the complex plane that encloses all the singularities of the integrand. Using complex variable theory this solution can be written in a more practical form as

$$B(y, t) = \sum \text{residues of } e^{st} \bar{B}(y, s).$$

3.4 Finite Interval with a Time-Modulated Flow

In this section we consider magnetic annihilation in a finite interval of space with a time-dependent stagnation-point flow. This problem can be written as

$$\frac{1}{R_m} B_{yy} + v(t) y B_y + v(t) B = B_t \quad 0 \leq y \leq 1 \quad 0 \leq t < \infty, \quad (3.33)$$

subject to initial condition

$$B(y, 0) = B_0(y) \quad 0 \leq y \leq 1 \quad (3.34)$$

and boundary conditions

$$B(0, t) = 0 \quad B(1, t) = B_b(t). \quad (3.35)$$

Equation (3.33) has already been solved for an infinite interval with prescribed initial condition and it was found that away from the origin, the behaviour of the magnetic field is controlled by magnetic advection.

Consider the finite interval to be a small section, $[0, 1]$, of the infinite interval. By taking the initial condition on $(-\infty, \infty)$ to be an odd function, the lower boundary condition in (3.35) is satisfied. By choosing the initial condition on $[0, 1]$ to be $B_0(y)$ the initial condition (3.34) is satisfied. By carefully selecting the initial condition on $(1, \infty)$, so that when it is advected the behaviour at $y = 1$ mimics $B_b(t)$, the upper boundary condition in (3.35) will be approximately satisfied. In this way the infinite

interval solution can supply an exact solution to equation (3.33) with an exact initial condition, exact lower boundary condition and approximate upper boundary condition.

The magnetic field under advection is given by

$$B(y, t) = g(t) B_0(yg(t)) \quad \text{where} \quad g(t) = e^{\int v(t) dt},$$

so, to mimic the upper boundary condition, we require

$$g(t) B_0(g(t)) = B_b(t),$$

which implies that

$$y B_0(y) = B_b(g^{-1}(y)),$$

where g^{-1} is the inverse function of g . Hence

$$B_0(y) = \frac{1}{y} B_b(g^{-1}(y))$$

is the required initial magnetic field.

This method for finding the solution on a finite interval is very powerful. Not only is it an exact solution with a good approximation to the boundary condition, but by relating the boundary condition on the finite interval to the initial condition on the infinite interval, use can be made of the investigation of the effect of different initial conditions on the magnetic field evolution already carried out. Thus it is possible to say which boundary conditions on the finite interval will lead to a steady state, which will cause it to increase and which will cause it to decay away.

Note that the approximation to the boundary condition will not be very good if the diffusion region spreads out and reaches the outer boundary. This will happen when v has been small or zero for any length of time.

Also note that if v is zero for any length of time then the function g will have no inverse. This problem can be overcome by switching to solving the diffusion equation, to which equation (3.33) reduces, during these periods.

3.5 Self-Similar Solutions

A self-similar solution of a partial differential equation is a type of solution in which one of the independent variables only appears in one particular combination with another. Physically these solutions occur when the system lacks a natural length scale, so they can be expected to exist far from any boundaries where the effect of boundary conditions is minimal. Starting with

$$\frac{1}{R_m} B_{yy} + v(t) y B_y + v(t) B = B_t,$$

then looking for self-similar solutions of the form

$$B(y, t) = B(\epsilon(y, t))$$

leads to

$$\frac{\epsilon_y^2}{R_m v} B'' + B' \left(y \epsilon_y + \frac{\epsilon_y y}{R_m v} - \frac{\epsilon_t}{v} \right) + B = 0,$$

where the primes denote differentiation with respect to ϵ . If this equation is to be solvable then both the coefficients of B'' and B' must be functions of ϵ . For simplicity we can assume that ϵ has a separable form, ie $\epsilon(y, t) = T(t)Y(y)$, so that the above equation becomes

$$\frac{(TY')^2}{R_m v} B'' + B' \left(y Y' T + \frac{TY''}{R_m v} - \frac{YT'}{v} \right) + B = 0. \quad (3.36)$$

To simplify this we can assume that

$$\frac{(TY')^2}{v} = 1.$$

Rearranging this into $Y' = v^{\frac{1}{2}}/T$ we obtain

$$Y' = \lambda \quad \text{and} \quad \frac{v^{\frac{1}{2}}}{T} = \lambda,$$

where λ is an arbitrary constant. These give

$$Y = \lambda y + c, \quad T = v^{\frac{1}{2}}/\lambda \quad \text{and hence} \quad \epsilon = yv^{\frac{1}{2}} + \frac{c}{\lambda}v^{\frac{1}{2}},$$

where c is another arbitrary constant. Equation (3.36) then becomes

$$\frac{1}{R_m}B'' + B' \left[y \left(v^{\frac{1}{2}} - \frac{1}{2}v^{-\frac{3}{2}}\dot{v} \right) \frac{1}{2}v^{-\frac{3}{2}}\dot{v}\frac{c}{\lambda} \right] + B = 0.$$

The only way for the coefficient of B' to be a function of ϵ is if $c = 0$ and $v^{\frac{1}{2}} - \frac{1}{2}v^{-\frac{3}{2}}\dot{v} = nv^{\frac{1}{2}}$, where n is arbitrary. This then gives

$$v = \frac{1}{2(n-1)t + m} \quad \text{and} \quad \frac{1}{R_m}B'' + n\epsilon B' + B = 0.$$

Note that if $n = 1$ the flow is steady state. As shown in appendix C, the equation for B has general solution

$$B = \alpha M \left(\frac{1}{2n}, \frac{1}{2}, -nR_m\epsilon^2 \right) + \beta \epsilon M \left(\frac{1}{2} + \frac{1}{2n}, \frac{3}{2}, -nR_m\epsilon^2 \right),$$

or, since $\epsilon = yv^{\frac{1}{2}}$,

$$B = \alpha M \left(\frac{1}{2n}, \frac{1}{2}, -nR_mvy^2 \right) + \beta yv^{\frac{1}{2}} M \left(\frac{1}{2} + \frac{1}{2n}, \frac{3}{2}, -nR_mvy^2 \right).$$

This will only satisfy the boundary condition $B(0) = 0$ if $\alpha = 0$, and so

$$B = \beta yv^{\frac{1}{2}} M \left(\frac{1}{2} + \frac{1}{2n}, \frac{3}{2}, -nR_mvy^2 \right).$$

As this solution supposedly exists far from the outer boundary then there is no boundary condition to determine β . Note that for the case of steady flow, where $n = 1$, this solution has the same form as the Sonnerup and Priest annihilation solution.

The reconnection rate $R_E = j_{np}/R_m = -\partial_y B(0, t)/R_m$ given by the above solution is

$$R_E = \frac{-\beta v^{\frac{1}{2}}}{R_m} = \frac{-\beta}{[2(n-1)t + m]R_m}.$$

If the flow is steady-state, with $n = 1$, then the reconnection rate decreases with R_m in contrast to the Sonnerup and Priest solution where it tends to a constant. This is due to the difference in outer boundary conditions.

3.6 Time-Dependent Diffusivity

Introduction

In previous sections the diffusivity, η , has been taken to be a constant. Physically, this is not strictly true as η may vary both in time and in space. In this section we follow a suggestion of Martin Heyn and consider η to be a function of time so that the induction equation becomes

$$\frac{\eta(t)}{R_m} B_{yy} + v(t) y B_y + v(t) B = B_t. \quad (3.37)$$

Changing the time variable from t to $T(t)$ gives

$$\frac{\eta(T)}{R_m} B_{yy} + v y B_y + v B = \dot{T} B_T$$

or

$$\frac{1}{R_m} B_{yy} + \frac{v}{\eta} y B_y + \frac{v}{\eta} B = \frac{\dot{T}}{\eta} B_T.$$

Choosing

$$\frac{\dot{T}}{\eta} = 1,$$

which defines T as

$$T = \int \eta dt,$$

gives

$$\frac{1}{R_m} B_{yy} + \frac{v}{\eta} y B_y + \frac{v}{\eta} B = B_T,$$

or

$$\frac{1}{R_m} B_{yy} + v^* y B_y + v^* B = B_T.$$

This equation has the same form as the equations obtained earlier when diffusivity was considered to be constant. A simple change of variables thus leads to an equation that has already been studied and solved.

Advection versus Diffusion

From our previous work it is known that balancing constant diffusion against a steady inflow gives a steady-state magnetic field. Intuitively therefore, it is to be expected that a steady-state magnetic field can be obtained by balancing a time varying flow against time varying diffusion.

If B is in a steady state and is not a function of t then equation (3.37) becomes

$$\frac{\eta(t)}{R_m} B_{yy} + v(t) y B_y + v(t) B = 0,$$

which can only be consistent if

$$\eta(t) = v(t)$$

leaving

$$\frac{1}{R_m} B'' + y B' + B = 0.$$

This equation is exactly the same as that determining the magnetic field in the Sonnerup and Priest case and has the same solution.

Chapter 4

Magnetic Annihilation in a Compressible, Inviscid Plasma

4.1 Introduction

Many annihilation and reconnection models assume, for simplicity, that the plasma is incompressible. In this section we examine annihilation models where the plasma density is allowed to vary spatially. Viscous effects are assumed to be negligible and the fluid flow, magnetic field and plasma density are taken to be of the form

$$\mathbf{v} = (u(x, y), v(x, y), 0), \quad \mathbf{B} = (B(y), 0, 0) \quad \text{and} \quad \rho = \rho(x, y). \quad (4.1)$$

Equations

The dimensionless, steady-state, resistive, inviscid MHD equations are

$$\begin{aligned} M_A^2 \rho (\mathbf{v} \cdot \nabla) \mathbf{v} &= -\nabla \left(\beta p + \frac{1}{2} B^2 \right) + (\mathbf{B} \cdot \nabla) \mathbf{B}, \\ \nabla \cdot (\rho \mathbf{v}) &= 0, \\ \mathbf{E} + \mathbf{v} \times \mathbf{B} &= \frac{1}{R_m} \mathbf{j}, \\ \nabla \times \mathbf{E} &= 0, \\ \mathbf{j} &= \nabla \times \mathbf{B}, \\ \nabla \cdot \mathbf{B} &= 0. \end{aligned}$$

Faraday's Law

With \mathbf{v} and \mathbf{B} of the forms (4.1) the components of Faraday's law are

$$\begin{aligned} \partial_y E_z &= 0, \\ \partial_x E_z &= 0, \\ \partial_x E_y - \partial_y E_x &= 0. \end{aligned} \quad (4.2)$$

The first two of these imply that $E_z = \text{constant} = k$.

Ohm's Law

With \mathbf{v} and \mathbf{B} of the forms (4.1) the components of Ohm's law are

$$\begin{aligned} E_{\hat{x}} &= 0, \\ E_{\hat{y}} &= 0, \\ E_{\hat{z}} - vB &= -\frac{1}{R_m} B'. \end{aligned}$$

The first two of these specify $E_{\hat{x}}$ and $E_{\hat{y}}$ (which now satisfy (4.2)) and the third becomes

$$\frac{1}{R_m} B' - vB = -k. \quad (4.3)$$

Since B is only a function of y this equation can only be consistent if $v = v(y)$.

Equation of Mass Continuity

With \mathbf{v} and ρ as in (4.1), the equation of mass continuity reduces to

$$\partial_x (\rho u) + \partial_y (\rho v) = 0. \quad (4.4)$$

Equation of Motion

The assumption of straight field lines reduces the equation of motion to

$$M_A^2 \rho (\mathbf{v} \cdot \nabla) \mathbf{v} = -\nabla \left(\beta p + \frac{1}{2} B^2 \right),$$

the components of which are

$$\begin{aligned} M_A^2 \rho (u \partial_x + v \partial_y) u &= -\partial_x \left(\beta p + \frac{1}{2} B^2 \right), \\ M_A^2 \rho (u \partial_x + v \partial_y) v &= -\partial_y \left(\beta p + \frac{1}{2} B^2 \right). \end{aligned}$$

The pressure terms can be eliminated by differentiating the first of these with respect to y , differentiating the second with respect to x and subtracting to give

$$\partial_y [\rho (u \partial_x + v \partial_y) u] - \partial_x [\rho (u \partial_x + v \partial_y) v] = 0.$$

Since v is only a function of y this simplifies to

$$\partial_y (\rho u u_x + \rho v u_y) - v v_y \rho_x = 0. \quad (4.5)$$

Summary

Equation (4.3) determines B once v is known and equations (4.4) and (4.5) form a pair of coupled non-linear partial differential equations in three unknowns, ρ , u and v . This set of equations is incomplete and to avoid the complexity of including an energy equation and equation of state we shall specify one of the velocity components. As in the earlier annihilation models, it will be assumed that $v(x, y) = -y$.

4.2 Assumptions

Looking for solutions of the form

$$\rho(x, y) = \rho(y) \quad \text{and} \quad u(x, y) = xf(y)$$

reduces the coupled partial differential equations (4.4) and (4.5) to the coupled ordinary differential equations

$$\begin{aligned} \rho f + d_y(\rho v) &= 0, \\ d_y(\rho f^2 + \rho v f') &= 0, \end{aligned}$$

or

$$\begin{aligned} \rho f + \rho' v + \rho v' &= 0, \\ f^2 + v f' &= \frac{k_0}{\rho}, \end{aligned}$$

where k_0 is an arbitrary constant. Dividing the first of these equations by $v\rho$ gives

$$\frac{f}{v} + \frac{\rho'}{\rho} + \frac{v'}{v} = 0,$$

which can be integrated to produce

$$\int \frac{f}{v} dy + \log \rho v = \text{const},$$

or

$$\rho v = k_1 e^{-\int f/v dy},$$

where k_1 is an arbitrary constant. The coupled equations thus become

$$\begin{aligned} \rho v &= k_1 e^{-\int f/v dy}, \\ f^2 + v f' &= \frac{k_0}{\rho}. \end{aligned}$$

These equations should have as a special case the incompressible solution where $v = -y$, $f = 1$ and $\rho = 1$. This is only possible if $k_0 = 1$ and $k_1 = -1$, giving

$$\begin{aligned} \rho v &= -e^{-\int f/v dy}, \\ f^2 + v f' &= \frac{1}{\rho}. \end{aligned}$$

The first of these equations hints at singularities in ρ where $v = 0$. To help avoid this let

$$f = -v' + g(y) \tag{4.6}$$

so that the equations become

$$\begin{aligned} \rho &= -e^{-\int g/v dy}, \\ v'^2 - 2v'g + g^2 + v(-v'' + g') &= \frac{1}{\rho}. \end{aligned} \tag{4.7}$$

To simplify these let

$$r = -e^{\int g/v dy} \tag{4.8}$$

implying that

$$r' = \frac{g}{v} r$$

and so

$$g = \frac{vr'}{r} \quad \text{and} \quad g' = \frac{v'r'}{r} + \frac{vr''}{r} - \frac{v'r'^2}{r^2}. \quad (4.9)$$

Substituting (4.8) and (4.9) into (4.7) gives

$$\begin{aligned} \rho &= \frac{1}{r}, \\ v'^2 - \frac{2v'vr'}{r} + v \left(-v'' + \frac{v'r'}{r} + \frac{vr''}{r} \right) &= \frac{1}{\rho}. \end{aligned} \quad (4.10)$$

Eliminating ρ between these produces

$$v^2 r'' - vv'r' + (v'^2 - vv'')r - r^2 = 0. \quad (4.11)$$

If v is now specified we have an equation which can, in principle, be solved for r . The density is then given by (4.10) and f is obtained from (4.6) with (4.9).

The assumption that $v = -y$ reduces (4.11) to

$$y^2 r'' - yr' + r - r^2 = 0 \quad (4.12)$$

and we can note that

- this is a second-order non-linear ordinary differential equation for r ,
- there is a trivial solution of $r = 1$ which corresponds to the incompressible case,
- the equation has even solutions with $r(-y) = r(y)$,
- at $y = 0$ this equation reduces to $r - r^2 = 0$ implying that $r = 0, 1$. Since $\rho = 1/r$, having $r = 0$ is obviously unphysical and so $r(0) = 1$.

4.3 Analytical Solution

Since (4.12) has even solutions, it need only be solved in the range $0 \leq y < \infty$. For $y > 0$ let $y = e^t$ so that

$$\frac{d}{dy} = \frac{1}{y} \frac{d}{dt}, \quad \frac{d^2}{dy^2} = -\frac{1}{y^2} \frac{d}{dt} + \frac{1}{y^2} \frac{d^2}{dt^2}$$

and the equation becomes

$$\ddot{r} - 2\dot{r} + r - r^2 = 0. \quad (4.13)$$

Information about solutions of this non-linear equation can be obtained through phase plane techniques. Letting $s = \dot{r}$ gives the almost-linear autonomous system

$$\begin{aligned} \dot{r} &= s, \\ \dot{s} &= 2s - r + r^2, \end{aligned} \quad (4.14)$$

which has critical points at $(r, s) = (0, 0)$ and $(1, 0)$.

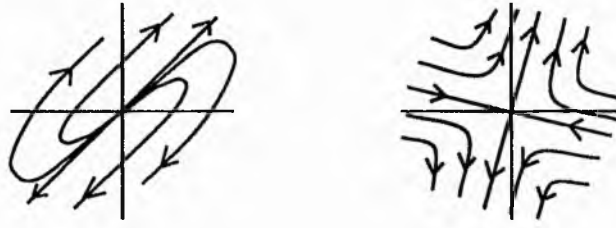
Close to the critical point $(0, 0)$ the system (4.14) reduces to

$$\begin{aligned} \dot{r} &= s, \\ \dot{s} &= 2s - r, \end{aligned}$$

which, as shown in appendix I, has the phase plane sketched in figure 4.1a.

For the critical point $(1, 0)$, changing coordinate system to $r_1 = r - 1$ transforms (4.14) to

$$\begin{aligned} \dot{r}_1 &= s, \\ \dot{s} &= 2s + r_1 + r_1^2. \end{aligned}$$

Figure 4.1: Phase plane near $(r, s) = (0,0)$ and $(1,0)$.

Close to the origin this reduces to

$$\begin{aligned}\dot{r}_1 &= s, \\ \dot{s} &= 2s + r_1,\end{aligned}$$

which, as shown in appendix J, has the phase plane sketched in figure 4.1b. Note that the trajectories through the origin have gradients $1 \pm \sqrt{2}$.

The phase plane for the almost-linear system (4.14) is obtained by “merging together” these two to obtain the phase plane sketch shown in figure 4.2.

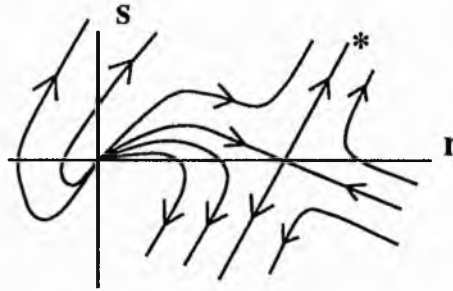


Figure 4.2: Phase plane for the almost-linear autonomous system.

The trajectories shown in this figure represent all the possible solutions of (4.13). Physically relevant solutions must

1. have $r > 0$ for all t (since $\rho = 1/r$ must be positive) and
2. tend to 1 as $t \rightarrow -\infty$ (since $r = 1$ at $y = 0$).

Only the asterisked trajectory meets both these requirements and is therefore the only physically relevant solution.

Boundary Conditions

Equation (4.13) is a second-order differential equation and its solution contains two arbitrary constants which will be determined by boundary conditions. In looking for an even solution we have effectively imposed the condition $r'(0) = 0$. Since r is related to both the density and the x -component of velocity, the other boundary condition can be either $\rho(1)$ or $v_x(0, 1)$.

Asymptotic Solution as $y \rightarrow 0$

As t tends to $-\infty$ (and hence y tends to zero) the asterisked solution becomes

$$s \rightarrow (1 + \sqrt{2})(r - 1) \quad \text{as} \quad y \rightarrow 0. \quad (4.15)$$

Substituting $s = \dot{r}$ into this and solving gives

$$r \rightarrow 1 + \ell e^{(1+\sqrt{2})t} \quad \text{as} \quad y \rightarrow 0,$$

where ℓ is an arbitrary constant. In terms of the original variable, y , this is

$$r \rightarrow 1 + \ell y^{1+\sqrt{2}} \quad \text{as} \quad y \rightarrow 0. \quad (4.16)$$

The arbitrary constant ℓ will be determined by the boundary condition on ρ or $v_{\hat{x}}$.

Asymptotic Solution as $y \rightarrow \infty$

From (4.14)

$$\frac{ds}{dr} = \frac{\dot{s}}{\dot{r}} = 2 + \frac{r^2 - r}{s}$$

and so

$$\frac{ds}{dr} \rightarrow 2 + \frac{r^2}{s} \quad \text{as} \quad r \rightarrow \infty. \quad (4.17)$$

As r becomes large, r^2/s tends to either a constant or infinity.

Assuming that r^2/s tends to a constant then (4.17) becomes

$$\frac{ds}{dr} \rightarrow 2 + c_0 \quad \text{as} \quad r \rightarrow \infty$$

with solution

$$s \rightarrow (2 + c_0)r + c_1 \quad \text{as} \quad r \rightarrow \infty.$$

However, this result gives

$$\frac{r^2}{s} \rightarrow \frac{r^2}{(2 + c_0)r + c_1} \quad \text{as} \quad r \rightarrow \infty,$$

which contradict the original assumption.

Assuming that r^2/s tends infinity as r increases then (4.17) becomes

$$\frac{ds}{dr} \rightarrow \frac{r^2}{s} \quad \text{as} \quad r \rightarrow \infty$$

with solution

$$s \rightarrow \sqrt{\frac{2}{3}} r^{\frac{3}{2}} \quad \text{as} \quad r \rightarrow \infty. \quad (4.18)$$

This solution does not contradict the original assumption. Substituting $s = \dot{r}$ into the above equation and solving gives

$$r \rightarrow \frac{4}{\left(\sqrt{\frac{2}{3}}t + c\right)^2} \quad \text{as} \quad r \rightarrow \infty,$$

or, in terms of y ,

$$r \rightarrow \frac{4}{\left(\sqrt{\frac{2}{3}} \log y + c\right)^2} \quad \text{as} \quad y \rightarrow \infty.$$

Streamlines

Streamlines are given by

$$\frac{dy}{dx} = \frac{v_y}{v_x} = \frac{v}{u} = \frac{v}{xf}.$$

Substituting for f from (4.6), then substituting g from (4.9) and setting $v = -y$, we obtain

$$\frac{dy}{dx} = \frac{-y}{x \left(-v' + \frac{vr'}{r}\right)}.$$

Rearranging this to

$$\frac{dx}{x} = \left(\frac{r'}{r} - \frac{1}{y} \right) dy$$

and integrating gives

$$x = \frac{\ell_0 r}{y}, \quad (4.19)$$

where ℓ_0 is an arbitrary constant. Once $r(y)$ is known, this expression allows the streamlines to be plotted.

4.4 Numerical Solution

Introduction

The equation

$$y^2 r'' - yr' + r - r^2 = 0 \quad (4.20)$$

has been analysed in the previous section and solutions in the limits of y tending to zero and infinity have been found. In this section numerical methods are used to obtain the solution for $r(y)$ over the whole range.

As previously detailed, equation (4.20) can be written as

$$\frac{ds}{dr} = 2 + \frac{r^2 - r}{s}, \quad (4.21)$$

where $s = r' = yr'$. Numerically solving both this equation, to obtain $s(r)$, and

$$\frac{dr}{dy} = \frac{1}{y} s(r), \quad (4.22)$$

will give $r(y)$.

Splitting the numerical solution into two separate steps allows the solution at each step to be compared to the analytical results. This gives verification that the numerical routines are working correctly and helps in tracking down and solving any numerical problems.

Initial Conditions

As the integration has to start from near the critical point and proceed outwards, the initial conditions can be obtained from the analytical work of the previous section. For the first step the initial condition is

$$s(1 + \delta_0) = (1 + \sqrt{2}) \delta_0, \quad (4.23)$$

where δ_0 is some small value that determines how close to the critical point the integration starting point is. Provided that δ_0 is small then the numerical solution should not be sensitive to its exact value.

For the second step the initial condition is

$$r(\delta_1) = 1 + \ell \delta_1^{1+\sqrt{2}}, \quad (4.24)$$

where δ_1 is some small value and ℓ is an arbitrary constant. Again, provided that δ_1 is small the numerical solution should not be sensitive to its exact value.

First Step

Numerically solving (4.21) with the initial condition (4.23) gave the solution plotted in figure 4.3a. This solution remained the same to over 4 decimal places as δ_0 was varied between 10^{-12} and $10^{-1.25}$. Figure 4.3b compares the numerical solution and the asymptotic solution (4.15). Figure 4.3c shows the percentage error between the numerical solution and the asymptotic solution (4.18).

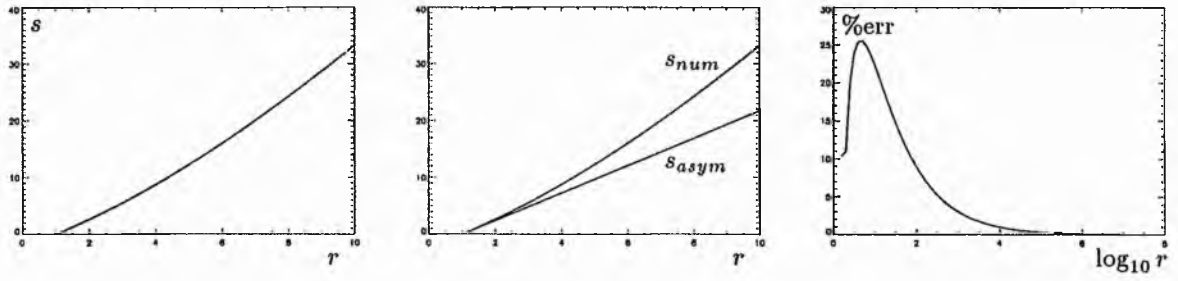


Figure 4.3: (a) Numerical solution for s , (b) and (c) comparison of numerical and asymptotic solutions for $y \rightarrow 0$ and ∞ .

Second Step

Equation (4.22) with initial condition (4.24) was solved numerically with several values of ℓ to give the solutions plotted in figure 4.4a. These solutions remained constant to 3 significant figures for δ_1 between $10^{-3.6}$ and $10^{-1.4}$. Figure 4.4b shows the percentage errors between the numerical solutions and the asymptotic solutions (4.16).

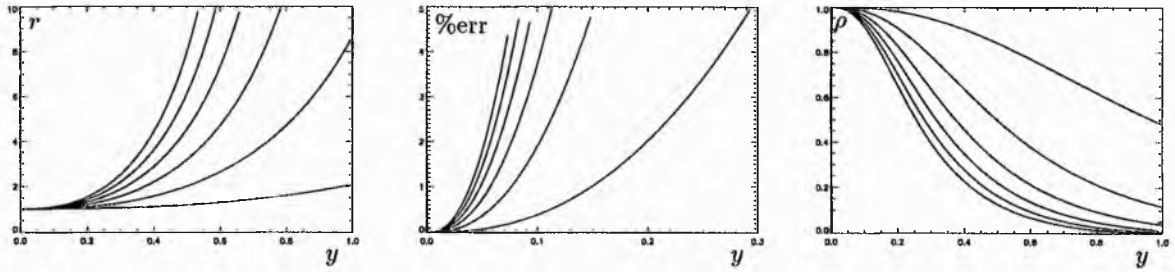


Figure 4.4: For $\ell = 1, 5, 10, 15, 20$ and 25 (a) numerical solution for r (b) error between numerical and asymptotic solutions (c) plasma density.

Plasma Density

Figure 4.4c shows the plasma density, $\rho = 1/r$, for several values of ℓ . Applying the boundary condition $\rho(1)$ is one way of determining a value for ℓ .

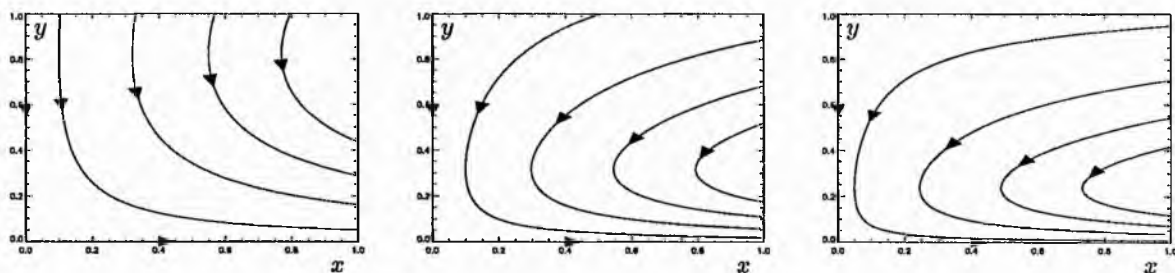
Streamlines

The numerical solution for $r(y)$ and the streamline equation, (4.19), gives the streamlines plotted in figure 4.5. These stream lines vary with ℓ and applying a boundary condition on $v_x(0, 1)$ is an alternative way of determining ℓ .

4.5 Magnetic Field

As it was assumed $v = -y$ the equation determining $B(y)$, (4.3), becomes

$$\frac{1}{R_m} B' + yB = -k.$$

Figure 4.5: Streamlines for $\ell = 1, 10$ and 20 .

This is the same equation for $B(y)$ considered in the models of annihilation in an incompressible plasma. Since the boundary conditions here ($B(0) = 0$ and $B(1) = 1$) are also the same the magnetic field will be identical. This is to be expected since v_y , the velocity component which advects the magnetic field and forces it to annihilate, is the same for both models.

4.6 Additional Thoughts

After discussion with the examiners of this thesis it has been agreed that the work in this chapter is not particularly realistic because of the freedom to choose one of the dependent variables.

To create a consistent set of equations which will determine all of the independent variables it is necessary to include an equation of state and an energy equation.

The simplest way of doing this is to assume that the temperature is constant (allowing the energy equation to be ignored) and considering the equation of state,

$$\bar{p} = RT_0 \bar{\rho}.$$

Non-dimensionalising this equation against $\bar{p} = p_0 p$, $\bar{\rho} = \rho_0 \rho$ gives

$$p = \frac{T}{\beta} \rho$$

where $T = \rho_0 R \beta T_0 / p_0$. Substituting this equation into the equation of motion and following the analysis in the first section of this chapter then gives the four equations

$$M_A^2 \rho (u \partial_x + v \partial_y) u = -T \rho_x, \quad (4.25)$$

$$M_A^2 \rho v v' = -T \rho_y - B B', \quad (4.26)$$

$$\partial_x (\rho u) + \partial_y (\rho v) = 0, \quad (4.27)$$

$$\frac{1}{R_m} B' + v B = -k, \quad (4.28)$$

for the four variables $B(y)$, $u(x, y)$, $v(y)$ and $\rho(x, y)$. Note that equation (4.26) is a first order ordinary differential equation for ρ and has the exact solution

$$\rho = e^{-\frac{1}{2} M_A^2 T^{-1} v^2} \left(-T^{-1} \int e^{\frac{1}{2} M_A^2 T^{-1} v^2} B B' dy + g(x) \right) \quad (4.29)$$

where $g(x)$ is an arbitrary function of x .

Asymptotic Solution

Here we give a brief treatment of the above four equations to demonstrate that realistic, sensible solutions can be found and to act as a possible guide for further research in this area. Since the limit of $T \rightarrow \infty$

is of interest (as it should give the incompressible case) then supposing solutions of the form

$$v = v_0 + T^{-1}v_1 \dots \quad B = B_0 + T^{-1}B_1 \dots \quad g = g_0 + T^{-1}g_1 \dots$$

simplifies (4.29) to

$$\rho = g_0 + T^{-1} \left(g_1 - \frac{1}{2}B_0^2 - \frac{1}{2}M_A^2 v_0^2 g_0 \right) + O(T^{-2}). \quad (4.30)$$

The equation of mass continuity, (4.27), will be satisfied identically if

$$\rho u = \Psi_y \quad \text{and} \quad \rho v = -\Psi_x. \quad (4.31)$$

and using the asymptotic forms for ρ and v in the second of these gives

$$\Psi_x = -g_0 v_0 + O(T^{-1}). \quad (4.32)$$

This can be integrated with respect to x and then differentiated with respect to y to obtain

$$\Psi_y = -G_0 v'_0 + O(T^{-1}), \quad (4.33)$$

where G_0 is the indefinite integral of g_0 (ie $G'_0 = g_0$). The second part of (4.31) then gives

$$u = \frac{\Psi_y}{\rho} = \frac{-G_0 v'_0 + O(T^{-1})}{g_0 + O(T^{-1})} = -\frac{G_0 v'_0}{g_0} + O(T^{-1}). \quad (4.34)$$

Equation (4.25) can be written as

$$(\Psi_y \partial_x - \Psi_x \partial_y) u = -T \rho_x,$$

which, on substituting in (4.32), (4.33) and (4.34), gives the $O(T)$ and $O(1)$ equations

$$g'_0 = 0 \quad \text{and} \quad -v'_0 v'_0 + v_0 v''_0 = -\frac{g'_1}{M_A^2 G_0}.$$

The first of these gives $g_0 = \ell_0$ and hence $G_0 = \ell_0 x + \ell_1$ where ℓ_0 and ℓ_1 are arbitrary constants. In the second equation the left hand side is a function of y and the right hand side is a function of x and so both sides must equal to some constant, $-\ell^2$ say. This leads to

$$\frac{g'_1}{M_A^2 G_0} = \ell^2,$$

(from which the solution

$$g_1 = \frac{1}{2}M_A^2 \ell^2 \ell_0 x^2 + \ell^2 M_A^2 \ell_1 x + \ell_2,$$

is obtained) and also

$$-v'_0 v'_0 + v_0 v''_0 = \ell_2.$$

Note that ℓ^2 cannot be zero or this equation will not have the required even solution for v_0 . Differentiating this leads to a solvable form (see equation (2.23) and its general solution in chapter 2) or the solution can be found by inspection to be

$$v_0 = \begin{cases} \ell x \\ \frac{\ell}{\lambda^2} \sin \lambda x \\ \frac{\ell}{\mu^2} \sinh \mu x. \end{cases}$$

Boundary conditions will determine which of these three cases applies and also the values of the arbitrary constants. This solution then allows equation (4.28) to be solved for the first order magnetic field.

Using the above solutions, equation (4.30) becomes

$$\rho = \ell_0 + T^{-1} \left(\frac{1}{2}M_A^2 \ell^2 \ell_0 x^2 + M_A^2 \ell^2 \ell_1 x + \ell_2 - \frac{1}{2}B_0^2 - \frac{1}{2}M_A^2 \ell_0 v_0^2 \right).$$

The boundary condition $\rho(0, 1) = 1$ fixes $\ell_0 = 1$ and the symmetry condition $\rho_x(0, y) = 0$ fixes $\ell_1 = 0$ giving

$$\rho = 1 + T^{-1} \left(\frac{1}{2} M_A^2 \ell^2 x^2 + \ell_2 - \frac{1}{2} B_0^2 - \frac{1}{2} M_A^2 v_0^2 \right).$$

Note that in the limit $T \rightarrow \infty$ this solution gives $\rho \rightarrow 1$ and $v \rightarrow v_0$ which is the annihilation solution for the incompressible case.

This brief analysis could be extended by solving for the first order terms in v , u and B or by examining the special case where ρ is independent of x .

Chapter 5

A Series Approach to Steady-State Magnetic Reconnection

5.1 Introduction

In this section the MHD equations are simplified into two non-linear coupled partial differential equations by assuming that the magnetic field and plasma flow are both two-dimensional. Looking for solutions that are a perturbation around the exact magnetic annihilation solution then yields two linear coupled partial differential equations. Series solutions to these equations are then obtained.

Equations

The steady-state, incompressible, resistive, viscous MHD equations are

$$\begin{aligned}M_A^2 (\mathbf{v} \cdot \nabla) \mathbf{v} &= -\beta \nabla p + \mathbf{j} \times \mathbf{B} + \frac{M_A^2}{R} \nabla^2 \mathbf{v}, \\ \mathbf{E} + \mathbf{v} \times \mathbf{B} &= \frac{1}{R_m} \mathbf{j}, \\ \nabla \times \mathbf{E} &= 0, \\ \nabla \cdot \mathbf{B} &= 0, \\ \nabla \cdot \mathbf{v} &= 0, \\ \mathbf{j} &= \nabla \times \mathbf{B}.\end{aligned}$$

Flux and Stream Functions

Assuming that the magnetic field and plasma flow are two-dimensional then, to satisfy $\nabla \cdot \mathbf{v} = \nabla \cdot \mathbf{B} = 0$, they must be of the form

$$\mathbf{v} = (\psi_y, -\psi_x, 0) \quad \text{and} \quad \mathbf{B} = (A_y, -A_x, 0), \quad (5.1)$$

where $A(x, y)$ is the flux function and $\psi(x, y)$ is the stream function.

Faraday's Equation

The components of Faraday's equation are

$$\begin{aligned}\partial_x E_z &= 0, \\ \partial_y E_z &= 0,\end{aligned}$$

$$\partial_x E_{\hat{y}} - \partial_y E_{\hat{x}} = 0. \quad (5.2)$$

The first two of these imply that

$$E_{\hat{z}} = \text{constant} = k.$$

Ohm's Law

The components of Ohm's Law are

$$\begin{aligned} E_{\hat{x}} &= 0, \\ E_{\hat{y}} &= 0, \\ E_{\hat{z}} + v_{\hat{x}} B_{\hat{y}} - v_{\hat{y}} B_{\hat{x}} &= \frac{1}{R_m} (\partial_x B_{\hat{y}} - \partial_y B_{\hat{x}}). \end{aligned}$$

The first two of these specify $E_{\hat{x}}$ and $E_{\hat{y}}$, which now satisfy (5.2). With \mathbf{B} and \mathbf{v} of the forms given in (5.1) and noting that $E_{\hat{z}} = k$, the third of these becomes

$$k - \psi_y A_x + \psi_x A_y = -\frac{1}{R_m} (A_{xx} + A_{yy})$$

or

$$\frac{1}{R_m} (A_{xx} + A_{yy}) - \psi_y A_x + \psi_x A_y = -k.$$

The Equation of Motion

The equation of motion can be written as

$$M_A^2 (\mathbf{v} \cdot \nabla) \mathbf{v} = -\nabla \left(\beta p + \frac{1}{2} B^2 \right) + (\mathbf{B} \cdot \nabla) \mathbf{B} + \frac{M_A^2}{R} \nabla^2 \mathbf{v}.$$

The pressure terms in this can be eliminated by taking the curl (see appendix A) to obtain

$$M_A^2 [(\mathbf{v} \cdot \nabla) \omega - (\omega \cdot \nabla) \mathbf{v}] = (\mathbf{B} \cdot \nabla) \mathbf{j} - (\mathbf{j} \cdot \nabla) \mathbf{B} + \frac{M_A^2}{R} \nabla^2 \omega,$$

where $\omega = \nabla \times \mathbf{v}$. As the problem is two-dimensional $\mathbf{j} = j \hat{\mathbf{z}}$, $\omega = \omega \hat{\mathbf{z}}$ and this equation reduces to

$$M_A^2 (\mathbf{v} \cdot \nabla) \omega = (\mathbf{B} \cdot \nabla) j + \frac{M_A^2}{R} \nabla^2 \omega.$$

With \mathbf{B} and \mathbf{v} of the form (5.1) this becomes

$$M_A^2 (\psi_y \partial_x - \psi_x \partial_y) (\psi_{xx} + \psi_{yy}) = (A_y \partial_x - A_x \partial_y) (A_{xx} + A_{yy}) + \frac{M_A^2}{R} (\partial_x^2 + \partial_y^2) (\psi_{xx} + \psi_{yy}).$$

Summary

If the magnetic field and flow have the two-dimensional forms $\mathbf{v} = (\psi_y, -\psi_x, 0)$ and $\mathbf{B} = (A_y, -A_x, 0)$, then the MHD equations reduce to

$$\frac{1}{R_m} (A_{xx} + A_{yy}) - \psi_y A_x + \psi_x A_y = -k \quad (5.3)$$

and

$$M_A^2 (\psi_y \partial_x - \psi_x \partial_y) (\psi_{xx} + \psi_{yy}) = (A_y \partial_x - A_x \partial_y) (A_{xx} + A_{yy}) + \frac{M_A^2}{R} (\partial_x^2 + \partial_y^2) (\psi_{xx} + \psi_{yy}). \quad (5.4)$$

5.2 Asymptotic Solution

Introduction

If we consider a magnetic reconnection scenario that is a perturbation of magnetic annihilation then we can look for solutions to equations (5.3) and (5.4) that are of the form

$$\psi(x, y) = xy + \frac{1}{R} \psi_1(x, y) \dots \quad \text{and} \quad A(x, y) = A_0(y) + \frac{1}{R} A_1(x, y) \dots \quad (5.5)$$

Ohm's Law

For solutions of the form (5.5), equation (5.3) leads to

$$\begin{aligned} \frac{1}{R_m} \left(\frac{1}{R} A_{1xx} + A_0'' + \frac{1}{R} A_{1yy} \right) - \left(x + \frac{1}{R} \psi_{1y} \right) \left(\frac{1}{R} A_{1x} \right) \\ + \left(y + \frac{1}{R} \psi_{1x} \right) \left(A_0' + \frac{1}{R} A_{1y} \right) + O\left(\frac{1}{R^2}\right) = -k \end{aligned}$$

which has zeroth-order part

$$\frac{1}{R_m} A_0'' + y A_0' = -k$$

and first-order part

$$\left(\frac{1}{R_m} \partial_{xx} + \frac{1}{R_m} \partial_{yy} - x \partial_x + y \partial_y \right) A_1 = -A_0' \partial_x \psi_1,$$

provided that $R \gg R_m \gg 1$.

Equation of Motion

With A and ψ of the forms (5.5), (5.4) yields

$$\begin{aligned} M_A^2 \left[\left(x + \frac{1}{R} \psi_{1y} \right) \partial_x - \left(y + \frac{1}{R} \psi_{1x} \right) \partial_y \right] \left(\frac{1}{R} \psi_{1xx} + \frac{1}{R} \psi_{1yy} \right) + O\left(\frac{1}{R^2}\right) \\ = \left[\left(A_0' + \frac{1}{R} A_{1y} \right) \partial_x - \left(\frac{1}{R} A_{1x} \right) \partial_y \right] \left(A_0'' + \frac{1}{R} A_{1xx} + \frac{1}{R} A_{1yy} \right) + \frac{M_A^2}{R} (\partial_x^2 + \partial_y^2) \left(\frac{1}{R} \psi_{1xx} + \frac{1}{R} \psi_{1yy} \right) \end{aligned}$$

The zeroth-order part of this is identically zero and the first-order part is

$$M_A^2 (x \partial_x - y \partial_y) (\partial_{xx} + \partial_{yy}) \psi_1 = A_0' \partial_x (\partial_{xx} + \partial_{yy}) A_1 - A_0''' \partial_x A_1,$$

provided that $R \gg M_A^2 \gg 1$.

Summary

Looking for perturbation solutions to equations (5.3), (5.4) of the form

$$\psi(x, y) = xy + \frac{1}{R} \psi_1(x, y) \dots \quad \text{and} \quad A(x, y) = A_0(y) + \frac{1}{R} A_1(x, y) \dots$$

leads to the zeroth-order equation

$$\frac{1}{R_m} A_0'' + y A_0' = -k \quad (5.6)$$

and first-order equations

$$\begin{aligned} \left(\frac{1}{R_m} \partial_{xx} + \frac{1}{R_m} \partial_{yy} - x \partial_x + y \partial_y \right) A_1 = -A_0' \partial_x \psi_1, \\ M_A^2 (x \partial_x - y \partial_y) (\partial_{xx} + \partial_{yy}) \psi_1 = A_0' \partial_x (\partial_{xx} + \partial_{yy}) A_1 - A_0''' \partial_x A_1. \end{aligned} \quad (5.7)$$

This approach is valid when $R \gg M_A^2 \gg 1$ and $R \gg R_m \gg 1$.

5.3 Zero-Order Equation

The zeroth-order equation, (5.6), can be written as

$$\frac{1}{R_m} \frac{d}{dy} (A'_0) + y (A'_0) = -k,$$

which is the Sonnerup and Priest magnetic annihilation equation examined earlier. The general solution of this is given in appendix D and applying the boundary conditions $A'_0(0) = 0$, $A'_0(1) = 1$ gives

$$A'_0(y) = \frac{yM \left(1, \frac{3}{2}, -\frac{1}{2}R_my^2\right)}{M \left(1, \frac{3}{2}, -\frac{1}{2}R_m\right)}.$$

Expressing the confluent hypergeometric function as a power series (see appendix B) and integrating gives

$$A_0(y) = \frac{y^2}{2M \left(1, \frac{3}{2}, -\frac{1}{2}R_m\right)} \sum_{j=0}^{\infty} \frac{(1)_j \left(-\frac{1}{2}R_my^2\right)^j}{\left(\frac{3}{2}\right)_j (j+1)!}. \quad (5.8)$$

Note that the constant of integration has been dropped as it is simply an additive constant to the flux function.

5.4 First-Order Equations

Introduction

The first-order equations (5.7) contain several parameters and prescribed functions (M_A^2 , R_m and A'_0) and can be simplified slightly by taking

$$y = R_m^{-\frac{1}{2}} Y, \quad x = R_m^{-\frac{1}{2}} X, \quad A'_0 = \kappa B(Y) \quad \text{and} \quad A_1 = \kappa R_m^{\frac{1}{2}} \bar{A}(Y), \quad \psi_1 = \bar{\psi}(Y),$$

where

$$\kappa = \frac{1}{M \left(1, \frac{3}{2}, -\frac{1}{2}R_m\right) R_m^{\frac{1}{2}}} \quad \text{and} \quad B = YM \left(1, \frac{3}{2}, -\frac{1}{2}Y^2\right), \quad (5.9)$$

to obtain

$$\bar{A}_{XX} + \bar{A}_{YY} - X\bar{A}_X + Y\bar{A}_Y = -\bar{\psi}_X B, \quad (5.10)$$

$$X\bar{\psi}_{XXX} + X\bar{\psi}_{XY} - Y\bar{\psi}_{XXY} - Y\bar{\psi}_{YY} = P(B\bar{A}_{XXX} + B\bar{A}_{XY} - \bar{A}_X B_{YY}), \quad (5.11)$$

where

$$P = \frac{1}{M_A^2 M^2 \left(1, \frac{3}{2}, -\frac{1}{2}R_m\right)}.$$

Series Solution

Equations (5.10) and (5.11) form a pair of coupled linear partial differential equations and are difficult to solve in general. We shall look for power series solutions. If the reconnection scenario is taken to be completely symmetric, ie $B_x(x, 0) = B_y(0, y) = v_y(x, 0) = v_x(0, y) = 0$, then A_1 must be an even function (in both x and y) and ψ_1 must be an odd function (in both x and y). Hence we look for solutions of the form

$$\bar{A} = \sum_{j=0}^{\infty} f_j(x) Y^{2j} \quad \text{and} \quad \bar{\psi} = \sum_{j=0}^{\infty} g_j(x) Y^{2j+1}, \quad (5.12)$$

where the f_j and g_j are, respectively, even and odd functions of x . This approach is similar to that of Cowley (1975) and Sonnerup (1988) except that these authors seek series solutions of the full (but inviscid) MHD equations whereas we seek asymptotic solutions of the first order MHD equations.

Series form of B

Expressing the confluent hypergeometric function M as a power series, the function B , defined in (5.9), becomes

$$B = \sum_{j=0}^{\infty} \alpha_j Y^{2j+1},$$

where

$$\alpha_j = \frac{(1)_j (-\frac{1}{2})^j}{(\frac{3}{2})_j j!}.$$

Differentiating this twice gives

$$B_{YY} = \sum_{j=0}^{\infty} \beta_j Y^{2j+1},$$

where

$$\beta_j = \alpha_{j+1} (2j+3)(2j+2).$$

First-Order Ohm's Law

Substituting the power series forms for \bar{A} , $\bar{\psi}$ and B into (5.10) gives

$$\sum_{j=0}^{\infty} f_j'' Y^{2j} + \sum_{j=0}^{\infty} f_{j+1} (2j+2)(2j+1) Y^{2j} - x \sum_{j=0}^{\infty} f_j' Y^{2j} + \sum_{j=1}^{\infty} 2j f_j Y^{2j} = - \sum_{j=1}^{\infty} \left(\sum_{k=0}^{j-1} g_k' \alpha_{j-1-k} \right) Y^{2j}$$

and equating the coefficients of the powers of Y yields

$$f_{j+1} = \frac{1}{(2j+2)(2j+1)} \left[x f_j' - f_j'' - 2j f_j - g_k' \sum_{k=0}^{j-1} \alpha_{j-1-k} g_k' \right]. \quad (5.13)$$

First-Order Equation of Motion

Substituting the power series forms for \bar{A} , $\bar{\psi}$, B and B_{YY} into (5.11) gives

$$\begin{aligned} & \sum_{j=0}^{\infty} [x g_j''' + x g_{j+1}' (2j+3)(2j+2) - g_j'' (2j+1) - g_{j+1} (2j+3)(2j+2)(2j+1)] Y^{2j+1} \\ &= P \sum_{j=0}^{\infty} \left[\sum_{k=0}^j f_k''' \alpha_{j-k} + f_{k+1}' (2k+2)(2k+1) \alpha_{j-k} - f_k' \beta_{j-k} \right] Y^{2j+1} \end{aligned}$$

and equating the coefficients of powers of Y produces

$$\begin{aligned} x g_{j+1}' - (2j+1) g_{j+1} &= \frac{1}{(2j+3)(2j+2)} \left[g_j'' (2j+1) - x g_j''' + \right. \\ & \quad \left. P \sum_{k=0}^j f_k''' \alpha_{j-k} + f_{k+1}' (2k+2)(2k+1) \alpha_{j-k} - f_k' \beta_{j-k} \right]. \quad (5.14) \end{aligned}$$

Summary

1. Equations (5.13) and (5.14) form a pair of recurrence relations; given f_0 and g_0 , these two equations can be used to generate all the other f_j and g_j . Solutions for \bar{A} and $\bar{\psi}$ can thus be derived from two arbitrary functions, f_0 and g_0 .
2. Changing from \bar{A} , $\bar{\psi}$ back to the original variables gives

$$A_1 = \kappa R_m^{\frac{1}{2}} \sum_{j=0}^{\infty} f_j (R_m^{\frac{1}{2}} x) R_m^j y^{2j} \quad \text{and} \quad \psi_1 = R_m^{\frac{1}{2}} \sum_{j=0}^{\infty} g_j (R_m^{\frac{1}{2}} x) R_m^j y^{2j+1} \quad (5.15)$$

and in appendix G it is proved that both of these series converge on the interval of interest, $|y| \leq 1$.

3. From (5.15), the first-order magnetic field in the \hat{y} direction is

$$B_{\hat{y}1}(x, 0) = \partial_x A_1(x, 0) = \kappa R_m f'_0(R_m^{\frac{1}{2}} x) \quad (5.16)$$

and the first-order flow in the \hat{x} direction is

$$v_{\hat{x}1}(x, 0) = \partial_y \psi_1(x, 0) = R_m^{\frac{1}{2}} g_0(R_m^{\frac{1}{2}} x), \quad (5.17)$$

so the arbitrary functions f_0 , g_0 can be determined from boundary conditions on $v_{\hat{x}1}(x, 0)$ and $B_{\hat{y}1}(x, 0)$.

5.5 Series Solutions for f and g

Introduction

If the boundary conditions $B_{\hat{y}1}(x, 0)$ and $v_{\hat{x}1}(x, 0)$ are of the form

$$B_{\hat{y}1}(x, 0) = \sum_{i=1}^{\infty} a_i^* x^{2i-1} \quad \text{and} \quad v_{\hat{x}1}(x, 0) = \sum_{i=0}^{\infty} b_i^* x^{2i+1}, \quad (5.18)$$

then equations (5.16) and (5.17) imply that

$$f_0 = \sum_{i=1}^{\infty} a_{0,i} X^{2i} \quad \text{and} \quad g_0 = \sum_{i=0}^{\infty} b_{0,i} X^{2i+1}, \quad (5.19)$$

where

$$a_{0,i} = -\frac{a_i^*}{\kappa R_m^{i+\frac{1}{2}}} \quad \text{and} \quad g_{0,i} = \frac{b_i^*}{R_m^{i+\frac{1}{2}}}. \quad (5.20)$$

The constant of integration in the expression for f_0 has been dropped as it is simply an additive constant to the flux function.

Series Solutions for f_{j+1}

If all the previous f_j and g_j are power series of the forms

$$f_j = \sum_{i=0}^{\infty} a_{j,i} x^{2i} \quad \text{and} \quad g_j = \sum_{i=0}^{\infty} b_{j,i} x^{2i+1},$$

then equation (5.13) becomes

$$f_{j+1}(x) = \sum_{i=0}^{\infty} \frac{1}{(2j+2)(2j+1)} \left[2(i-j)a_{j,i} - (2i+2)(2i+1)a_{j,i+1} - \sum_{k=0}^{j-1} \alpha_{j-1-k} b_{k,i}(2i+1) \right] x^{2j}$$

which can be written

$$f_{j+1}(x) = \sum_{i=0}^{\infty} a_{j+1,i} X^{2i},$$

where

$$a_{j+1,i} = \frac{1}{(2j+2)(2j+1)} \left[2(i-j)a_{j,i} - (2i+2)(2i+1)a_{j,i+1} - \sum_{k=0}^{j-1} \alpha_{j-1-k} b_{k,i}(2i+1) \right]. \quad (5.21)$$

Series Solutions for g_{j+1}

If all the previous f_j and g_j are of power series form then equation (5.14) becomes

$$xg'_{j+1} - (2j+1)g_{j+1} = \sum_{i=0}^{\infty} c_{j,i} x^{2i+1}, \quad (5.22)$$

where

$$c_{j,i} = \frac{2i+2}{(2j+3)(2j+2)} \left[2(2i+3)(j-i)b_{j,i+1} + P \sum_{k=0}^j (2i+4)(2i+3)\alpha_{j-k}a_{k,i+2} + (2k+2)(2k+1)\alpha_{j-k}a_{k+1,i+1} - \beta_{j-k}a_{k,i+1} \right]. \quad (5.23)$$

Solving (5.22) by means of an integrating factor yields

$$g_{j+1} = \sum_{\substack{i=0 \\ i \neq j}}^{\infty} \frac{c_{j,i}}{2(i-j)} x^{2i+1} + c_{j,j} x^{2j+1} \log x + c_j^* x^{2j+1},$$

where the c_j^* are arbitrary constants. The log-type singularities will give unphysical behaviour near $x=0$ and to avoid this we must have

$$c_{j,j} = 0, \quad (5.24)$$

leaving

$$g_{j+1} = \sum_{\substack{i=0 \\ i \neq j}}^{\infty} \frac{c_{j,i}}{2(i-j)} x^{2i+1} + c_j^* x^{2j+1},$$

which can be written as

$$g_{j+1}(x) = \sum_{i=0}^{\infty} b_{j+1,i} x^{2i+1},$$

where

$$b_{j+1,i} = \begin{cases} \frac{c_{j,i}}{2(i-j)} & i \neq j \\ c_j^* & i = j. \end{cases} \quad (5.25)$$

Note that with $c_{j,i}$ defined in (5.23), the condition (5.24) becomes

$$\sum_{k=0}^j (2i+4)(2i+3)\alpha_{j-k}a_{k,i+2} + (2k+2)(2k+1)\alpha_{j-k}a_{k+1,i+1} - \beta_{j-k}a_{k,i+1} = 0. \quad (5.26)$$

Summary

1. If the functions f_0 and g_0 are power series in x then all the f_j and g_j will also be power series in x .
2. To avoid unphysical log-type singularities the coefficients $a_{j,i}$ and $b_{j,i}$ must satisfy equation (5.26). This suggests that there are restrictions on the form of the boundary conditions, B_{j1} and $v_{\pm 1}$.
3. The first-order solutions (5.12) can now be written as

$$\bar{A} = \sum_{j=0}^{\infty} \sum_{i=0}^{\infty} a_{j,i} Y^{2j} x^{2i} \quad \text{and} \quad \bar{\psi} = \sum_{j=0}^{\infty} \sum_{i=0}^{\infty} b_{j,i} Y^{2j+1} x^{2i+1}$$

and changing back to the original variables produces

$$A_1 = \kappa R_m^{\frac{1}{2}} \sum_{j=0}^{\infty} \sum_{i=0}^{\infty} a_{j,i} R_m^{i+j} y^{2j} x^{2i} \quad \text{and} \quad \psi_1 = R_m \sum_{j=0}^{\infty} \sum_{i=0}^{\infty} b_{j,i} R_m^{i+j} y^{2j+1} x^{2i+1}. \quad (5.27)$$

Given the boundary conditions (5.18) then the $a_{0,i}$ and $b_{0,i}$ can be obtained from (5.20) which then allows equations (5.25) and (5.26) to be used to give all the remaining $a_{j,i}$ and $b_{j,i}$.

4. The arbitrary constants c_j^* that occur in each g_j are determined by applying additional boundary conditions. The simplest additional boundary conditions to apply involve specifying v_{y1} or v_{x1} on $x = 1$ or $y = 1$.

5.6 Boundary Conditions

Physically, the only first-order boundary condition of any importance is $B_{y1}(x, 0)$ as the behaviour of the zeroth-order solutions will dominate on all other boundaries.

5.7 Solutions for the Flux and Stream Functions

With the series solutions (5.27) and (5.8), the flux and stream functions,

$$A(x, y) = A_0(y) + \frac{1}{R} A_1(x, y) \quad \text{and} \quad \psi(x, y) = xy(y) + \frac{1}{R} \psi_1(x, y),$$

become

$$A = \frac{1}{2} R_m^{\frac{1}{2}} \kappa y^2 \sum_{j=0}^{\infty} \frac{(1)_j (-\frac{1}{2} R_m y^2)^j}{(\frac{3}{2})_j (j+1)!} + \frac{\kappa R_m^{\frac{1}{2}}}{R} \sum_{j=0}^{\infty} \sum_{i=0}^{\infty} a_{j,i} R_m^{i+j} y^{2j} x^{2i} \quad (5.28)$$

and

$$\psi = xy + \frac{R_m}{R} \sum_{j=0}^{\infty} \sum_{i=0}^{\infty} b_{j,i} R_m^{i+j} y^{2j+1} x^{2i+1}. \quad (5.29)$$

5.8 Magnetic Field Lines

Magnetic field lines are given by plotting the contours of the flux function. Due to the complicated nature of the solution (5.28) this can only be done numerically. However, close to the origin (5.28) reduces to

$$A = \frac{1}{2} R_m^{\frac{1}{2}} \kappa y^2 + \frac{\kappa R_m^{\frac{1}{2}}}{R} a_{0,n} R_m^n x^{2n},$$

where $a_{0,n}$ is the first non-zero coefficient in $f_0 = a_{0,1}x^2 + a_{0,2}x^4 \dots$. From (5.20) this becomes

$$A = \frac{1}{2} R_m^{\frac{1}{2}} \kappa y^2 - \frac{a_n^*}{R n R_m^n} x^{2n},$$

where a_n^* is the first non-zero coefficient in $B_{y1} = a_1^*x + a_2^*x^3 \dots$. Since A is zero at the origin the equation of the magnetic field line through the origin is given by

$$0 = \frac{1}{2} R_m^{\frac{1}{2}} \kappa y^2 - \frac{a_n^*}{R n R_m^n} x^{2n},$$

which can be rearranged to give

$$y = \left(\frac{2a_n^*}{\kappa R_m^{n+\frac{1}{2}} R n} \right)^{\frac{1}{2}} x^n. \quad (5.30)$$

From this equation we find that if a_1^* is non-zero (so that $n = 1$) the magnetic field through the origin is a straight line, giving an x-type neutral point. However, if a_1^* is zero (so that $n > 1$) the magnetic field through the origin touches the x-axis, giving a magnetic cusp.

After applying the Kummer identity to the definition of κ in (5.9), the asymptotic approximation $M(a, b, z) \rightarrow \Gamma(b) e^z z^{a-b} / \Gamma(a)$ as $z \rightarrow \infty$ gives

$$\kappa \rightarrow R_m^{\frac{1}{2}} \quad \text{as} \quad R_m \rightarrow \infty,$$

so equation (5.30) becomes

$$y = \left(\frac{2a_n^*}{R_m^{n+1} R n} \right)^{\frac{1}{2}} x^n \quad \text{as} \quad R_m \rightarrow \infty.$$

This implies that as R_m increases the field line through the origin moves towards the x -axis.

5.9 Necessary Conditions

If f_0 and g_0 are power series of the form (5.19) then the first two conditions given by (5.26) are

$$\begin{aligned} 12a_{0,2} + 2a_{1,1} + 2a_{0,1} &= 0, \\ -4a_{0,3} + \frac{4}{3}a_{1,2} - \frac{4}{3}a_{0,2} + 12a_{1,3} + 12a_{2,2} &= 0. \end{aligned}$$

Using (5.21) to express the $a_{i,j}$ in terms of $a_{0,i}$ and $b_{0,i}$ these conditions become

$$a_{0,1} = 0, \quad (5.31)$$

$$\frac{16}{3}a_{0,2} - 58a_{0,3} + 504a_{0,4} - 5b_{0,2} = 0. \quad (5.32)$$

Since $a_{0,1} = 0$, equation (5.20) implies that a_1^* must also be zero. Hence, in the analysis of the previous section we must have $n > 1$ and so the magnetic field at the origin forms a magnetic cusp rather than an x -type neutral point.

5.10 Examples

Introduction

In this section the series solution for A is implemented in a computer program and experimented with. It was found that as R_m is increased, more terms have to be taken in the series solution to ensure convergence and the slower the programs become. This puts a practical limit of about $R_m = 100$ on the investigations. The simplest boundary conditions possible,

$$B_{\bar{y}1} = a_2^* x^3 \quad \text{and} \quad v_{\bar{x}1} = -\frac{16}{30} a_2^* R_m^{\frac{1}{2}} \kappa^{-1} x^5,$$

where a_2^* is an arbitrary constant, were used and these give

$$f_0 = -\frac{1}{2} a_2^* \kappa^{-1} R_m^{-\frac{5}{2}} x^4 \quad \text{and} \quad g_0 = -\frac{16}{30} a_2^* \kappa^{-1} R_m^{-\frac{5}{2}} x^5,$$

which satisfy the conditions (5.31) and (5.32). All the other conditions given by (5.26) are satisfied identically, due to the truncated power series forms of f_0 and g_0 . The c_j^* are taken to be zero on the grounds that they have no significant effect on the overall behaviour of the solution.

Note that although the boundary condition for $v_{\bar{x}1}$ is a function of R_m , the previous result that $\kappa \rightarrow R_m^{\frac{1}{2}}$ as $R_m \rightarrow \infty$ shows that

$$v_{\bar{x}1} \rightarrow -\frac{16}{30} a_2^* x^5$$

as R_m becomes large.

Varying R_m

With $M_A^2 = a_2^* = 1$ and $R = 10^3$, the results of varying R_m are plotted in figure 5.1. As R_m is increased the separatrix moves closer to the x -axis (agreeing with the analytical result in section (5.8)) and the magnetic field becomes more and more similar to the magnetic annihilation configuration.

The reconnection rate $R_E = j(0,0)/R_m$ is plotted in figure 5.2. As R_m is increased the reconnection rate tends towards 1.

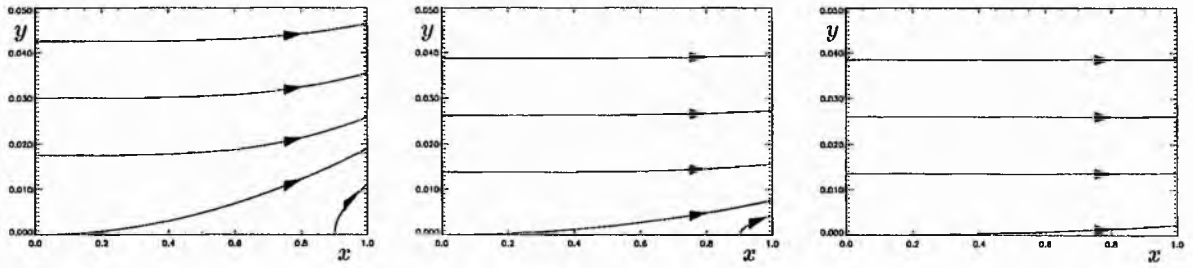


Figure 5.1: Magnetic field lines for $R_m = 10^0, 10^1, 10^2$. (All with $R = 10^3$, and $a_2^* = 1$)

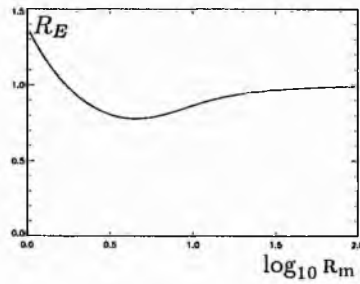


Figure 5.2: The reconnection rate as a function of R_m .

Varying the Boundary Condition

With $R_m = 10^2$ and $R = 10^3$ the value of a_2^* was varied to give the results plotted in figure 5.3. As a_2^* is increased the separatrix widens out and eventually reverse current appears on the x -axis. The reverse current only appears when a_2^* is so large that the idea of this field being a perturbation starts to look a little shaky. However, investigations seem to indicate that the value of a_2^* at which reverse currents occur becomes smaller as R_m increases.

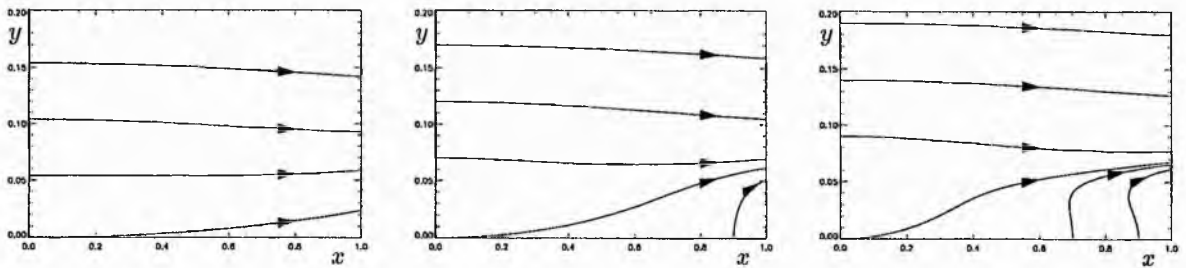


Figure 5.3: Magnetic field lines for $a_2^* = 10^2, 10^3, 10^4$. (All with $R = 10^3$ and $R_m = 10^2$.)

Chapter 6

Magnetic Reconnection in a Viscous Plasma

6.1 Introduction

If viscous forces are assumed to be dominant, then the MHD equation of motion reduces to

$$\nabla^2 \mathbf{v} = 0. \quad (6.1)$$

This assumption has decoupled the equation of motion from the induction equation and it is now possible to solve the above equation of motion for \mathbf{v} , insert it into the induction equation

$$\frac{1}{R_m} \nabla^2 \mathbf{B} + \nabla \times (\mathbf{v} \times \mathbf{B}) = 0$$

and solve for the magnetic field. This approach may be compared with kinematic reconnection where the flow is prescribed, the equation of motion ignored and the induction equation solved to obtain the magnetic field.

6.2 Plasma Flow

Solving the Equation of Motion

Using the vector identity $\nabla \times (\nabla \times \mathbf{v}) = \nabla (\nabla \cdot \mathbf{v}) - \nabla^2 \mathbf{v}$, equation (6.1) becomes

$$\nabla (\nabla \cdot \mathbf{v}) - \nabla \times \boldsymbol{\omega} = 0 \quad (6.2)$$

where $\boldsymbol{\omega} = \nabla \times \mathbf{v}$ is the vorticity. For simplicity the flow can be taken to be incompressible so that $\nabla \cdot \mathbf{v} = 0$. If the flow is also taken to be two-dimensional then this implies $\mathbf{v} = \nabla \times \psi(x, y) \hat{\mathbf{z}} = (\psi_y, -\psi_x, 0)$ and equation (6.2) becomes

$$\psi_{xx} + \psi_{yy} = 0. \quad (6.3)$$

Looking for separable solutions of the form $\psi(x, y) = X(x)Y(y)$ leads to

$$X'' - \ell X = 0 \quad \text{and} \quad Y'' + \ell Y = 0$$

where ℓ is an arbitrary constant. These equations have three different cases, depending on whether ℓ is greater than, less than or equal to zero and give the solution

$$\psi = \begin{cases} (ax + b)(cy + d) & \ell = 0 \\ (a \sin \mu x + b \cos \mu x)(c \sinh \mu y + d \cosh \mu y) & \ell = -\mu^2 \\ (a \sinh \lambda x + b \cosh \lambda x)(c \sin \lambda y + d \cos \lambda y) & \ell = \lambda^2, \end{cases}$$

where a, b, c and d are arbitrary constants.

Boundary Conditions

Taking the scenario to be symmetric, so that only the quadrant $0 \leq x, y \leq 1$ has to be considered, gives the boundary conditions $v_{\hat{x}} = 0$ on $x = 0$ and $v_{\hat{y}} = 0$ on $y = 0$. To satisfy these conditions the solution for the stream function reduces to

$$\psi = \begin{cases} axy & \ell = 0 \\ a \sin \mu x \sinh \mu y & \ell = -\mu^2 \\ a \sinh \lambda x \sin \lambda y & \ell = \lambda^2. \end{cases}$$

Note that

1. For the $\ell = 0$ case, $\psi = axy$ giving the simple stagnation-point flow $\mathbf{v} = a(x, -y, 0)$.
2. As equation (6.3) is linear, these three basic solutions can be superimposed to satisfy boundary conditions on $y = 1$ and $x = 1$.

6.3 Magnetic Field

Introduction

For a two-dimensional model, where $\mathbf{B} = (A_y, -A_x, 0)$, Ohm's and Faraday's laws (or equivalently the induction equation) reduce to

$$\frac{1}{R_m} A_{xx} + \frac{1}{R_m} A_{yy} - v_{\hat{x}} A_x - v_{\hat{y}} A_y = -k \quad (6.4)$$

where $k = E_{\hat{z}}$ is the constant electric field in the \hat{z} direction. If $v_{\hat{y}}$ and $v_{\hat{x}}$ are known functions then this gives a second-order inhomogeneous partial differential equation for A which can in principle be solved subject to prescribed boundary conditions. Considering a symmetric situation, so that only the quadrant $0 \leq x, y \leq 1$ has to be considered, gives the boundary conditions $B_{\hat{x}} = 0$ on $y = 0$ and $B_{\hat{y}} = 0$ on $x = 0$ or

$$A_y = 0 \quad \text{on} \quad y = 0 \quad \text{and} \quad A_x = 0 \quad \text{on} \quad x = 0$$

as boundary conditions for the flux function. There are a variety of possible forms for the two remaining boundary conditions.

Assuming that the plasma flow is the simple stagnation-point flow $\mathbf{v} = (x, -y, 0)$, equation (6.4) becomes

$$\frac{1}{R_m} A_{xx} + \frac{1}{R_m} A_{yy} - x A_x + y A_y = -k. \quad (6.5)$$

Solving for the Flux Function

The simplest way of solving equation (6.5) is to find the complementary function and a particular integral. Their sum then gives the general solution.

Particular Integral

If the particular integral is considered to be a function of y only, equation (6.5) reduces to

$$\frac{1}{R_m} A'' + y A' = -k.$$

This is the magnetic annihilation equation and, as shown in appendix D, has the general solution

$$A' = -R_m k y M \left(1, \frac{3}{2}, -\frac{1}{2} R_m y^2 \right) + c_0 e^{-\frac{1}{2} R_m y^2}.$$

Applying the boundary condition $A'(0) = 0$ gives $c_0 = 0$ and so

$$A' = -R_m k y M \left(1, \frac{3}{2}, -\frac{1}{2} R_m y^2 \right).$$

To obtain A , the Kummer function in the above equation can be written as a power series and integrated term by term or, alternatively, the solution can be expressed as

$$A = -R_m k \int_0^y \xi M \left(1, \frac{3}{2}, -\frac{1}{2} R_m \xi^2 \right) d\xi \quad (6.6)$$

and evaluated by numerical methods.

Complementary Function

The homogeneous equation,

$$\frac{1}{R_m} A_{xx} + \frac{1}{R_m} A_{yy} - x A_x + y A_y = 0,$$

is separable and looking for solutions of the form $A(x, y) = X(x)Y(y)$ leads to

$$\frac{1}{R_m} X'' - x X' - \lambda X = 0 \quad \text{and} \quad \frac{1}{R_m} Y'' + y Y' + \lambda Y = 0,$$

where λ is an arbitrary constant. As shown in appendix C these equations have general solutions

$$X = c_0 M \left(\frac{\lambda}{2}, \frac{1}{2}, \frac{1}{2} R_m x^2 \right) + c_1 x M \left(\frac{1}{2} + \frac{\lambda}{2}, \frac{3}{2}, \frac{1}{2} R_m x^2 \right)$$

and

$$Y = k_0 e^{-\frac{1}{2} R_m y^2} M \left(\frac{1}{2} - \frac{\lambda}{2}, \frac{1}{2}, \frac{1}{2} R_m y^2 \right) + k_1 y e^{-\frac{1}{2} R_m y^2} M \left(1 - \frac{\lambda}{2}, \frac{3}{2}, \frac{1}{2} R_m y^2 \right).$$

The boundary condition $A_x(0, y) = 0$ implies that $X'(0) = 0$ giving $c_1 = 0$. Similarly, the boundary condition $A_y(x, 0) = 0$ implies that $Y'(0) = 0$ giving $k_1 = 0$. The complementary function is thus

$$A_{cf} = \sum_{\text{all } \lambda} c_\lambda M \left(\frac{\lambda}{2}, \frac{1}{2}, \frac{1}{2} R_m x^2 \right) e^{-\frac{1}{2} y^2} M \left(\frac{1}{2} - \frac{\lambda}{2}, \frac{1}{2}, \frac{1}{2} R_m y^2 \right),$$

where the λ and c_λ are determined by conditions on the outer boundaries.

General Solution

The general solution can be written as

$$A(x, y) = -k A_{pi}(y) + A_{cf}(x, y) \quad (6.7)$$

where

$$A_{pi}(y) = R_m \int_0^y \xi M \left(1, \frac{3}{2}, -\frac{1}{2} R_m \xi^2 \right) d\xi, \quad A_{cf}(x, y) = \sum_{\lambda} c_\lambda X_\lambda(x) Y_\lambda(y)$$

and

$$X_\lambda(x) = M \left(\frac{1}{2} \lambda, \frac{1}{2}, \frac{1}{2} R_m x^2 \right), \quad Y_\lambda(y) = e^{-\frac{1}{2} R_m y^2} M \left(\frac{1}{2} - \frac{1}{2} \lambda, \frac{1}{2}, \frac{1}{2} R_m y^2 \right). \quad (6.8)$$

Outer Boundary Conditions

Applying the boundary condition $B_y = 0$ on $y = 1$ to the general solution (6.7) leads to

$$\partial_x A_{cf}(x, 1) = \sum_{\lambda} X'_{\lambda}(x) Y_{\lambda}(1) = 0,$$

which is only possible if $Y_{\lambda}(1) = 0$. Using (6.8) this condition becomes

$$M\left(\frac{1}{2} - \frac{\lambda}{2}, \frac{1}{2}, \frac{1}{2} R_m\right) = 0,$$

which will only be satisfied by certain values of λ denoted by λ_n . The complementary function can thus be written as

$$A_{cf}(x, y) = \sum_{n=0}^{\infty} c_n X_n(x) Y_n(y) \quad (6.9)$$

where

$$X_n(x) = M\left(\frac{1}{2} \lambda_n, \frac{1}{2}, \frac{1}{2} R_m x^2\right), \quad Y_n(y) = e^{-\frac{1}{2} R_m y^2} M\left(\frac{1}{2} - \frac{1}{2} \lambda_n, \frac{1}{2}, \frac{1}{2} R_m y^2\right) \quad (6.10)$$

and the λ_n satisfy

$$M\left(\frac{1}{2} - \frac{1}{2} \lambda_n, \frac{1}{2}, \frac{1}{2} R_m\right) = 0. \quad (6.11)$$

Although the set of functions Y_n are not mutually orthogonal, appendix F shows that as $Y'_n(0) = Y_n(1) = 0$ there is an "orthogonal" function

$$Y_n^*(y) = e^{\frac{1}{2} R_m y^2} Y_n(y) = M\left(\frac{1}{2} - \frac{1}{2} \lambda_n, \frac{1}{2}, \frac{1}{2} R_m y^2\right) \quad (6.12)$$

such that

$$\int_0^1 Y_n(y) Y_m^*(y) dy \begin{cases} = 0 & n \neq m \\ \neq 0 & n = m. \end{cases}$$

Note that from (6.11) this function will satisfy $Y_n^*(1) = 0$.

The last boundary condition is taken to be $B_y(1, y) = f(y)$ so that, when applied to (6.7), we obtain

$$-\partial_x A_{cf}(1, y) = -\sum_{n=0}^{\infty} c_n X'_n(1) Y_n(y) = f(y).$$

This can now be multiplied by $Y_n^*(y)$ and integrated from 0 to 1 to give

$$c_n = \frac{-\int_0^1 f(y) Y_n^*(y) dy}{X'_n(1) \int_0^1 Y_n Y_n^* dy}. \quad (6.13)$$

The solution for the flux function is not yet complete as k is still a free parameter. However, applying the boundary condition $B_x(0, 1) = 1$ (which arises from the non-dimensionalisation) to (6.7) allows k to be determined as

$$k = \frac{\partial_y A_{cf}(0, 1) - 1}{A'_{pi}(1)}.$$

With A_{cf} of the form (6.9) and noting that $X(0) = M(\frac{1}{2} \lambda_n, \frac{1}{2}, 0) = 1$ this becomes

$$k = \frac{\sum_{n=0}^{\infty} c_n Y'_n(0) - 1}{A'_{pi}(1)}. \quad (6.14)$$

Magnetic Field Near the Origin

Using the power series representation of the Kummer function we find that near the origin the solutions (6.6) and (6.10) become

$$A_{pi} \approx -\frac{1}{2}R_m y^2, \quad X_n \approx 1 + \frac{1}{2}\lambda_n R_m x^2, \quad Y_n \approx 1 - \frac{1}{2}\lambda_n R_m y^2$$

and hence

$$B_{\bar{y}} = -A_x = \sum_{n=0}^{\infty} X'_n Y_n \approx -R_m x \sum_{n=0}^{\infty} c_n \lambda_n$$

and

$$B_{\bar{x}} = A_y = A'_{pi} + \sum_{n=0}^{\infty} X_n Y'_n \approx -R_m y \left(\frac{1}{2}k + \sum_{n=0}^{\infty} c_n \lambda_n \right).$$

The field lines near the origin are thus given by

$$\frac{dy}{dx} = \frac{B_{\bar{y}}}{B_{\bar{x}}} = \frac{x \sum_{n=0}^{\infty} c_n \lambda_n}{y \left(\frac{1}{2}k + \sum_{n=0}^{\infty} c_n \lambda_n \right)}$$

or

$$\frac{dy}{dx} = \frac{\kappa x}{y} \quad \text{where} \quad \kappa = \frac{\sum_{n=0}^{\infty} c_n \lambda_n}{\left(\frac{1}{2}k + \sum_{n=0}^{\infty} c_n \lambda_n \right)}.$$

This equation can be solved to give $y^2 = \kappa x^2 + \ell_0$ where ℓ_0 is an arbitrary constant. At the origin ℓ_0 must be zero and so the equation of the field lines through the origin is $y^2 = \kappa x^2$ or $y = \pm\sqrt{\kappa}x$. This implies that the magnetic field near the origin takes the form of an x-point and that the angle between the arms of the x is governed by the value of κ .

6.4 Large R_m

Introduction

In this section we examine how the flux function and the magnetic field behave as R_m becomes large.

The λ_n

As R_m tends to infinity the asymptotic approximation

$$M(a, b, z) \rightarrow \frac{\Gamma(b)}{\Gamma(a)} e^z z^{a-b} \quad \text{as } z \rightarrow \infty \quad (6.15)$$

implies that the equation defining the λ_n , (6.11), becomes

$$\frac{\Gamma\left(\frac{1}{2}\right) \left(\frac{1}{2}R_m\right)^{-\frac{\lambda}{2}}}{\Gamma\left(\frac{1}{2} - \frac{\lambda}{2}\right)} = 0.$$

This will only be satisfied if

$$\frac{1}{2} - \frac{\lambda}{2} = -n \quad n = 0, 1, 2, \dots$$

and so

$$\lambda_n \rightarrow 2n + 1 \quad n = 0, 1, 2, \dots \quad \text{as } R_m \rightarrow \infty.$$

The X_n

Applying $\lambda_n \rightarrow 2n + 1$ and the asymptotic approximation (6.15) to equation (6.10) yields

$$X_n \rightarrow \frac{\Gamma\left(\frac{1}{2}\right)}{\Gamma\left(n + \frac{1}{2}\right)} e^{\frac{1}{2}R_m x^2} \left(\frac{1}{2}R_m x^2\right)^{-n}.$$

The Y_n^*

If $\lambda_n \rightarrow 2n + 1$ then $Y_n^* = M(\frac{1}{2} - \frac{1}{2}\lambda_n, \frac{1}{2}, \frac{1}{2}R_m y^2)$ becomes

$$Y_n^* \rightarrow M\left(-n, \frac{1}{2}, \frac{1}{2}R_m y^2\right) \quad \text{as } R_m \rightarrow \infty$$

and since $M(-n, b, z)$ (where n is a positive integer and b is non-integer) is a polynomial of order n this implies

$$Y_n^* \rightarrow a_n (R_m y^2)^n \quad \text{as } R_m \rightarrow \infty.$$

This result appears to contradict the boundary condition $Y(1) = 0$ but numerical solutions for Y_n^* as R_m becomes large show that this result is correct and that a boundary layer forms at $y = 1$ so that $Y_n^*(1)$ is always zero. The thickness of this boundary layer decreases as R_m increases.

The Y_n

As $Y_n = e^{-\frac{1}{2}R_m y^2} Y_n^*$ then making use of the above result for the asymptotic behaviour of Y_n^* gives

$$Y_n \rightarrow a_n e^{-\frac{1}{2}R_m y^2} (R_m y^2)^n \quad \text{as } R_m \rightarrow \infty.$$

The c_n

Using the asymptotic forms of Y_n and Y_n^* in (6.13) gives

$$c_n \rightarrow \frac{-\int_0^1 f(x) y^{2n} dy}{a_n X_n'(1) \left(\frac{1}{2}R_m\right)^n \int_0^1 e^{-R_m y^2} y^{4n} dy} \quad \text{as } R_m \rightarrow \infty. \quad (6.16)$$

Since

$$\int_0^1 e^{-R_m y^2} y^{2N} dy \rightarrow (2N-1)!! 2^{-2N} R_m^{-N-\frac{1}{2}} \quad \text{as } R_m \rightarrow \infty$$

(which is proved in appendix H) equation (6.16) becomes

$$c_n \rightarrow \frac{-2^{2n} \left(\frac{1}{2}R_m\right)^{n+\frac{1}{2}} \int_0^1 f(x) y^{2n} dy}{a_n X_n'(1) (4n-1)!!} \quad \text{as } R_m \rightarrow \infty$$

and using of the asymptotic form of X_n we obtain

$$c_n \rightarrow \frac{-2^{2n} \Gamma\left(n + \frac{1}{2}\right) \left(\frac{1}{2}R_m\right)^{n+\frac{1}{2}} \int_0^1 f(x) y^{2n} dy}{a_n \Gamma\left(\frac{1}{2}\right) e^{\frac{1}{2}R_m} R_m \left[1 + n \left(\frac{1}{2}R_m\right)^{n-1}\right] (4n-1)!!} \quad \text{as } R_m \rightarrow \infty. \quad (6.17)$$

Electric Field

Using the asymptotic forms of c_n and Y_n in (6.14) we find that

$$k \rightarrow -\frac{1}{A_{pi}'(1)} \quad \text{as } R_m \rightarrow \infty. \quad (6.18)$$

Complementary Function

Using the above asymptotic forms of X_n , Y_n and c_n in (6.9) we find that

$$A_{cf} \rightarrow \sum_{n=0}^{\infty} \frac{-e^{\frac{1}{2}(x^2-y^2-1)} (2xy)^{2n} \left(\frac{1}{2}R_m\right)^{3n-\frac{1}{2}} \int_0^1 f(y) y^{2n} dy}{\left[1 + n \left(\frac{1}{2}R_m\right)^{n-1}\right] (4n-1)!!} \quad \text{as } R_m \rightarrow \infty$$

and, since $x^2 \leq 1$, this implies that $A_{cf} \rightarrow 0$ as R_m becomes large.

Magnetic Field

Since the complementary function tends to zero we find that $A \rightarrow -kA_{pi}(y)$ as R_m becomes large. Making use of (6.18) this becomes

$$A \rightarrow \frac{A_{pi}(y)}{A'_{pi}(1)} \quad \text{as } R_m \rightarrow \infty.$$

From this and (6.6) we find that

$$\mathbf{B} \rightarrow \left(\frac{yM \left(1, \frac{3}{2} - \frac{1}{2}R_m y^2\right)}{M \left(1, \frac{3}{2} - \frac{1}{2}R_m\right)}, 0, 0 \right) \quad \text{as } R_m \rightarrow \infty,$$

which is the same magnetic field as in the steady-state magnetic annihilation model examined earlier. It thus appears that, irrespective of the boundary conditions on $x = 1$, magnetic reconnection of the kind we are investigating in a viscous plasma tends towards magnetic annihilation as R_m becomes large.

Reconnection Rates

As the magnetic field tends towards the magnetic annihilation scenario as R_m becomes large the reconnection and ohmic heating rates must also be the same in this limit, ie

$$R_E \rightarrow 1 \quad \text{and} \quad R_\Omega \rightarrow R_m^{\frac{1}{2}} \quad \text{as } R_m \rightarrow \infty.$$

For R_E this is easily confirmed since, as since $R_E = |k|$, we obtain from (6.18) and (6.6)

$$R_E \rightarrow \frac{1}{M \left(1, \frac{3}{2}, -\frac{1}{2}R_m\right)}$$

and applying the Kummer identity and the asymptotic approximation (6.15) gives $R_E \rightarrow 1$ as $R_m \rightarrow \infty$.

6.5 Numerical Investigation of the Analytical Solution

Introduction

In this section the analytical solution is investigated numerically to see if it behaves as expected in the limit of large R_m . This is slightly difficult because

1. as R_m increases the X_n start to behave as $e^{\frac{1}{2}R_m x^2}$ and become difficult to evaluate accurately, and
2. as R_m is increased, more terms in the solution have to be calculated to give convergence to $f(y)$ on the boundary and this results in unacceptably long running computer programs.

The first of these problems puts a limit of about $R_m = 10^3$ on the investigations. The second problem can be overcome to some extent by choosing certain boundary conditions that give fast convergence at the upper range of R_m . For example, the boundary condition

$$f(y) = e^{-\frac{1}{2} \cdot 10^3 \cdot y^2}$$

requires about 30 terms for convergence at $R_m = 10^2$ and, since Y_0 behaves as $e^{-\frac{1}{2}R_m y^2}$, it only requires one term at $R_m = 10^3$. Note that with this particular boundary condition B_y is only large close to $y = 0$ and we are restricted to investigating very narrow current sheets.

Magnetic Field

With the boundary conditions

$$B_y(1, y) = e^{-\frac{1}{2}10^3 y^2} \quad \text{and} \quad B_x(0, 1) = 1 \quad (6.19)$$

the magnetic field was calculated for various values of R_m and plotted in figure (6.1). As expected the field lines become horizontal as R_m increases and the solution tends towards magnetic annihilation.

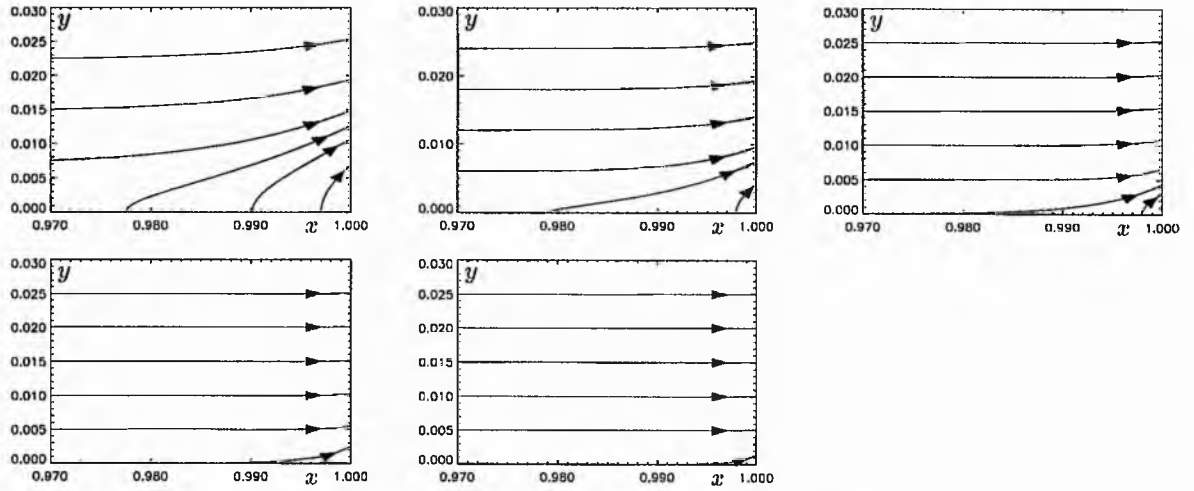


Figure 6.1: Magnetic field lines for $R_m = 10^2, 10^{2.25}, 10^{2.5}, 10^{2.75}, 10^3$.

Reconnection Rate

For the boundary conditions (6.19) the reconnection rate was calculated at various values of R_m and plotted in figure (6.2). As expected, the reconnection rate tends to one as R_m increases.

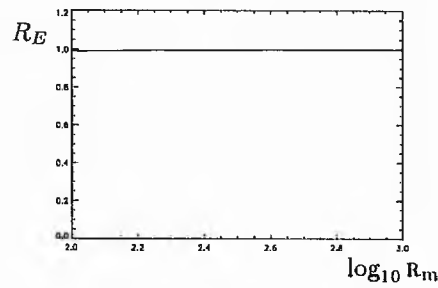


Figure 6.2: The reconnection rate as a function of R_m .

Chapter 7

Magnetic Flipping

7.1 Introduction

As shown in chapter 5, for any two-dimensional, steady-state, model with an incompressible flow the MHD equations reduce to two coupled partial differential equations (the induction and vorticity equations) in two variables (A and ψ).

In the annihilation models examined earlier these equations were decoupled by the assumption that the field lines were straight. The vorticity equation could then be solved for the plasma flow and the induction equation for the magnetic field.

In a slightly different approach, Priest and Forbes (1992) specify the magnetic field as $2\frac{1}{2}$ -dimensional and solve the induction equation for the $2\frac{1}{2}$ -dimensional plasma flow. The solution they obtained possesses a singularity which they then investigated in more detail by constructing approximate patched solutions which include viscous effects.

In the next section it will be shown that the Priest and Forbes solution for the plasma flow can be refined so that it also satisfies the vorticity equation. In the process it becomes apparent that the plasma streamlines are straight. This knowledge simplifies further analysis and allows exact analytical solutions, which include viscous effects, to be found.

7.2 Refining the Priest and Forbes Solution

Following Priest and Forbes (1992), assume that the magnetic field is an x-type neutral point field,

$$\mathbf{B} = (y, x, -\ell), \quad (7.1)$$

that the plasma flow is incompressible,

$$\mathbf{v} = (\psi_y(x, y), -\psi_x(x, y), v_z(x, y)), \quad (7.2)$$

and examine the steady-state, inviscid MHD equations

$$\begin{aligned} \nabla \times \mathbf{E} &= 0, \\ \mathbf{E} + \mathbf{v} \times \mathbf{B} &= \frac{1}{R_m} \mathbf{j}, \\ M_A^2 (\mathbf{v} \cdot \nabla) \mathbf{v} &= -\beta \nabla p + \mathbf{j} \times \mathbf{B}. \end{aligned}$$

Note that as the viscous term in the equation of motion has been dropped, the solution obtained for \mathbf{v} will not possess any viscous effects and is said to be "ideal".

Faraday's Law

The components of Faraday's Law are

$$\begin{aligned}\partial_y E_z &= 0, \\ \partial_x E_z &= 0, \\ \partial_x E_y - \partial_y E_x &= 0.\end{aligned}\tag{7.3}$$

The first two of these imply that $E_z = \text{constant} = k$.

Ohm's Law

With \mathbf{B} and \mathbf{v} of the forms (7.1) and (7.2), the components of Ohm's Law are

$$E_x + \ell \psi_x - x v_z = 0, \tag{7.4}$$

$$E_y + \ell \psi_y + y v_z = 0, \tag{7.5}$$

$$k + x \psi_y + y \psi_x = 0.$$

The third of these is a first-order partial differential equation for ψ which is easily solved by the method of characteristics to obtain

$$\psi = -k \sinh^{-1} \left(\frac{x}{\sqrt{y^2 - x^2}} \right) + g(\xi), \tag{7.6}$$

where $\xi = y^2 - x^2$. The \hat{x} and \hat{y} components of the plasma velocity are then

$$v_x = \frac{kx}{y^2 - x^2} + 2yg' \quad \text{and} \quad v_y = \frac{ky}{y^2 - x^2} + 2xg', \tag{7.7}$$

where the derivative of g is with respect to the independent variable ξ .

Substituting equations (7.4) and (7.5) into (7.3) gives

$$y \partial_x v_z + x \partial_y v_z = 0,$$

which can be solved by the method of characteristics to obtain

$$v_z = f(y^2 - x^2). \tag{7.8}$$

The plasma flow given by components (7.7) and (7.8) is the solution obtained by Priest and Forbes in which the plasma flow is determined to within two arbitrary functions, f and g . Note that the third component of the magnetic field, the arbitrary constant ℓ , does not appear in the solution and is therefore not essential to the problem.

The Equation of Motion

With \mathbf{v} of the form (7.2) the components of the equation of motion are

$$\begin{aligned}M_A^2 (\psi_y \psi_{xy} - \psi_x \psi_{yy}) &= -\beta p_x, \\ M_A^2 (-\psi_y \psi_{xx} + \psi_x \psi_{xy}) &= -\beta p_y, \\ \psi_y \partial_x v_z - \psi_x \partial_y v_z &= 0.\end{aligned}\tag{7.9}$$

Eliminating p by differentiating the first of these with respect to y , the second with respect to x and subtracting, gives

$$(\psi_y \partial_x - \psi_x \partial_y)(\psi_{xx} + \psi_{yy}) = 0.$$

Substituting in the solution for ψ , (7.6), into this produces

$$xy \left(\frac{k^2}{\xi^3} + 4g'g'' \right) + \frac{k(x^2 + y^2)}{\xi} \left(g'''\xi + g'' - \frac{g'}{\xi} \right) = 0,$$

where $\xi = y^2 - x^2$ and the derivatives of g are with respect to ξ . The function g has to satisfy this equation. Since g is a function of ξ this equation can only be consistent if

$$\frac{k^2}{\xi^3} + 4g'g'' = 0 \quad (7.10)$$

leaving

$$g'''\xi + g'' - \frac{g'}{\xi} = 0. \quad (7.11)$$

The second of this pair, (7.11), can be written as

$$\xi^2 (g')'' + \xi (g')' - (g') = 0,$$

which is an Euler-type equation with the general solution

$$g' = a\xi + \frac{b}{\xi}$$

where a and b are two arbitrary constants. Substituting this into (7.10) gives

$$\frac{k^2 - 4b^2}{\xi^3} + 4a^2\xi = 0,$$

which can only be satisfied if $a = 0$ and $b = \pm k/2$.

Thus, the stream function ψ will satisfy the equation of motion if

$$g' = \pm \frac{k}{2\xi},$$

which can be integrated to yield

$$g = \pm \frac{1}{2}k \log \xi + c.$$

In terms of x and y

$$g = \pm \frac{1}{2}k \log (y^2 - x^2) + c$$

and so

$$\psi = -k \sinh^{-1} \left(\frac{x}{\sqrt{y^2 - x^2}} \right) \pm \frac{k}{2} \log (y^2 - x^2) + c.$$

The constant of integration, c , can be dropped as only the derivatives of the stream function are important.

Substituting this solution for ψ into equation (7.9) gives

$$\partial_x v_z \pm \partial_y v_z = 0,$$

which can be solved by the method of characteristics to obtain

$$v_z = h(y \mp x).$$

The only way that this solution can be consistent with (7.8) is if the arbitrary functions h and f are both equal to some constant, c_0 .

Summary

If

$$\mathbf{B} = (y, x, -\ell) \quad \text{and} \quad \mathbf{v} = (\psi_y, -\psi_x, v_z)$$

then the steady-state, incompressible, inviscid MHD equations will only be satisfied if the stream function is

$$\psi = -k \sinh^{-1} \left(\frac{x}{\sqrt{y^2 - x^2}} \right) \pm \frac{k}{2} \log (y^2 - x^2).$$

This gives two possible solutions for the plasma flow, either

$$\mathbf{v} = \left(\frac{k}{y-x}, \frac{k}{y-x}, c_0 \right) \quad \text{or} \quad \mathbf{v} = \left(-\frac{k}{y+x}, \frac{k}{y+x}, c_0 \right).$$

Note that both of these solutions have straight streamlines (parallel to $y = x$ and $y = -x$, respectively) and both have a singularity (on $y = x$ and $y = -x$, respectively).

Rotating Through 45 Degrees

The plasma flows in the above solutions are parallel to $y = \pm x$. It is convenient to rotate everything through 45 degrees so that the plasma flow is along one of the coordinate axes. This leads to

$$\mathbf{B} = (x, -y, -\ell),$$

an x-type neutral point field with separatrices along $x, y = 0$, and either

$$\mathbf{v} = \left(\frac{k}{y}, 0, c_0 \right) \quad \text{or} \quad \mathbf{v} = \left(0, \frac{k}{x}, c_0 \right), \quad (7.12)$$

which have streamlines parallel to and a singularity on $y = 0$ and $x = 0$, respectively.

Singularities and Viscosity

The solutions (7.12) for the flow are singular on $y = 0$ or $x = 0$. This gives unphysical behaviour near these lines which can only be eliminated if some non-ideal effect, not included in the ideal analysis, becomes important near $y = 0$ or $x = 0$, creating a boundary layer.

Physically, note that with $\mathbf{v} = (k/y, 0, 0)$ the plasma above the y -axis is flowing in the positive x -direction and below the y -axis it is flowing in the negative x -direction. These adjacent streams of plasma will not simply slip past each other; they will exert a viscous drag on each other. The effects of viscosity were not included in the previous analysis.

Mathematically, we can note that the viscous term, $M_A^2 \nabla^2 \mathbf{v} / R$, was dropped on the basis that its magnitude is small as R is large. With $\mathbf{v} = (k/y, 0, 0)$ the viscous term is

$$\frac{M_A^2}{R} \nabla^2 \mathbf{v} = \frac{M_A^2}{R} \frac{2}{y^3},$$

which is negligible if y is large but, irrespective of the magnitude of R , becomes non-negligible close to $y = 0$.

From these physical and mathematical arguments, it can be surmised that near $y = 0$ the inviscid approximation becomes untenable and viscous effects become important, creating a viscous boundary layer. This viscous boundary layer will slightly distort the given magnetic field, giving some resistive effects as field lines slip through the plasma.

Boundary Conditions

The solutions (7.12) have k as an arbitrary parameter. The condition that $v = 1$ on the boundary (which arises from the non-dimensionalisation) can be applied to obtain

$$\mathbf{v} = \left(\frac{1}{y}, 0, c_0 \right) \quad \text{or} \quad \mathbf{v} = \left(0, \frac{1}{x}, c_0 \right). \quad (7.13)$$

7.3 Straight Stream Lines

Introduction

The solutions for \mathbf{v} given in (7.12) have streamlines parallel to either the x - or y -axes. It is natural to assume that the streamlines are going to be straight everywhere, both outside and inside the viscous boundary layer. This assumption removes many non-linear terms from the MHD equations and simplifies further analysis. With

$$\mathbf{v} = (v(y), 0, 0) \quad \text{and} \quad \mathbf{B} = \nabla \times A(x, y) \hat{\mathbf{z}} = (A_y, -A_x, 0) \quad (7.14)$$

the steady-state MHD equations become

$$\begin{aligned} \nabla \times \mathbf{E} &= 0, \\ \mathbf{E} + \mathbf{v} \times \mathbf{B} &= \frac{1}{R_m} \mathbf{j}, \\ 0 &= -\nabla \left(\beta p + \frac{1}{2} B^2 \right) + (\mathbf{B} \cdot \nabla) \mathbf{B} + \frac{M_A^2}{R} \nabla^2 \mathbf{v}. \end{aligned} \quad (7.15)$$

From the ideal solutions, given in (7.13), v can be expected to behave like $1/y$ when the effects of viscosity are negligible.

Faraday's Law

The components of Faraday's Law are

$$\begin{aligned} \partial_y E_z &= 0, \\ \partial_x E_z &= 0, \\ \partial_x E_y - \partial_y E_x &= 0. \end{aligned} \quad (7.16)$$

The first two of these imply that $E_z = \text{constant} = k$.

Ohm's Law

With \mathbf{v} and \mathbf{B} of the form (7.14) the components of Ohm's Law are

$$\begin{aligned} E_x &= 0, \\ E_y &= 0, \\ E_z - v A_x &= -\frac{1}{R_m} (A_{xx} + A_{yy}). \end{aligned}$$

The first two of these specify E_x and E_y (which now satisfy (7.16)) and the third becomes

$$\frac{1}{R_m} (A_{xx} + A_{yy}) - v A_x = -k. \quad (7.17)$$

The Equation of Motion

The pressure terms in the equation of motion (7.15) can be eliminated by taking the curl (see appendix A) to obtain the vorticity equation

$$0 = (\mathbf{B} \cdot \nabla) \mathbf{j} - (\mathbf{j} \cdot \nabla) \mathbf{B} + \frac{M_A^2}{R} \nabla^2 \boldsymbol{\omega}.$$

With \mathbf{v} and \mathbf{B} of the forms (7.14) the only non-zero component of this is

$$0 = (A_y \partial_x - A_x \partial_y) (-A_{xx} - A_{yy}) - \frac{M_A^2}{R} v'''$$

and using (7.17) to substitute for $-A_{xx} - A_{yy}$ produces

$$0 = R_m (A_y \partial_x - A_x \partial_y) (k - v A_x) - \frac{M_A^2}{R} v'''$$

or

$$0 = (A_y \partial_x - A_x \partial_y) (v A_x) + \epsilon v''', \quad (7.18)$$

where $\epsilon = M_A^2 / (R R_m)$. Since v is only a function of y this equation can only be consistent if

$$A_x = f(y)$$

implying that

$$A = x f(y) + g(y) \quad (7.19)$$

and reducing equation (7.18) to

$$\epsilon v''' - f^2 v' - f f' v = 0.$$

Back to Ohm's Law

Substituting A of the form (7.19) into equation (7.17) gives

$$\frac{1}{R_m} (x f'' + g'') - v f = -k. \quad (7.20)$$

Since v , f and g are functions of y this will only be consistent if

$$f'' = 0$$

implying that

$$f = k_1 y + k_2$$

(where k_1, k_2 are arbitrary constants) and equation (7.20) becomes

$$\frac{1}{R_m} g'' - v f = -k.$$

Summary

If

$$\mathbf{v} = (v(y), 0, 0) \quad \text{and} \quad \mathbf{B} = (A_y, -A_x, 0)$$

then the MHD equations are satisfied if

$$\begin{aligned} A &= x f(y) + g(y), \\ f &= k_1 y + k_2, \\ \frac{1}{R_m} g'' - v f &= -k, \\ \epsilon v''' - f^2 v' - f f' v &= 0, \end{aligned}$$

where k_1, k_2 are arbitrary constants, k is the electric field in z -direction and

$$\epsilon = \frac{M_A^2}{RR_m}.$$

Note that ϵ becomes small if R or R_m become large.

Boundary Conditions

As $B_y = f(y) = -k_1 y - k_2$, assuming that B_y is an odd function (so that only the region $0 \leq y \leq 1$ has to be considered) and that $B_y(1) = -1$ (arising from the non-dimensionalisation) gives $k_1 = 1$ and $k_2 = 0$. Thus

$$\mathbf{B} = (x + g', -y, 0) \quad \text{and} \quad \mathbf{v} = (v, 0, 0)$$

where

$$\begin{aligned} \epsilon v''' - y^2 v' - yv &= 0, \\ \frac{1}{R_m} g'' &= yv - k. \end{aligned} \quad (7.21)$$

The boundary conditions for v are

$$v(0) = 0, \quad v''(0) = 0 \quad \text{and} \quad v(1) = 1. \quad (7.22)$$

The first two of these arise from assuming v to be an odd function and the third from the non-dimensionalisation.

The boundary conditions for g are

$$g'(0) = 0 \quad \text{and} \quad g'(1) = 0.$$

The first of these ensures that B_x is an odd function in y and the second ensures that B_x on the boundary is the same as the ideal case.

There is an alternative outer boundary condition for g , namely $g''(1) = 0$, which is chosen so that $\mathbf{j} = -(A_{xx} + A_{yy})\hat{\mathbf{z}} = -g''\hat{\mathbf{z}}$ is zero on the boundary. It will be shown later that both outer boundary conditions give the same reconnection rates.

7.4 Plasma Flow

Outer Solution

If the viscous term in (7.21) is assumed to be negligible then the equation becomes

$$yv' + v = 0,$$

which can be written as

$$\frac{d}{dy}(yv) = 0$$

and integrated to give

$$v = \frac{c_1}{y}.$$

Applying the boundary condition $v(1) = 1$ fixes $c_1 = 1$ and so the outer solution of (7.21) is the expected ideal solution, $v = 1/y$.

Complete Solution

Equation (7.21) has been solved analytically by Kenny (1992) who found solutions in terms of modified Bessel functions. These solutions do not show clearly the different types of asymptotic behaviour that are possible and so a slightly different analysis is followed here.

Changing the independent variable from y to

$$Y = \epsilon^{-\frac{1}{4}} y,$$

equation (7.21) becomes

$$v''' - Y^2 v' - Y v = 0, \quad (7.23)$$

where the dot (\cdot) denotes differentiation with respect to Y . Note that this change of variable suggests that the boundary layer width varies as $\epsilon^{\frac{1}{4}}$. Equation (7.23) can be written as

$$v''' + 2 \left(-\frac{1}{2} Y^2 \right) v' + \left(-\frac{1}{2} Y^2 \right)' v = 0$$

and is a particular case of

$$v''' + 2f(y)v' + f'(y)v = 0,$$

which (see Murphy (1960)) has general solution

$$v = c_1 v_1^2 + c_2 v_1 v_2 + c_3 v_2^2$$

where v_1 and v_2 are the two linearly independent solutions of

$$v'' + \frac{1}{2} f(y) v = 0.$$

Equation (7.23) therefore has the general solution

$$v = c_1 v_1^2 + c_2 v_1 v_2 + c_3 v_2^2,$$

where v_1, v_2 are the linearly independent solutions of

$$v'' - \frac{1}{4} Y^2 v = 0. \quad (7.24)$$

Changing the dependent variable from v to w where

$$v = e^{-\frac{1}{4} Y^2} w,$$

equation (7.24) becomes

$$w'' - Y w' - \frac{1}{2} w = 0$$

and changing the independent variable from Y to $z = \frac{1}{2} Y^2$ transforms this to

$$zw'' + \left(\frac{1}{2} - z \right) w' - \frac{1}{4} w = 0, \quad (7.25)$$

which is a particular case of Kummer's equation,

$$zw'' + (b - z) w' - aw = 0.$$

The general solution of Kummer's equation can be expressed in several different forms, for example as

$$w = \alpha M(a, b, z) + \beta U(a, b, z)$$

or

$$w = \alpha M(a, b, z) + \beta z^{1-b} M(1+a-b, 2-b, z)$$

or

$$w = \alpha U(a, b, z) + \beta z^{1-b} M(1+a-b, 2-b, z).$$

For our particular situation, the last of these proves to be the most useful.

The two independent solutions of equation (7.25) are thus

$$U\left(\frac{1}{4}, \frac{1}{2}, z\right) \quad \text{and} \quad z^{\frac{1}{2}} M\left(\frac{3}{4}, \frac{3}{2}, z\right)$$

which gives the two independent solutions v_1, v_2 as

$$e^{-\frac{1}{2}Y^2} U\left(\frac{1}{4}, \frac{1}{2}, \frac{1}{2}Y^2\right) \quad \text{and} \quad e^{-\frac{1}{2}Y^2} Y M\left(\frac{3}{4}, \frac{3}{2}, \frac{1}{2}Y^2\right).$$

The general solution for v is then

$$\begin{aligned} v = & c_1 e^{-\frac{1}{2}Y^2} U^2\left(\frac{1}{4}, \frac{1}{2}, \frac{1}{2}Y^2\right) + c_2 Y e^{-\frac{1}{2}Y^2} U\left(\frac{1}{4}, \frac{1}{2}, \frac{1}{2}Y^2\right) M\left(\frac{3}{4}, \frac{3}{2}, \frac{1}{2}Y^2\right) \\ & + c_3 Y^2 e^{-\frac{1}{2}Y^2} M^2\left(\frac{3}{4}, \frac{3}{2}, \frac{1}{2}Y^2\right), \end{aligned}$$

or, in terms of y ,

$$\begin{aligned} v = & k_1 e^{-\frac{1}{2}\epsilon^{-\frac{1}{2}}y^2} U^2\left(\frac{1}{4}, \frac{1}{2}, \frac{1}{2}\epsilon^{-\frac{1}{2}}y^2\right) + k_2 y e^{-\frac{1}{2}\epsilon^{-\frac{1}{2}}y^2} U\left(\frac{1}{4}, \frac{1}{2}, \frac{1}{2}\epsilon^{-\frac{1}{2}}y^2\right) M\left(\frac{3}{4}, \frac{3}{2}, \frac{1}{2}\epsilon^{-\frac{1}{2}}y^2\right) \\ & + k_3 y^2 e^{-\frac{1}{2}\epsilon^{-\frac{1}{2}}y^2} M^2\left(\frac{3}{4}, \frac{3}{2}, \frac{1}{2}\epsilon^{-\frac{1}{2}}y^2\right). \end{aligned} \quad (7.26)$$

Note that

1. The general solution (7.26) is a linear superposition of three functions, two of which are even and one of which is odd.
2. If the effects of viscosity are reduced, R becomes large and ϵ becomes small. In this limit the asymptotic approximations

$$M(a, b, z) \rightarrow \frac{\Gamma(b)}{\Gamma(a)} e^z z^{a-b} \quad \text{and} \quad U(a, b, z) \rightarrow z^{-a} \quad \text{as} \quad z \rightarrow \infty \quad (7.27)$$

can be used on the general solution (7.26) to yield

$$v \rightarrow 2^{\frac{1}{2}} k_1 \epsilon^{\frac{1}{4}} y^{-1} e^{-\frac{1}{2}\epsilon^{-\frac{1}{2}}y^2} + 2k_2 \epsilon^{\frac{1}{2}} \frac{\Gamma(\frac{3}{2})}{\Gamma(\frac{3}{4})} y^{-1} + 2^{\frac{3}{2}} k_3 \epsilon^{\frac{3}{4}} \frac{\Gamma^2(\frac{3}{2})}{\Gamma^2(\frac{3}{4})} y^{-1} e^{\frac{1}{2}\epsilon^{-\frac{1}{2}}y^2}.$$

This has an exponentially increasing term and will only match to the outer ideal solution, $v = 1/y$, if $k_3 = 0$.

Boundary Conditions

Applying the boundary conditions (7.22) to (7.26) gives

$$k_1 = 0, \quad k_3 = 0, \quad k_2 = \frac{1}{e^{-\frac{1}{2}\epsilon^{-\frac{1}{2}}y^2} U\left(\frac{1}{4}, \frac{1}{2}, \frac{1}{2}\epsilon^{-\frac{1}{2}}y^2\right) M\left(\frac{3}{4}, \frac{3}{2}, \frac{1}{2}\epsilon^{-\frac{1}{2}}y^2\right)}$$

and so

$$v = \frac{y e^{-\frac{1}{2}\epsilon^{-\frac{1}{2}}y^2} U\left(\frac{1}{4}, \frac{1}{2}, \frac{1}{2}\epsilon^{-\frac{1}{2}}y^2\right) M\left(\frac{3}{4}, \frac{3}{2}, \frac{1}{2}\epsilon^{-\frac{1}{2}}y^2\right)}{e^{-\frac{1}{2}\epsilon^{-\frac{1}{2}}y^2} U\left(\frac{1}{4}, \frac{1}{2}, \frac{1}{2}\epsilon^{-\frac{1}{2}}y^2\right) M\left(\frac{3}{4}, \frac{3}{2}, \frac{1}{2}\epsilon^{-\frac{1}{2}}y^2\right)}. \quad (7.28)$$

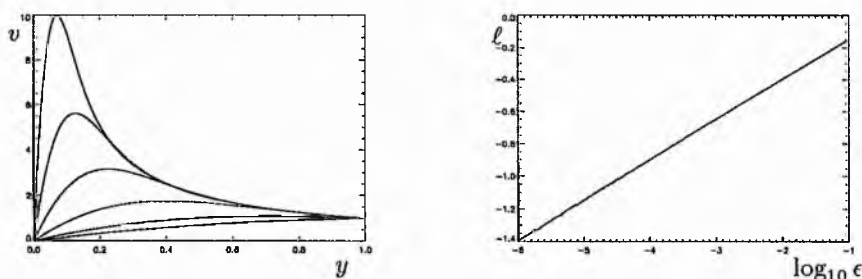


Figure 7.1: (a) $v(y)$ for several values of ϵ (b) boundary layer width as a function of ϵ .

This solution is plotted in figure 7.1a. As ϵ tends to zero the viscous boundary layer becomes narrower and the solution becomes more like $1/y$.

Figure 7.1b is a plot of boundary layer width as a function of ϵ . The line has a gradient of 0.25 showing that $\ell \sim \epsilon^{0.25}$, as expected.

Asymptotic Behaviour of v

If ϵ becomes small then the approximations (7.27) can be used on (7.28) to give $v \rightarrow 1/y$, which agrees with the outer ideal solution.

As $z \rightarrow 0$, $M(a, b, z) \rightarrow 1$ and, provided that $0 < b < 1$, $U(a, b, z) \rightarrow \Gamma(1-b)/\Gamma(1-b+a)$. As y tends to zero these approximations can be used on (7.28) to yield

$$v \rightarrow \frac{\Gamma\left(\frac{1}{2}\right) y}{\Gamma\left(\frac{1}{4}\right) e^{-\frac{1}{2}\epsilon^{-\frac{1}{2}}} U\left(\frac{1}{4}, \frac{1}{2}, \frac{1}{2}\epsilon^{-\frac{1}{2}}\right) M\left(\frac{3}{4}, \frac{3}{2}, \frac{1}{2}\epsilon^{-\frac{1}{2}}\right)} \quad \text{as } y \rightarrow 0.$$

If ϵ is small then the asymptotic approximations in (7.27) can be used on this to give $v \rightarrow \epsilon^{-\frac{1}{2}} y$.

Since the boundary layer width varies as $\epsilon^{\frac{1}{4}}$ then these two results can be used to construct a patched solution for v , namely

$$v \approx \begin{cases} \epsilon^{-\frac{1}{2}} y & 0 \leq y \leq \epsilon^{\frac{1}{4}} \\ \frac{1}{y} & \epsilon^{\frac{1}{4}} \leq y \leq 1 \end{cases} \quad \text{as } \epsilon \rightarrow 0. \quad (7.29)$$

7.5 Magnetic Field

Introduction

The magnetic field is of the form

$$\mathbf{B} = (x + g'(y), -y, 0),$$

where g satisfies

$$g'' = R_m(yv(y) - k) \quad (7.30)$$

and the boundary conditions $g(0) = g'(1) = 0$.

Integrating (7.30) once gives

$$g' = R_m \int_0^1 \xi v(\xi) d\xi - R_m k y + c_0,$$

where c_0 is an arbitrary constant of integration. Applying the boundary conditions $g'(0) = g'(1) = 0$ gives $c_0 = 0$ and

$$k = \int_0^1 d\xi v(\xi) d\xi. \quad (7.31)$$

Approximating v by the patched solution (7.29) this becomes

$$k = \int_0^{\epsilon^{\frac{1}{4}}} \epsilon^{-\frac{1}{2}} y^2 dy + \int_{\epsilon^{\frac{1}{4}}}^1 dy = 1 - \frac{2}{3} \epsilon^{\frac{1}{4}} = 1 - \frac{2}{3} M_A^{\frac{1}{2}} R^{-\frac{1}{4}} R_m^{-\frac{1}{4}}$$

which tends to 1 as R_m or R becomes large.

Equation (7.31) can also be evaluated numerically to give the results plotted in figure 7.2. Figure 7.2a shows that as ϵ becomes small k tends to 1. Figure 7.2b is a plot of $1 - k$ against ϵ and as the gradient of the line is 0.25 and the y -axis intercept of the extrapolated straight line is zero this suggests that $1 - k = \epsilon^{\frac{1}{4}}$ which is in good agreement with the approximate analytical result above.

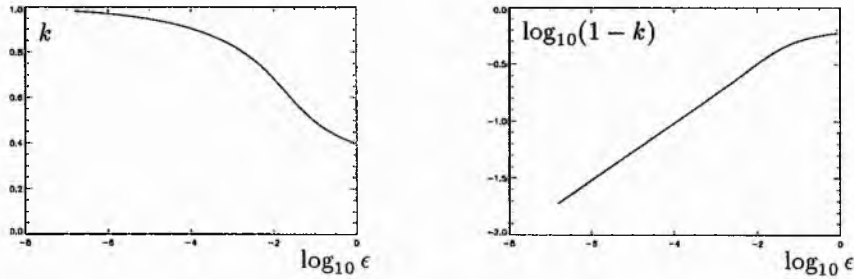


Figure 7.2: (a) k and (b) $\log_{10}(1 - k)$ as functions of ϵ .

Field Lines

General

The magnetic field lines are given by

$$\frac{dx}{dy} = \frac{B_x}{B_y} = \frac{x + g'(y)}{-y},$$

which can be rewritten as

$$y \frac{dx}{dy} + x = -g'$$

or

$$\frac{d}{dy}(yx) = -g'.$$

Integrating this with respect to y and rearranging slightly gives

$$x = \frac{\ell_0 - g(y)}{y}, \quad (7.32)$$

where ℓ_0 is an arbitrary constant. If $g(y)$ is known this expression allows the field lines to be plotted.

Outer Region

For the outer region where $v \approx 1/y$ equation (7.30) becomes

$$g'' = R_m(1 - k).$$

If R or R_m are large then $k = 1 - \epsilon^{\frac{1}{4}}$ and this becomes

$$g'' = R_m \epsilon^{\frac{1}{4}} = M_A^{\frac{1}{2}} R_m^{\frac{3}{4}} R^{-\frac{1}{4}}.$$

Integrating and applying the outer boundary condition $g'(1) = 0$ gives

$$g' = M_A^{\frac{1}{2}} R_m^{\frac{3}{4}} R^{-\frac{1}{4}}(y - 1)$$

and the gradient of the field lines in the outer region is then

$$\frac{dy}{dx} = \frac{B_y}{B_x} = \frac{-y}{x + g'} = \frac{-y}{x + M_A^{\frac{1}{2}} R_m^{\frac{3}{2}} R^{-\frac{1}{4}} (y - 1)}.$$

As R_m becomes large $dy/dx \rightarrow 0$ and the field lines become horizontal. As R becomes large $dy/dx \rightarrow -y/x$ giving an x-point field.

Inner Region

For the inner region where $v \approx \epsilon^{-\frac{1}{2}} y$ equation (7.30) is approximately

$$g'' = R_m \left(\epsilon^{-\frac{1}{2}} y^2 - k \right)$$

and if R or R_m is large, $k = 1 - \epsilon^{\frac{1}{4}}$ and this becomes

$$g'' = R_m \left(\epsilon^{-\frac{1}{2}} y^2 - 1 + \epsilon^{\frac{1}{4}} \right).$$

Integrating and applying the boundary condition $g'(0) = 0$ gives

$$g = R_m \left(\frac{1}{12} \epsilon^{-\frac{1}{2}} y^4 - \frac{1}{2} y^2 + \frac{1}{2} \epsilon^{\frac{1}{4}} y^2 \right) + c_0,$$

where c_0 is an arbitrary constant which, since only the derivatives of g have any meaning, can be taken to be zero. If y lies within the boundary layer then we can write $y = f \epsilon^{\frac{1}{4}}$ (where $0 \leq f \leq 1$) to obtain

$$g = R_m \left(\frac{1}{12} \epsilon^{\frac{1}{2}} f^4 - \frac{1}{2} \epsilon^{\frac{1}{2}} f^2 + \frac{1}{2} \epsilon^{\frac{3}{4}} f^2 \right).$$

If f and ϵ are both small then the dominant term is $\epsilon^{\frac{1}{2}} f^2$. Thus for small ϵ and close to the origin we have

$$g \approx -\frac{1}{2} R_m \epsilon^{\frac{1}{2}} f^2 = -\frac{1}{2} R_m y^2.$$

and the equation for the field lines, (7.32), becomes

$$x = \frac{\ell_0 + \frac{1}{2} R_m y^2}{y}$$

or

$$y \left(x - \frac{1}{2} R_m y \right) = \ell_0.$$

At the origin $\ell_0 = 0$, therefore the equation of the fieldlines passing through the origin is given by $y(x - \frac{1}{2} R_m y) = 0$ which has solution $y = 0$ or $y = 2R_m^{-1}x$. This implies that the field near the origin takes the form of an x-point and that the angle between the arms of the x decreases as R_m increases. This ties in with the previous result in which the magnetic field in the outer region becomes more horizontal as R_m increases.

Numerical Solutions

Solving equation (7.30) numerically subject to the boundary conditions and plotting contours of the flux function $A = xy + g(y)$ gives the field lines shown in figures 7.3 and 7.4. In figure 7.3 M_A^2 and R_m are kept constant and R is varied. As R is increased the field becomes more like a neutral point field, as expected from the above analytical work. In figure 7.4 M_A^2 and R are kept constant and R_m is varied. As R_m is increased the field lines become almost horizontal, again as expected.

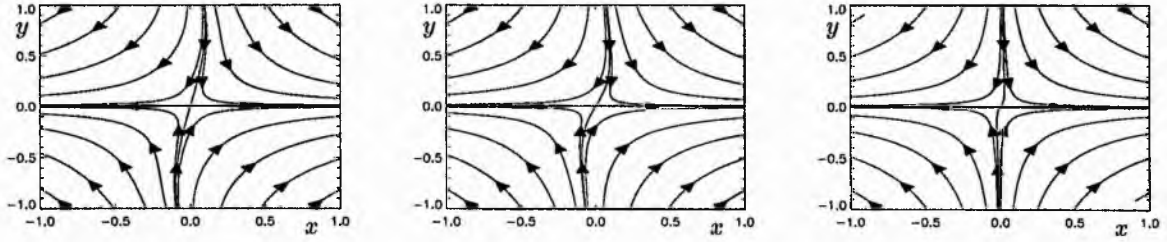


Figure 7.3: Magnetic field lines for $R =$ (a) 10^0 , (b) 10^3 and (c) 10^6 , all with $R_m = M_A^2 = 1$.

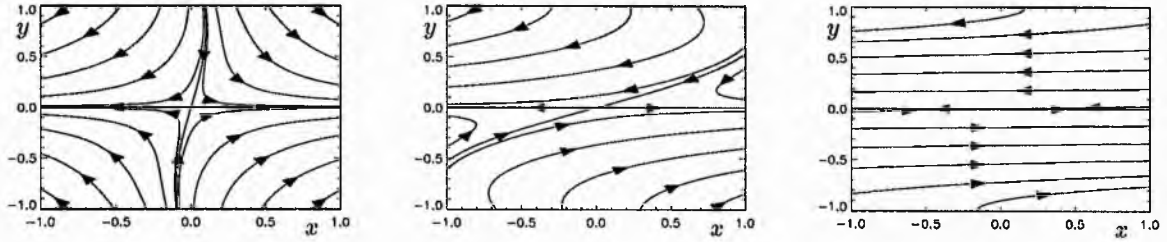


Figure 7.4: Magnetic field lines for $R_m =$ (a) 10^0 , (b) 10^1 and (c) 10^2 , all with $R = M_A^2 = 1$.

7.6 Reconnection Rates

The Reconnection Rate

The reconnection rate is

$$R_E = k$$

and since $k \rightarrow 1 - \epsilon^{\frac{1}{4}}$ as R_m or R become large we obtain

$$R_E \rightarrow 1 - M_A^{\frac{1}{2}} R^{-\frac{1}{4}} R_m^{-\frac{1}{4}} \quad \text{as } R, R_m \rightarrow \infty,$$

which tends to 1 as R or R_m increases.

The Ohmic Heating Rate

The ohmic heating rate is

$$R_\Omega = \frac{1}{R_m} \int_0^1 j^2 dy$$

and since

$$j = -g'' = -R_m (yv(y) - k)$$

this becomes

$$R_\Omega = R_m \int_0^1 (yv(y) - k)^2 dy. \quad (7.33)$$

Approximating v by the patched solution (7.29) gives

$$R_\Omega = R_\Omega^i + R_\Omega^o,$$

where

$$R_\Omega^i = R_m \int_0^{\epsilon^{\frac{1}{4}}} \left(\epsilon^{-\frac{1}{2}} y^2 - k \right)^2 dy = R_m \epsilon^{\frac{1}{4}} \left(\frac{1}{5} - \frac{2}{3} k + k^2 \right)$$

is the ohmic heating within the viscous boundary layer and

$$R_{\Omega}^o = R_m \int_{\epsilon^{\frac{1}{4}}}^1 (1-k)^2 dy = R_m (1-k)^2 \left(1 - \epsilon^{\frac{1}{4}}\right)$$

is the ohmic heating outside it. Since $k \rightarrow 1 - \epsilon^{\frac{1}{4}}$ as R or $R_m \rightarrow \infty$ we obtain

$$R_{\Omega}^i \rightarrow \frac{8}{15} R_m \epsilon^{\frac{1}{4}} \quad \text{and} \quad R_{\Omega}^o \rightarrow R_m \epsilon^{\frac{1}{2}} \quad \text{as } R, R_m \rightarrow \infty$$

or,

$$R_{\Omega}^i \rightarrow R_m M_A^{\frac{1}{2}} R_m^{\frac{3}{4}} R^{-\frac{1}{4}} \quad \text{and} \quad R_{\Omega}^o \rightarrow M_A R_m^{\frac{1}{2}} R^{-\frac{1}{2}} \quad \text{as } R, R_m \rightarrow \infty.$$

In the limit of large R or large R_m , $R_{\Omega}^i \gg R_{\Omega}^o$ showing that most of the ohmic heating is produced within the viscous boundary layer and so

$$R_{\Omega} \rightarrow R_{\Omega}^i = \frac{8}{15} M_A^{\frac{1}{2}} R_m^{\frac{3}{4}} R^{-\frac{1}{4}} \quad \text{as } R, R_m \rightarrow \infty.$$

Numerical Results

Equation (7.33) can be evaluated numerically to give the results shown in figure 7.5. Figure 7.5a shows R_{Ω}^i and R_{Ω}^o as functions of R_m with R fixed at 10^2 . The two lines have gradients 0.78 and 0.6 which are in good agreement with the values of 0.75 and 0.5 suggested by the above analytical approximation. Figure 7.5b shows R_{Ω}^i and R_{Ω}^o as functions of R with R_m fixed at 10^2 . The two lines have gradients -0.22 and -0.4 which are close to the expected -0.25 and -0.5.

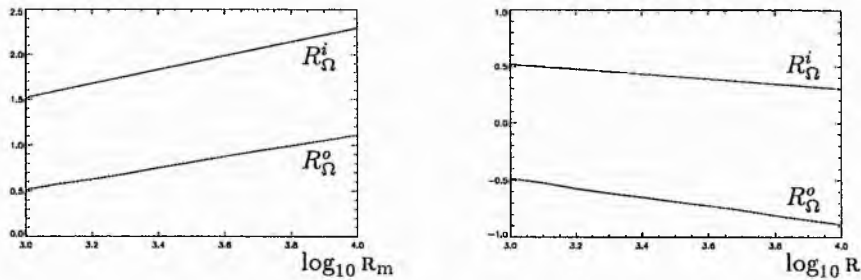


Figure 7.5: The ohmic heating rates as a function of (a) R_m and (b) R .

Alternative Boundary Conditions

Applying the alternative boundary condition $g''(1) = 0$ to equation (7.30) gives $k = 1$. This changes the reconnection rate from $1 - M_A^2 R_m^{-\frac{1}{4}} R^{-\frac{1}{4}}$ to 1. In the limit of large R_m or R these become identical. In the ohmic heating rate the only change is that $R_{\Omega}^o = 0$ but this does not affect the result that $R_{\Omega} \rightarrow R_{\Omega}^i = \frac{8}{15} M_A^{\frac{1}{2}} R_m^{\frac{3}{4}} R^{-\frac{1}{4}}$.

Conclusions

This thesis investigates several models of magnetic annihilation and reconnection, namely

1. **Steady-state magnetic annihilation.** Analytical solutions to the MHD equations were found for an annihilating magnetic field with various stagnation-point flows. For the case of a simple stagnation-point flow the solutions were exact and for a wider class of flows asymptotic solutions were obtained. As R_m is increased it is found that the current sheet width decreases, the current sheet strength increases and the reconnection and ohmic heating rates tend to 1 and $R_m^{-1/2}$, respectively. It is shown that the advection process is important in creating strong magnetic field and strong currents, hence part of the energy released as heat has its origin in whatever process is driving the plasma flow.

This work could be extended by, for instance, considering a more complete version of Ohm's law which would then allow the behaviour of the current sheet to be examined when the normal form fails.

2. **Time-dependent magnetic annihilation.** Exact, analytical solutions to the MHD equations are found for an annihilating magnetic field with a time-modulated stagnation-point flow. On an infinite interval both analytical and computer investigations show that the initial magnetic field, through advection, has a strong influence on the reconnection and ohmic heating rates.

In future a more extensive examination of the effects of the initial magnetic field could be made, in particular looking at initial conditions that are even functions and sums of even and odd functions.

3. **Annihilation in a compressible, inviscid plasma.** The steady-state annihilation model is extended to the compressible case and, assuming the form of the y -component of the flow and that the density varies in only one dimension, analytical solutions for the flow, plasma density and magnetic field are obtained. The flow is of stagnation-point type and the plasma has a maximum density within the current sheet. The magnetic field is determined by the y -component of the flow and is the same as in the incompressible case.

This area of work could be extended by considering the case in which plasma density varies in two dimensions or by considering the y -component of the flow to be arbitrary (which would involve including an energy equation and an equation of state).

4. **Steady-state magnetic reconnection.** The steady-state, incompressible MHD equations are reduced to two non-linear coupled partial differential equations. Reconnection solutions are sought by an asymptotic approach using the already known annihilation solutions. The resulting first-order equations were dealt with by looking for power series solutions. The solution for the magnetic field was found to possess only a magnetic cusp and not an x-type neutral point. Also, some types of boundary conditions were able to produce reverse current at the end of the current sheet.

Only one form of boundary condition was studied in any detail and further work could examine the effects of more general boundary conditions. Also, the boundary conditions are applied on $y = 0$

and it should be possible (using symbolic evaluation of the series solution) to apply boundary conditions on $y = 1$, which will give greater insight to the behaviour of the model in response to conditions on the outer boundary.

5. **Reconnection in a viscous plasma.** The assumption that viscous forces are dominant decouples the equation of motion from the induction equation. The simple stagnation-point flow is an exact solution and allows an exact analytical series solution for the magnetic field to be obtained. For the case where the incoming magnetic field lines are straight it was shown that the magnetic field tends towards the magnetic annihilation solution as R_m increases, irrespective of the right-hand boundary condition.

This work could be extended in several areas by considering different boundary conditions and more general fluid flows.

6. **Magnetic flipping.** We consider a previous ideal model of magnetic flipping and assume that the streamlines are straight. This simplifies the MHD equations to such an extent that an analytical solution for the plasma flow can be found, the odd part of which matches to the ideal solution and exhibits a viscous boundary layer. The solution for the magnetic field is found to be of an x-point type with the angle between the separatrices determined by the Reynolds and magnetic Reynolds numbers. It is shown that the bulk of the ohmic heating occurs within the viscous boundary layer. Possible extensions to this work involve considering the general solution for the fluid flow and its effect on the magnetic field. It should also be possible to examine the case of slightly curved streamlines by assuming that the curvature is small and comes in at a lower order.

Appendix A

Relationships between \mathbf{B} and \mathbf{j}

The vector identities

$$\nabla(\mathbf{a} \cdot \mathbf{b}) = (\mathbf{b} \cdot \nabla)\mathbf{a} + (\mathbf{a} \cdot \nabla)\mathbf{b} + \mathbf{b} \times (\nabla \times \mathbf{a}) + \mathbf{a} \times (\nabla \times \mathbf{b}), \quad (\text{A.1})$$

$$\nabla \times (\mathbf{a} \times \mathbf{b}) = (\mathbf{b} \cdot \nabla)\mathbf{a} - \mathbf{b}(\nabla \cdot \mathbf{a}) - (\mathbf{a} \cdot \nabla)\mathbf{b} + \mathbf{a}(\nabla \cdot \mathbf{b}), \quad (\text{A.2})$$

$$\nabla \cdot (\nabla \times \mathbf{a}) = 0 \quad (\text{A.3})$$

will be used to derive some standard relationships between a vector function and its curl.

1. In (A.1), setting $\mathbf{a} = \mathbf{b} = \mathbf{B}$ gives

$$\nabla B^2 = 2(\mathbf{B} \cdot \nabla)\mathbf{B} + 2\mathbf{B} \times \mathbf{j}$$

and hence

$$\mathbf{j} \times \mathbf{B} = (\mathbf{B} \cdot \nabla)\mathbf{B} - \frac{1}{2}\nabla B^2. \quad (\text{A.4})$$

2. In (A.3), setting $\mathbf{a} = \mathbf{B}$ gives

$$\nabla \cdot \mathbf{j} = 0. \quad (\text{A.5})$$

3. In (A.2), setting $\mathbf{a} = \mathbf{j}$ and $\mathbf{b} = \mathbf{B}$ gives

$$\nabla \times (\mathbf{j} \times \mathbf{B}) = (\mathbf{B} \cdot \nabla)\mathbf{j} - \mathbf{B}(\nabla \cdot \mathbf{j}) - (\mathbf{j} \cdot \nabla)\mathbf{B} + \mathbf{j}(\nabla \cdot \mathbf{B}).$$

Making use of (A.5) and $\nabla \cdot \mathbf{B} = 0$ reduces this to

$$\nabla \times (\mathbf{j} \times \mathbf{B}) = (\mathbf{B} \cdot \nabla)\mathbf{j} - (\mathbf{j} \cdot \nabla)\mathbf{B}. \quad (\text{A.6})$$

4. The curl of (A.4) is

$$\nabla \times (\mathbf{j} \times \mathbf{B}) = \nabla \times (\mathbf{B} \cdot \nabla)\mathbf{B}$$

and substituting this into (A.6) yields

$$\nabla \times (\mathbf{B} \cdot \nabla)\mathbf{B} = (\mathbf{B} \cdot \nabla)\mathbf{j} - (\mathbf{j} \cdot \nabla)\mathbf{B}. \quad (\text{A.7})$$

Appendix B

Some Properties of the Confluent Hypergeometric Kummer Function

From Abramowitz and Stegun (1972)

1. The function $M(a, b, z)$ is a solution to Kummer's equation,

$$z \frac{d^2 w}{dz^2} + (b - z) \frac{dw}{dz} - aw = 0.$$

2. $M(a, b, z)$ can be expressed as an infinite series,

$$M(a, b, z) = \sum_{n=0}^{\infty} \frac{(a)_n z^n}{(b)_n n!}, \quad (\text{B.1})$$

where

$$(a)_0 = 1 \quad \text{and} \quad (a)_n = a(a+1)(a+2)\dots(a+n-1).$$

3. The derivative of $M(a, b, z)$ is given by

$$\frac{d}{dz} M(a, b, z) = \frac{a}{b} M(a+1, b+1, z). \quad (\text{B.2})$$

4. If $|z| \rightarrow \infty$ with a and b fixed then

$$M(a, b, z) \rightarrow \frac{\Gamma(b)}{\Gamma(a)} e^z z^{a-b}. \quad (\text{B.3})$$

5. If $a \rightarrow -\infty$ with b bounded and z real then

$$M(a, b, z) \rightarrow \Gamma(b) e^{\frac{1}{2}z} \left(\frac{1}{2}bz - az \right)^{\frac{1}{4} - \frac{1}{2}b} \pi^{-\frac{1}{2}} \cos \left(\sqrt{2bz - 4az} - \frac{1}{2}b\pi + \frac{1}{4}\pi \right). \quad (\text{B.4})$$

6. Kummer's identity is

$$M(a, b, z) = e^z M(b-a, b, -z). \quad (\text{B.5})$$

Appendix C

The solution of $y'' + axy' + by = 0$

For the equation

$$y'' + axy' + by = 0$$

changing independent variables from x to $z = -\frac{1}{2}ax^2$ gives

$$z\ddot{y} + \dot{y}\left(\frac{1}{2} - z\right) - \frac{b}{2a}y = 0. \quad (\text{C.1})$$

This can be compared with Kummer's equation,

$$z\ddot{w} + (B - z)\dot{w} - Aw = 0,$$

which has the general solution

$$w = \alpha M(A, B, z) + \beta z^{1-B} M(1 + A - B, 2 - B, z).$$

Equation (C.1) thus has the general solution

$$y = \alpha M\left(\frac{b}{2a}, \frac{1}{2}, z\right) + \beta z^{\frac{1}{2}} M\left(\frac{1}{2} + \frac{b}{2a}, \frac{3}{2}, z\right),$$

or, in terms of the original variable x ,

$$y = \alpha M\left(\frac{b}{2a}, \frac{1}{2}, -\frac{1}{2}ax^2\right) + \beta x M\left(\frac{1}{2} + \frac{b}{2a}, \frac{3}{2}, -\frac{1}{2}ax^2\right).$$

Note that by using Kummer's identity this solution can be written as

$$y = \alpha e^{-\frac{1}{2}ax^2} M\left(\frac{1}{2} - \frac{b}{2a}, \frac{1}{2}, \frac{1}{2}ax^2\right) + \beta' x e^{-\frac{1}{2}ax^2} M\left(1 - \frac{b}{2a}, \frac{3}{2}, \frac{1}{2}ax^2\right).$$

Appendix D

Solution to $\frac{1}{R_m}B' + yB = -k$

The equation

$$\frac{1}{R_m}B' + yB = -k \quad (D.1)$$

can be differentiated to obtain

$$\frac{1}{R_m}B'' + yB' + B = 0,$$

which (see appendix C) has the general solution

$$B = c_0 e^{-\frac{1}{2}R_m y^2} + c_1 y M\left(1, \frac{3}{2}, -\frac{1}{2}R_m y^2\right). \quad (D.2)$$

This solution contains two arbitrary constants whereas any solution to (D.1) should only contain one arbitrary constant and should contain the variable k . This implies that either c_0 or c_1 can be expressed in terms of k .

Substituting (D.2) back into (D.1) gives

$$\frac{2c_1}{R_m} \left[M\left(1, \frac{3}{2}, z\right) \left(\frac{1}{2} - z\right) + z M'\left(1, \frac{3}{2}, z\right) \right] = -k,$$

where $z = -\frac{1}{2}R_m y^2$. Using the identity

$$(b-1)M(a-1, b-1, z) = (b-1-z)M(a, b, z) + zM'(a, b, z)$$

(see Abramowitz and Stegun) this becomes

$$\frac{2c_1}{R_m} \left[\frac{1}{2} M\left(0, \frac{3}{2}, z\right) \right] = -k,$$

or, since $M(0, b, z) = 1$,

$$c_1 = -R_m k$$

The solution (D.2) thus becomes

$$B = c_0 e^{-\frac{1}{2}R_m y^2} - R_m k y M\left(1, \frac{3}{2}, -\frac{1}{2}R_m y^2\right),$$

which, using Kummer's identity, can be written as

$$B = c_0 e^{-\frac{1}{2}R_m y^2} - R_m k y e^{-\frac{1}{2}y^2} M\left(\frac{1}{2}, \frac{3}{2}, \frac{1}{2}R_m y^2\right).$$

Appendix E

Orthogonal Functions 1

The set of functions

$$y_n = x e^{-\frac{1}{2} a x^2} M \left(1 - \frac{b_n}{2a}, \frac{3}{2}, \frac{1}{2} a x^2 \right),$$

satisfying $y_n(0) = y_n(1) = 0$, are solutions of

$$y'' + a x y' + b_n y = 0. \quad (\text{E.1})$$

Consider the equation

$$h'' - a x h' + (\mu_n - a) h = 0 \quad (\text{E.2})$$

, which, as shown in appendix C, has the solution

$$h_n = x M \left(1 - \frac{b_n}{2a}, \frac{3}{2}, \frac{1}{2} a x^2 \right) = e^{\frac{1}{2} a x^2} y_n.$$

Note that the h_n will also be zero on $x = 0, 1$.

Multiplying equation (E.1) by h_m and integrating by parts from 0 to 1 gives

$$[h_m y_n']_0^1 - [h_m' y_n]_0^1 - [x h_m y_n]_0^1 + \int_0^1 y_n (h_m'' - a x h_m' - a h_m) dx + b_n \int_0^1 h_m y_n dx = 0.$$

As the y_n and h_m are zero on $x = 0, 1$ this reduces to

$$\int_0^1 y_n (h_m'' - a x h_m' - a h_m) dx + b_n \int_0^1 h_m y_n dx = 0$$

and making use of (E.2) this becomes

$$-b_m \int_0^1 y_n h_m - \mu_n dx + b_n \int_0^1 h_m y_n dx = 0$$

or

$$(b_n - b_m) \int_0^1 y_n h_m dx = 0.$$

From this equation it is seen that if $n \neq m$ then the integral must vanish. If $n = m$ then

$$\int_0^1 y_n h_n dx = \int_0^1 e^{\frac{1}{2} a x^2} y_n^2 dx \neq 0,$$

and so y_n and $h_n = e^{\frac{1}{2} a x^2} y_n$ are orthogonal functions.

Appendix F

Orthogonal Functions 2

The set of functions

$$y_n = e^{-\frac{1}{2}ax^2} M\left(\frac{1}{2} - \frac{b_n}{2a}, \frac{1}{2}, \frac{1}{2}ax^2\right),$$

satisfying $y'_n(0) = y_n(1) = 0$, are solutions of

$$y'' + axy' + b_n y = 0. \quad (\text{F.1})$$

Consider the equation

$$h'' - axh' + (\mu_n - a)h = 0, \quad (\text{F.2})$$

which, as shown in appendix C, has the solution

$$h_n = M\left(\frac{1}{2} - \frac{b_n}{2a}, \frac{1}{2}, \frac{1}{2}ax^2\right) = e^{\frac{1}{2}ax^2} y_n.$$

Note that the h_n satisfy $h'(0) = h(1) = 0$.

Multiplying equation (F.1) by h_m and integrating by parts from 0 to 1 gives

$$[h_m y'_n]_0^1 - [h'_m y_n]_0^1 - [x h_m y_n]_0^1 + \int_0^1 y_n (h''_m - axh'_m - ah_m) dx + b_n \int_0^1 h_m y_n dx = 0.$$

As the y_n , h_m are zero on $x = 1$ and y'_n , h'_m are zero on $x = 0$ this reduces to

$$\int_0^1 y_n (h''_m - axh'_m - ah_m) dx + b_n \int_0^1 h_m y_n dx = 0$$

and making use of (F.2) this becomes

$$-b_m \int_0^1 y_n h_m dx - \mu_n \int_0^1 h_m y_n dx + b_n \int_0^1 h_m y_n dx = 0$$

or

$$(b_n - b_m) \int_0^1 y_n h_m dx = 0.$$

From this equation, if $n \neq m$ then the integral must vanish. If $n = m$ then

$$\int_0^1 y_n h_n dx = \int_0^1 e^{\frac{1}{2}ax^2} y_n^2 dx \neq 0,$$

and so y_n and $h_n = e^{\frac{1}{2}ax^2} y_n$ are orthogonal functions.

Appendix G

Convergence of A_1 and ψ_1

Introduction

Given f_0 and g_0 , the equations

$$f_{j+1} = \frac{1}{(2j+2)(2j+1)} \left[x f'_j - f''_j - 2j f_j - \sum_{k=0}^{j-1} \alpha_{j-1-k} g'_k \right] \quad (G.1)$$

and

$$x g'_{j+1} - (2j+1) g_{j+1} = \frac{1}{(2j+3)(2j+2)} \left[g''_j (2j+1) - x g'''_j + \right. \\ \left. P \sum_{k=0}^j f'''_k \alpha_{j-k} + f'_{k+1} (2k+2)(2k+1) \alpha_{j-k} - f'_k \beta_{j-k} \right] \quad (G.2)$$

generate the complete set of f_j and g_j to give the solutions

$$\bar{A} = \sum_{j=0}^{\infty} f_j Y^{2j}, \quad \text{and} \quad \bar{\psi} = \sum_{j=0}^{\infty} g_j Y^{2j+1}.$$

Changing back to the parameterised variables (where $x = R_m^{\frac{1}{2}} x$, $Y = R_m^{\frac{1}{2}} y$, $\psi_1 = \bar{\psi}$ and $A_1 = \kappa R_m^{\frac{1}{2}} \bar{A}$) gives

$$A_1 = \kappa R_m^{\frac{1}{2}} \sum_{j=0}^{\infty} F_j y^{2j} \quad \text{and} \quad \psi_1 = R_m^{\frac{1}{2}} \sum_{j=0}^{\infty} G_j y^{2j+1},$$

where

$$F_j = f_j R_m^j \quad \text{and} \quad G_j = g_j R_m^j.$$

It is important to determine if these two series are convergent on the interval of interest, $0 \leq y \leq 1$.

Expression for $|F_{j+1}^{(n)}|$

If $f_j = R_m^{-j} F_j$ and $g_j = R_m^{-j} G_j$ then equation (G.1) becomes

$$F_{j+1} = \frac{R_m}{(2j+2)(2j+1)} \left[x F'_j - F''_j - 2j F_j - R_m \sum_{k=0}^{j-1} \alpha_{j-1-k} R_m^{j-1-k} G'_k \right],$$

which can be differentiated n times to obtain

$$F_{j+1}^{(n)} = \frac{R_m}{(2j+2)(2j+1)} \left[x F_j^{(n+1)} + n F_j^{(n)} - F_j^{(n+2)} - 2j F_j^{(n)} - R_m \sum_{k=0}^{j-1} \alpha_{j-1-k} R_m^{j-1-k} G_k^{(n+1)} \right].$$

As we are only interested in the range $|x| \leq R_m^{\frac{1}{2}}$ the above equation gives

$$\begin{aligned} |F_{j+1}^{(n)}| \leq & \frac{R_m}{(2j+2)(2j+1)} \left[R_m^{\frac{1}{2}} |F_j^{(n+1)}| + n |F_j^{(n)}| + |F_j^{(n+2)}| + 2j |F_j^{(n)}| + \right. \\ & \left. R_m \sum_{k=0}^{j-1} |\alpha_{j-1-k}| R_m^{j-1-k} |G_k^{(n+1)}| \right]. \end{aligned} \quad (G.3)$$

Expression for $|G_{j+1}^{(n)}|$

If $F_j = R_m^j f_j$ and $G_j = R_m^j g_j$ then equation (G.2) becomes

$$\begin{aligned} xG_{j+1}' - (2j+1)G_{j+1} = & \frac{R_m}{(2j+3)(2j+2)} \left[G_j''(2j+1) - xG_j''' + \right. \\ & \left. P \sum_{k=0}^j F_k''' \alpha_{j-k} R_m^{j-k} + F_{k+1}'(2k+2)(2k+1) \alpha_{j-k} R_m^{j-k-1} - F_k' \beta_{j-k} R_m^{j-k} \right], \end{aligned}$$

which can be differentiated n times to obtain

$$\begin{aligned} xG_{j+1}^{(n+1)} - (2j-n+1)G_{j+1}^{(n)} = & \frac{R_m}{(2j+3)(2j+2)} \left[(2j+1)G_j^{(n+2)} - xG_j^{(n+3)} - nG_j^{(n+2)} + \right. \\ & \left. P \sum_{k=0}^j F_k^{(n+3)} \alpha_{j-k} R_m^{j-k} + F_{k+1}^{(n+1)}(2k+2)(2k+1) \alpha_{j-k} R_m^{j-k-1} - F_k^{(n+1)} \beta_{j-k} R_m^{j-k} \right]. \end{aligned}$$

This equation is of the form

$$xG_{j+1}^{(n+1)} - (2j-n+1)G_{j+1}^{(n)} = \frac{R_m h_j^{(n)}(x)}{(2j+3)(2j+2)},$$

which has solution

$$G_{j+1}^{(n)} = \frac{1}{(2j+3)(2j+2)} x^{2j-n+1} \int x^{-(2j-n+1)-1} h_j^{(n)}(x) dx + c_{j+1} x^{2j-n+1},$$

where the c_{j+1} are arbitrary constants. This implies that

$$|G_{j+1}^{(n)}| \leq \frac{R_m}{(2j+3)(2j+2)} \left| x^{2j-n+1} \int x^{-(2j-n+1)-1} h_j^{(n)}(x) dx \right| + |c_{j+1}| R_m^{\frac{1}{2}(2j-n+1)}.$$

If $|h_j^{(n)}(x)| \leq h_j^n$ then

$$|G_{j+1}^{(n)}| \leq \frac{R_m h_j^n}{(2j+3)(2j+2)} \left| x^{2j-n+1} \int x^{-(2j-n+1)-1} dx \right| + |c_{j+1}| R_m^{\frac{1}{2}(2j-n+1)}$$

and evaluating the integral gives

$$|G_{j+1}^{(n)}| \leq \frac{R_m h_j^n}{(2j+3)(2j+2)(2j-n+1)} + |c_{j+1}| R_m^{\frac{1}{2}(2j-n+1)}. \quad (G.4)$$

Also, as

$$\begin{aligned} h_j^{(n)}(x) = & (2j+1)G_j^{(n+2)} - xG_j^{(n+3)} - nG_j^{(n+2)} + \\ & P \sum_{k=0}^j F_k^{(n+3)} \alpha_{j-k} R_m^{j-k} + F_{k+1}^{(n+1)}(2k+2)(2k+1) \alpha_{j-k} R_m^{j-k-1} - F_k^{(n+1)} \beta_{j-k} R_m^{j-k} \end{aligned}$$

this implies

$$\begin{aligned} h_j^n \leq & (2j+1) |G_j^{(n+2)}| + R_m^{\frac{1}{2}} |G_j^{(n+3)}| + n |G_j^{(n+2)}| + P \sum_{k=0}^j \left[|F_k^{(n+3)}| |\alpha_{j-k}| R_m^{j-k} \right. \\ & \left. + |F_{k+1}^{(n+1)}| (2k+2)(2k+1) |\alpha_{j-k}| R_m^{j-k-1} + |F_k^{(n+1)}| |\beta_{j-k}| R_m^{j-k} \right]. \end{aligned} \quad (G.5)$$

Simple Bound on F_{j+1}

Let m_0 be the maximum of $|F_k^{(N)}|$ and $|G_k^{(N)}|$ where $0 \leq k \leq j$ and $N \in (0, 1, 2, 3)$. Then, from equation (G.3), we obtain

$$|F_{j+1}^{(N)}| \leq \frac{m_0 R_m}{(2j+2)(2j+1)} \left[R_m^{\frac{1}{2}} + N + 1 + 2j + R_m \sum_{k=0}^{j-1} |\alpha_{j-1-k}| R_m^{j-1-k} \right].$$

Now

$$\begin{aligned} \sum_{k=0}^{j-1} |\alpha_{j-1-k}| R_m^{j-1-k} &= \sum_{k=0}^{j-1} |\alpha_k| R_m^k \\ &= \sum_{k=0}^{j-1} \frac{(1)_k (\frac{1}{2})^k}{(\frac{3}{2})_k k!} R_m^k \\ &< \sum_{k=0}^{\infty} \frac{(1)_k (\frac{1}{2})^k}{(\frac{3}{2})_k k!} R_m^k \\ &= M \left(1, \frac{3}{2}, \frac{1}{2} R_m \right) \\ &= m_1 \end{aligned} \tag{G.6}$$

and so

$$|F_{j+1}^{(N)}| \leq \frac{R_m^{\frac{1}{2}} + N + 1 + 2j + R_m m_1}{(2j+2)(2j+1)} R_m m_0.$$

Since $N \leq 3$ this becomes

$$|F_{j+1}^{(N)}| \leq \frac{m_2 + m_3 j}{(2j+2)(2j+1)}, \tag{G.7}$$

where $m_2 = (R_m^{\frac{1}{2}} + 4 + R_m m_1) R_m m_0$ and $m_3 = 2 R_m m_0$. Note that the right-hand side decreases with j and so for j greater than a certain value the $|F_{j+1}^{(N)}|$ will be less than m_0 .

Simple Bound on G_{j+1}

As before, with m_0 the maximum of $|F_k^{(N)}|$ and $|G_k^{(N)}|$, where $N \in (0, 1, 2, 3)$ and $0 \leq k \leq j$, equation (G.5) gives

$$h_j^N \leq m_0 \left((2j+1) + R_m^{\frac{1}{2}} + N + P \sum_{k=0}^j |\alpha_{j-k}| R_m^{j-k} + (2k+2)(2k+1) |\alpha_{j-k}| R_m^{j-k-1} + |\beta_{j-k}| R_m^{j-k} \right).$$

As

$$\sum_{k=0}^j |\alpha_{j-k}| R_m^{j-k} = \sum_{k=0}^j |\alpha_k| R_m^k < m_1 \tag{G.8}$$

and

$$\begin{aligned} \sum_{k=0}^j |\alpha_{j-k}| (2k+2)(2k+1) R_m^{j-k} &< (2j+2)(2j+1) \sum_{k=0}^j |\alpha_{j-k}| R_m^{j-k} \\ &< (2j+2)(2j+1) m_1 \end{aligned}$$

and

$$\sum_{k=0}^j |\beta_{j-k}| R_m^{j-k-1} = R_m^{-1} \sum_{k=0}^j |\beta_{j-k}| R_m^{j-k}$$

$$\begin{aligned}
&= R_m^{-1} \sum_{k=0}^j |\beta_k| R_m^k \\
&< R_m^{-1} \sum_{k=0}^{\infty} |\beta_k| R_m^k \\
&= R_m^{-1} \sum_{k=0}^{\infty} (2k+2)(2k+1) |\alpha_k| R_m^k \\
&= R_m^{-1} M'' \left(1, \frac{3}{2}, \frac{1}{2} R_m^{\frac{1}{2}} \right) \\
&= m_4,
\end{aligned} \tag{G.9}$$

we thus have

$$h_j^N \leq m_0 \left((2j+1) + R_m^{\frac{1}{2}} + N + Pm_1 + P(2j+2)(2j+1)m_1 + Pm_4 \right).$$

Equation (G.4) now becomes

$$\left| G_{j+1}^{(N)} \right| \leq \frac{(2j+1) + R_m^{\frac{1}{2}} + N + Pm_1 + P(2j+2)(2j+1)m_1 + Pm_4}{(2j+3)(2j+2)(2j-n+1)} R_m m_0 + |c_{j+1}| R_m^{\frac{1}{2}(2j-n+1)}$$

and since $N \leq 3$ we obtain

$$\left| G_{j+1}^{(N)} \right| \leq \frac{m_5 + (2j+1) + (2j+2)(2j+1)m_6}{(2j+3)(2j+2)(2j+1)} + C_j, \tag{G.10}$$

where $m_5 = (R_m^{\frac{1}{2}} + Pm_1 + Pm_4 + 3)R_m m_0$ and $m_6 = Pm_1 R_m m_0$. Note that the first term on the right-hand side decreases with j and, provided the second term also decreases with j (by choosing the constants c_{j+1} in a certain fashion), then for j greater than a certain value, $\left| G_{j+1}^{(N)} \right|$ will be less than m_0 .

Bounds on F_j and G_j , $0 \leq j \leq \infty$

Providing that the arbitrary constants c_{j+1} are chosen carefully, then equations (G.7) and (G.10) show that if j is greater than or equal to a certain value, J say, then $\left| F_{j+1}^{(N)} \right|$ and $\left| G_{j+1}^{(N)} \right|$ ($N \in (0, 1, 2, 3)$) will be less than m_0 . This allows the procedure to become recursive and gives the result that

$$\left| F_j^{(N)} \right| \leq \begin{cases} m_0 & 0 \leq j \leq J \\ \frac{m_2 + m_3(j-1)}{(2j)(2j-1)} & J < j < \infty \end{cases} \tag{G.11}$$

$$\left| G_j^{(N)} \right| \leq \begin{cases} m_0 & 0 \leq j \leq J \\ \frac{m_5 + (2j-1) + (2j)(2j-1)m_6}{(2j+1)(2j)(2j-1)} + C_j & J < j < \infty. \end{cases} \tag{G.12}$$

The less strict version of this is simply

$$\left| F_j^{(N)} \right|, \left| G_j^{(N)} \right| \leq m_0 \quad 0 \leq n \leq 3 \quad 0 \leq j < \infty. \tag{G.13}$$

A stronger bound on F_{j+1}

The expressions (G.11) and (G.12) aren't quite strong enough to prove convergence. However, we can obtain a much stronger result by putting them back into the original equations. If

$$|F_{j+1}| \leq \frac{R_m}{(2j+2)(2j+1)} \left[R_m^{\frac{1}{2}} |F_j'| + |F_j''| + 2j |F_j| + R_m \sum_{k=0}^{j-1} |\alpha_{j-1-k}| R_m^{j-1-k} |G_k'| \right]$$

then, using (G.13) and (G.6), we obtain

$$|F_{j+1}| \leq \frac{R_m}{(2j+2)(2j+1)} \left[R_m^{\frac{1}{2}} m_0 + m_0 + 2j |F_j| + R_m m_0 m_1 \right]$$

or

$$|F_{j+1}| \leq \frac{R_m}{(2j+2)(2j+1)} [m_7 + 2j |F_j|],$$

where $m_7 = R_m^{\frac{1}{2}} m_0 + m_0 + R_m m_0 m_1$. If $j > J$ we can use (G.11) to replace the $|F_j|$ term to obtain

$$|F_{j+1}| \leq \frac{R_m}{(2j+2)(2j+1)} \left[m_7 + 2j \frac{m_2 + m_3(j-1)}{(2j)(2j-1)} \right] \quad j > J$$

or

$$|F_{j+1}| \leq \frac{R_m m_7}{(2j+2)(2j+1)} + \frac{R_m 2j(m_2 + m_3(j-1))}{(2j+2)(2j+1)(2j)(2j-1)} \quad j > J. \quad (G.14)$$

Convergence of A_1

As the series

$$\sum_{j=0}^{\infty} \frac{R_m m_7}{(2j+2)(2j+1)} \quad \text{and} \quad \sum_{j=0}^{\infty} \frac{R_m 2j(m_2 + m_3(j-1))}{(2j+2)(2j+1)(2j)(2j-1)}$$

both converge, the inequality (G.14) shows that

$$\sum_{j=0}^{\infty} F_j$$

also converges. Thus

$$A_1 = \kappa R_m^{\frac{1}{2}} \sum_{j=0}^{\infty} F_j y^{2j}$$

will be convergent for all $y \leq 1$.

A stronger bound on G_{j+1}

From (G.4) and (G.5)

$$|G_{j+1}| \leq \frac{R_m}{(2j+3)(2j+2)(2j+1)} \left[(2j+1) |G_j''| + R_m^{\frac{1}{2}} |G_j'''| + P \sum_{k=0}^j |F_k'''| |\alpha_{j-k}| R_m^{j-k} + |F_{k+1}'| (2k+2)(2k+1) |\alpha_{j-k}| R_m^{j-k-1} + |F_k'| |\beta_{j-k}| R_m^{j-k} \right] + C_j$$

and using (G.13), (G.8) and (G.9) produces

$$|G_{j+1}| \leq \frac{R_m}{(2j+3)(2j+2)(2j+1)} \left[(2j+1)m_0 + R_m^{\frac{1}{2}} m_0 + P m_1 m_0 + P m_4 m_0 + P \sum_{k=0}^j |F_{k+1}'| (2k+2)(2k+1) |\alpha_{j-k}| R_m^{j-k-1} \right] + C_j$$

or

$$|G_{j+1}| \leq \frac{R_m}{(2j+3)(2j+2)(2j+1)} [(2j+1)m_0 + m_8 + PS] + C_j, \quad (G.15)$$

where $m_8 = R_m^{\frac{1}{2}} m_0 + P m_1 m_0 + P m_4 m_0$ and

$$S = \sum_{k=0}^j |F_{k+1}'| (2k+2)(2k+1) |\alpha_{j-k}| R_m^{j-k-1}.$$

If $j > J$

$$\begin{aligned} S &= \sum_{k=0}^J |F'_{k+1}| (2k+2)(2k+1) |\alpha_{j-k}| R_m^{j-k-1} + \sum_{k=J+1}^j |F'_{k+1}| (2k+2)(2k+1) |\alpha_{j-k}| R_m^{j-k-1} \\ &\leq (2J+2)(2J+1) \sum_{k=0}^J |F'_{k+1}| |\alpha_{j-k}| + \sum_{k=J+1}^j |F'_{k+1}| (2k+2)(2k+1) |\alpha_{j-k}| R_m^{j-k-1} \end{aligned}$$

and using (G.13) and then (G.6) gives

$$S \leq m_9 + \sum_{k=J+1}^j |F'_{k+1}| (2k+2)(2k+1) |\alpha_{j-k}| R_m^{j-k-1},$$

where $m_9 = (2J+2)(2J+1)m_0m_1$. Using (G.11) to replace the F'_{k+1} term yields

$$\begin{aligned} S &\leq m_9 + \sum_{k=J+1}^j (m_2 + m_3k) |\alpha_{j-k}| R_m^{j-k-1} \\ &\leq m_9 + (m_2 + m_3j) \sum_{k=J+1}^j |\alpha_{j-k}| R_m^{j-k-1} \\ &\leq m_9 + (m_2 + m_3j) \sum_{k=0}^j |\alpha_{j-k}| R_m^{j-k-1}, \end{aligned}$$

which can be written as

$$S \leq m_9 + (m_2 + m_3j) R_m^{-1} \sum_{k=0}^j |\alpha_k| R_m^k.$$

Making use of (G.6) gives

$$S \leq m_9 + (m_2 + m_3j) R_m^{-1} m_1$$

and hence $S \leq m_{10}$ where $m_{10} = m_9 + (m_2 + m_3j) R_m^{-1} m_1$. Equation (G.15) thus becomes

$$|G_{j+1}| \leq \frac{R_m}{(2j+3)(2j+2)(2j+1)} [(2j+1)m_0 + m_8 + Pm_{10}] + C_j \quad (G.16)$$

Convergence of ψ_1

As

$$\frac{R_m(2j+1)m_0}{(2j+3)(2j+2)(2j+1)} \quad \text{and} \quad \frac{R_m(m_8 + Pm_{10})}{(2j+3)(2j+2)(2j+1)}$$

are both convergent, then, providing

$$\sum_{j=0}^{\infty} C_j$$

converges, the inequality (G.16) shows that

$$\sum_{j=0}^{\infty} G_j$$

also converges. Thus

$$\psi_1 = R_m^{\frac{1}{2}} \sum_{j=0}^{\infty} G_j y^{2j+1}$$

will be convergent for all $y \leq 1$.

Appendix H

Some Integrals

In this appendix the integrals

$$\int_0^1 e^{-ay^2} dy, \quad \int_0^1 y^2 e^{-ay^2} dy, \quad \text{and} \quad \int_0^1 y^4 e^{-ay^2} dy$$

are evaluated in the limit as $a \rightarrow \infty$.

1. For the first integral, a change of variable from y to $u = a^{\frac{1}{2}}y$ gives

$$\int_0^1 e^{-ay^2} dy = a^{-\frac{1}{2}} \int_0^{a^{\frac{1}{2}}} e^{-u^2} du = a^{-\frac{1}{2}} \operatorname{erf} \left(a^{\frac{1}{2}} \right)$$

and taking the limit as $a \rightarrow \infty$ we obtain

$$\int_0^1 e^{-ay^2} dy \rightarrow a^{-\frac{1}{2}}. \quad (\text{H.1})$$

2. For the second integral, integrating by parts gives

$$\int_0^1 y^2 e^{-ay^2} dy = -\frac{1}{2} a^{-1} e^{-a} + \frac{1}{2} a^{-1} \int_0^1 e^{-ay^2} dy.$$

Taking the limit as $a \rightarrow \infty$ and using (H.1) yields

$$\int_0^1 y^2 e^{-ay^2} dy \rightarrow \frac{1}{2} a^{-\frac{3}{2}}. \quad (\text{H.2})$$

3. For the third integral, integrating by parts gives

$$\int_0^1 y^4 e^{-ay^2} dy = -\frac{1}{2} a^{-1} e^{-a} + \frac{3}{2} a^{-1} \int_0^1 y^2 e^{-ay^2} dy.$$

and taking the limit and using (H.2) produces

$$\int_0^1 y^4 e^{-ay^2} dy \rightarrow \frac{3}{4} a^{-\frac{5}{2}}. \quad (\text{H.3})$$

These results allow the proposition

$$P(n) = \int_0^1 y^{2n} e^{-ay^2} dy \rightarrow \frac{(2n-1)!!}{2^{2n}} a^{-n-\frac{1}{2}} \quad \text{as } a \rightarrow \infty$$

to be proved by induction. Equation (H.2) can be used as an anchor and the inductive step is to integrate

$$\int_0^1 y^{2(n+1)} e^{-ay^2} dy$$

by parts to obtain

$$\int_0^1 y^{2(n+1)} e^{-ay^2} dy = -\frac{1}{2} a^{-1} e^{-ay^2} + \frac{2n+1}{2a} \int_0^1 y^{2n} e^{-ay^2} dy.$$

Taking the limit as $a \rightarrow \infty$ and using $P(n)$ gives

$$\int_0^1 y^{2(n+1)} e^{-ay^2} dy \rightarrow \frac{(2n+1)(2n-1)!!}{2 \cdot 2^{2n}} a^{-1-n-\frac{1}{2}} = \frac{(2(n+1)-1)!!}{2^{n+1}} a^{-(n+1)-\frac{1}{2}}$$

which is $P(n+1)$, completing the inductive proof.

Appendix I

Linear Autonomous System 1

Consider the linear autonomous system

$$\dot{x} = y, \quad (\text{I.1})$$

$$\dot{y} = 2y - x. \quad (\text{I.2})$$

1. Differentiating (I.2) with respect to t and substituting for \dot{x} from (I.1) gives

$$\ddot{y} - 2\dot{y} + y = 0,$$

which has the general solution

$$y = ae^t + bte^t.$$

Substituting this into (I.2) gives

$$x = ae^t + bte^t - be^t.$$

The system is thus an unstable improper node.

2. With the above solutions

$$\frac{y}{x} = \frac{ae^t + bte^t}{ae^t + bte^t - be^t} = \frac{a + bt}{(a - b) + bt},$$

which implies that $y \rightarrow x$ as $t \rightarrow \pm\infty$.

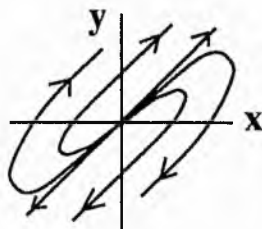
3. With

$$\frac{dy}{dx} = \frac{\dot{y}}{\dot{x}} = \frac{2y - x}{y} = 2 - \frac{x}{y},$$

looking for solutions of the form $y = mx$ gives $y = x$.

4. The trajectories of the system are horizontal ($\dot{y} = 0$) on $y = 0$ and vertical ($\dot{x} = 0$) on $y = \frac{1}{2}x$.

The above pieces of evidence allow the behaviour of the system to be sketched as



Appendix J

Linear Autonomous System 2

Consider the linear autonomous system

$$\dot{x} = y, \quad (\text{J.1})$$

$$\dot{y} = 2y + x, \quad (\text{J.2})$$

1. Differentiating (J.2) with respect to t and substituting for \dot{x} from (J.1) gives

$$\ddot{y} - 2\dot{y} - y = 0,$$

which has the general solution

$$y = ae^{(1+\sqrt{2})t} + be^{(1-\sqrt{2})t}.$$

Substituting this into (J.2) gives

$$x = a(-1 + \sqrt{2})e^{(1+\sqrt{2})t} + b(-1 - \sqrt{2})e^{(1-\sqrt{2})t}.$$

The system is thus a saddle point.

2. With the above solutions

$$\frac{y}{x} = \frac{ae^{(1+\sqrt{2})t} + be^{(1-\sqrt{2})t}}{a(-1 + \sqrt{2})e^{(1+\sqrt{2})t} + b(-1 - \sqrt{2})e^{(1-\sqrt{2})t}},$$

which implies that as $t \rightarrow \infty$, $y/x \rightarrow 1 + \sqrt{2}$ and as $t \rightarrow -\infty$, $y/x \rightarrow 1 - \sqrt{2}$.

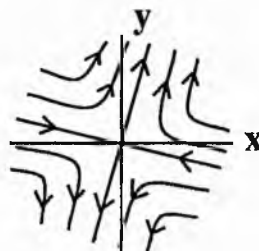
3. With

$$\frac{dy}{dx} = \frac{\dot{y}}{\dot{x}} = \frac{2y + x}{y} = 2 + \frac{x}{y},$$

looking for solutions of the form $y = mx$ yields $y = (1 \pm \sqrt{2})x$.

4. The trajectories are vertical ($\dot{x} = 0$) on $y = 0$ and horizontal ($\dot{y} = 0$) on $y = -\frac{1}{2}x$.

The above pieces of evidence allow the behaviour of the system near this point to be sketched as



References

- Abramowitz and Stegun (1972), *Handbook of Mathematical Functions*, Dover.
- Axford WI (1984), *Magnetic Reconnection in Space and Laboratory Plasmas* (ed. Hones W), Geophysical Monograph 30, p1.
- Biskamp D (1984), 'Magnetic reconnection across an x-type neutral point, slow shocks versus current sheets', *Phys. Lett.* **105A**, 124.
- Biskamp D (1986), 'Magnetic reconnection via current sheets', *Phys. of Fluids* **29**, 1520-1531.
- Biskamp D & Welter H (1980), 'Coalescence of Magnetic Islands', *Phys. Rev. Lett.* **44**, 1069-1072.
- Chester CR (1971), *Techniques in Partial Differential Equations*, McGraw-Hill, pp 118-121
- Clark A (1964), 'Production & dissipation of magnetic energy by differential fluid motions', *Phys. of Fluids* **7**, 1299-1305.
- Cowley SWH (1975) 'Magnetic field line reconnection in a conducting incompressible fluid: properties of the diffusion region', *J. Plasma Phys.* **14**, 475.
- DeLuca EE & Craig IJD (1992), 'Magnetic reconnection in incompressible fluids', *Astrophys. J.* **390**, 679-686.
- Forbes TG & Priest ER (1982), 'Numerical study of line-tied magnetic reconnection', *Solar Phys.* **81**, 303.
- Forbes TG & Priest ER (1983), 'Numerical experiment relevant to line-tied reconnection in two-ribbon flares', *Solar Phys.* **84**, 169.
- Forbes TG & Priest ER (1984), 'Numerical simulation of reconnection in an emerging magnetic flux region', *Solar Phys.* **94**, 315.
- Fu ZF & Lee LC (1986), 'Multiple X line reconnection 2: the dynamics', *J. Geophys. Res.* **91**, 13373.
- Gratton FT, Heyn MF, Biernat HK, Rijnbeek RP & Gnavi G (1988) 'MHD stagnation point flows in the presence of viscosity and resistivity', *J. Geophys. Res.* **93**, 7318.
- Habbal SR & Tuan TF (1979), 'Plane MHD flows in hyperbolic magnetic field, implications for the problem of magnetic field line reconnection', *J. Plasma Phys.* **21**, 85.
- Hayashi T & Sato T (1978), 'Magnetic reconnection: acceleration, heating and shock formation', *J. Geophys. Res.* **83**, 217-220.
- Jardine M & Priest ER (1988a), 'Weakly nonlinear theory of fast steady-state magnetic reconnection', *J. Plasma Phys.* **40**, 143.

- Jardine M & Priest ER (1988b), 'Global energetics of fast magnetic reconnection', *J. Plasma Phys.* **40**, 505.
- Jardine M & Priest ER (1988c), *Proc. of workshop on reconnection in space plasmas*, ESA SP-285, Vol II, p45.
- Jardine M & Priest ER (1988d), 'Reverse currents in fast magnetic reconnection', *J. Geophys. Astrophys. Fluid Dyn.* **42**, 163.
- Jardine M, Allen HR, Priest ER & Grundy RE (1992), 'A family of two-dimensional nonlinear solutions for magnetic field annihilation', *J. Geophys. Res.* **97**, 4199–4208.
- Jardine M, Allen HR & Grundy RE (1993), 'Three-dimensional magnetic field annihilation', *J. Geophys. Res.* **98**, 19409–19417.
- Jeffries JT, Smith EVP & Smith HJ (1959), 'The flare of September 18th, 1957', *Astrophys. J.* **129**, 146–163.
- Jeffries JT & Orrall FQ (1961), 'On the interpretation of prominence spectra II', *Astrophys. J.* **133**, 946–942.
- Kenny RG (1992), 'Liquid-metal flows near a magnetic neutral point', *J. Fluid. Mech.* **244**, 201–224.
- Kirkland KB & Sonnerup BUÖ (1979), 'Self similar resistive decay of a current sheet in a compressible plasma', *J. Plasma Phys.* **22**, 289–302.
- Lee LC (1986), *Solar wind-magnetosphere coupling* (ed. Kamide Y & Slavin JA), Terra Scientific, p297.
- Lee LC & Fu ZF (1986), 'Multiple X line reconnection 1', *J. Geophys. Res.* **91**, 6807.
- Murphy GM (1960), *Ordinary Differential Equations and Their Solutions*, Van Nostrand
- Parker EN (1957), 'Acceleration of cosmic rays in solar flares', *Phys. Rev.* **107**, 830–836.
- Parker EN (1963), 'Solar-flare phenomenon and the theory of reconnection and annihilation of magnetic fields', *Phys. Rev.* **99**, 177–211.
- Parker EN (1973), 'Comments on the reconnection rate of magnetic fields', *J. Plasma Phys.* **9**, 49.
- Petschek HE (1964), *AAS-NASA Symp. on the Phys. of Solar Flares*, NASA SP-50 p 425.
- Phan TD & Sonnerup BUÖ (1990), 'MHD stagnation-point flows at a current sheet including viscous and resistive effects: general two-dimensional solutions', *J. Plasma. Phys.* **44**, 525–546.
- Priest ER & Forbes TG (1986), 'New models for fast steady state magnetic reconnection' *J. Geophys. Res.* **91**, 5579.
- Priest ER & Lee LC (1990), 'Non-linear reconnection models with separatrix jets', *J. Plasma Phys.* **44**, 337–360.
- Priest ER & Forbes TG (1992), 'Magnetic flipping: reconnection in three dimensions without null points', *J. Geophys. Res.* **97**, 1521.
- Rickard GJ & Craig IJD (1993), 'Fast magnetic reconnection and the coalescence instability', *Phys. Fluids B* **5**, 956–964.
- Scholer M (1989), 'Undriven magnetic reconnection in an isolate current sheet', *J. Geophys. Res.* **94**, 8805.

- Sonnerup BUÖ (1970), 'Magnetic field reconnexion in a highly conducting incompressible fluid', *J. Plasma Phys.* **4**, 161.
- Sonnerup BUÖ & Priest ER (1975), 'Resistive MHD stagnation-point flows at a current sheet', *J. Plasma Phys.* **14**, 283.
- Sonnerup BUÖ (1988), 'On the theory of steady-state reconnection', *Computer Phys. Communications.* **49**, 143–159.
- Soward AM & Priest ER (1986), 'Magnetic field-line reconnection with jets', *J. Plasma Phys.* **35**, 333.
- Sonnerup BUÖ & Wang DJ (1987), 'Structure of boundary layers in incompressible MHD', *J. Geophys. Res.* **92**, 8621.
- Strachan NR & Priest ER (1994), 'A general family of nonuniform reconnection models with separatrix jets', *J. Geophys. Astrophys. Fluid Dyn.*, in press.
- Sweet PA (1958), *IAU Symp.* **6**, 123.
- Tsuda T & Ugai M (1977), 'Magnetic field line reconnection by localised enhancement of resistivity. Part 2.', *J. Plasma Phys.* **18**, 451.
- Vasyliunas VM (1975), 'Theoretical models of magnetic field line merging', *Rev. of Geophys. and Space Phys.* **13**, 303–336.